

<https://doi.org/10.15388/vu.thesis.761>

<https://orcid.org/0009-0006-9103-1938>

VILNIUS UNIVERSITY

CENTER FOR PHYSICAL SCIENCES AND TECHNOLOGY

Julija Pupeikė

# Development and Research of Electrically Conductive and Wear Resistant Textiles by Coating with PEDOT:PSS Polymer

**DOCTORAL DISSERTATION**

Technology Sciences

Material Engineering, T 008

VILNIUS 2025

The dissertation was prepared between 2019 and 2024 at Center for Physical Sciences and Technology.

**Academic Supervisor – Dr. Audronė Sankauskaitė** (Center for Physical Sciences and Technology, Technological Sciences, Material Engineering, T 008).

This doctoral dissertation will be defended in a public meeting of the Dissertation Defence Panel:

**Chairman** – Prof. Habil. Dr. Nerija Žurauskienė (Center for Physical Sciences and Technology, Technological Sciences, Materials Engineering, T 008).

**Members:**

Prof. Dr. Daiva Mikučionienė (Kaunas University of Technology, Technological Sciences, Materials Engineering, T.008),

Prof. Habil. Dr. Linas Labanauskas (Center for Physical Sciences and Technology, Natural Sciences, Chemistry, N 003),

Dr. Eglė Fataraitė-Urbonienė (Kaunas University of Technology, Technological Sciences, Materials Engineering, T 008),

Assoc. Prof. Dr. Jolanta Rousseau (University of Artois, France, Technological Sciences, Chemical Engineering, T 005).

The dissertation shall be defended at a public meeting of the Dissertation Defence Panel at 12:00 on 6 June 2024 in meeting room D401 of the Center for physical sciences and technology.

Address: Sauletekio av. 3, Vilnius, Lithuania

Tel. +370 264 9211; e-mail: office@ftmc.lt

The text of this dissertation can be accessed at the libraries of Center for Physical Sciences and Technology, as well as on the website of Vilnius University:

[www.vu.lt/lt/naujienos/ivykiu-kalendorius](http://www.vu.lt/lt/naujienos/ivykiu-kalendorius)

VILNIAUS UNIVERSITETAS  
FIZINIŲ IR TECHNOLOGIJOS MOKSLŲ CENTRAS

Julija Pupeikė

# Elektrai laidžių ir dėvėjimui atsparių tekstilės medžiagų kūrimas ir tyrimas padengiant PEDOT:PSS polimeru

**DAKTARO DISERTACIJA**

Technologijos mokslai  
Medžiagų inžinerija, T 008

VILNIUS 2025

Disertacija rengta 2019–2024 metais VMTI Fizinių ir technologijos mokslų centre.

**Mokslinė vadovė – dr. Audronė Sankauskaitė** (Fizinių ir technologijos mokslų centras, technologiniai mokslai, medžiagų inžinerija, T 008).

Gynimo taryba:

**Pirmininkė** –prof. habil. dr. Nerija Žurauskienė (Fizinių ir technologijos mokslų centras, technologijos mokslai, medžiagų inžinerija – T 008)

**Nariai:**

Prof. dr. Daiva Mikučionienė (Kauno technologijos universitetas, technologijos mokslai, medžiagų inžinerija, T 008),

Habil. prof. dr. Linas Labanauskas (Fizinių ir technologijos mokslų centras, gamtos mokslai, chemija, N 003),

Dr. Eglė Fataraitė-Urbonienė (Kauno technologijos universitetas, technologijos mokslai, medžiagų inžinerija, T 008),

Doc. dr. Jolanta Rousseau (Artois universitetas, Prancūzija, technologijos mokslai, chemijos inžinerija, T 005).

Disertacija ginama viešame Gynimo tarybos posėdyje 2025 m. birželio mėn. 6 d. 12 val. Fizinių ir technologinių mokslų centre D401 posėdžių salėje. Adresas: Saulėtekio al. 3, D401 salė, Vilnius, Lietuva, tel. +370 264 9211; el. paštas [office@ftmc.lt](mailto:office@ftmc.lt)

Disertaciją galima peržiūrėti Fizinių ir technologijos mokslų centro, Vilniaus Universiteto bibliotekose ir VU interneto svetainėje adresu:

<https://www.vu.lt/naujienos/ivykiu-kalendorius>

## LIST OF ABBREVIATIONS

<b>CB</b>	Carbon Black
<b>CNTs</b>	Carbon Nanotubes
<b>CS-AFM</b>	Current Sensing Atomic Force Microscopy
<b>CV</b>	Cyclic Voltammetry
<b>CPC</b>	Conductive Polymer Composite
<b>DBU</b>	Deutsche Bundesstiftung Umwelt (German Federal Environmental Foundation)
<b>EMI</b>	Electromagnetic Interference
<b>EMR</b>	Electromagnetic Radiation
<b>ESD</b>	Electrostatic Discharge
<b>FTIR-ATR</b>	Fourier Transform Infrared Spectroscopy with Attenuated Total Reflectance
<b>FTMC</b>	Center for Physical Sciences and Technology
<b>G</b>	Graphene
<b>GO</b>	Graphene Oxide
<b>Gr</b>	Graphite
<b>ICPs</b>	Intrinsically Conductive Polymers
<b>MXene</b>	2D Materials Made of Transition Metal Carbides/Nitrides
<b>PA</b>	Polyacetylene
<b>PA</b>	Polyamide
<b>PANI</b>	Polyaniline
<b>PEDOT: PSS</b>	Poly(3,4-ethylene dioxythiophene): Poly(styrenesulfonate)
<b>PET</b>	Polyethylene Terephthalate
<b>PP</b>	Polypropylene
<b>PPy</b>	Polypyrrole
<b>PPS</b>	Polyphenylene Sulphide
<b>PTh</b>	Polythiophene
<b>PVA</b>	Poly(vinyl alcohol)
<b>PVA-KOH</b>	Polyvinyl Alcohol-Potassium Hydroxide
<b>PVAc</b>	Poly(vinyl acetate)
<b>PVB</b>	Poly(vinyl butyral)
<b>Py</b>	Pyrrole
<b>RAM</b>	Radar Absorbing Materials
<b>SE</b>	Shielding Effectiveness
<b>SEM</b>	Scanning Electron Microscopy
<b>Vis-NIR</b>	Visible-Near Infrared
<b>XPS</b>	X-ray Photoelectron Spectroscopy

## CONTENTS

INTRODUCTION.....	8
THESIS DESCRIPTION.....	11
LITERATURE OVERVIEW.....	14
1. CONDUCTIVE MATERIALS FOR TEXTILE APPLICATION.....	14
1.1 Definition of the concept.....	14
1.2 Electroconductive additives.....	15
1.2.1 Metal applications.....	17
1.2.2 Carbon and its derivatives applications.....	17
1.2.3 Intrinsically conducting polymers for textile.....	18
2. INTRINSICALLY CONDUCTIVE POLYMER PEDOT:PSS.....	21
2.1 PEDOT:PSS properties.....	21
2.1.2 PEDOT: PSS as “conductive acid dye“.....	23
2.1.3 PEDOT:PSS crosslinking materials.....	24
2.2 PEDOT: PSS applications.....	30
2.3 Methods of inserting ICPs into textiles.....	33
3. CONDUCTIVE TEXTILES.....	37
3.1 Antistatic textiles.....	37
3.1.1 Guidelines and policies.....	37
3.2 Electromagnetic interference shielding (EMI) textiles.....	39
3.2.1 Mechanisms of EMI shielding.....	44
3.2.2 EMI shielding textile application.....	44
3.3 Electroconductive additives and application for Smart/E-Textiles.....	45
3.3.1 Smart textiles past, present and future.....	46
3.3.2 Passive smart textiles.....	49
3.3.3 Active smart textiles.....	49
3.3.4 Ultra-smart or intelligent textiles.....	49
3.3.5 Applications and testing methods for smart textile.....	50
3.3.6 Conductive textiles testing methods.....	51
4. EXPERIMENTAL PART.....	54
4.1 Materials.....	54
4.1.1 Textile materials.....	54
4.1.2 Conductive polymers and auxiliaries.....	54
4. 2 Methodology.....	55
4.2.1 Sample low pressure plasma treatment.....	55
4.2.2 Dyeing with Clevios F ET.....	56
4.2.3 Flatbed screen printing with Clevios S V3.....	57

4.2.4 Digital printing with Clevios F ET and Clevios S V3.....	58
4.3 Materials characterization.....	59
4.3.1 Aqueous liquid repellence water/alcohol solution resistance test.....	59
4.3.2 SEM analysis.....	59
4.3.3 Fourier transform infrared spectroscopy.....	59
4.3.4 X-Ray Photoelectron Spectroscopy.....	60
4.3.5 Vis-NIR spectroscopy.....	60
4.3.6 Current sensing atomic force microscopy (CS-AFM) techniqu.....	61
4.3.7 Cyclic Voltammetry (CV) electrochemical technique.....	61
4.3.8 Colour fastness to washing and rubbing .....	63
4.3.9 Electrical conductivity measurements.....	65
4.3.10 Electrical resistance measurement.....	66
5.1 Results.....	69
5.1.1 Aqueous liquid repellency analysis.....	69
5.1.2. Coding of samples according to modifying type.....	69
5.1.3 SEM analysis.....	70
5.1.4 Fabric analysis by weight.....	77
5.1.5 Spectrophotometric measurements of color difference.....	77
5.1.6 Evaluation of conductive PEDOT:PSS coating durability after washing cycles.....	78
5.1.7 Color fastness to dry rubbing analysis.....	82
5.1.8 Comparison of color diffrencece results.....	83
5.1.9 Specific surface resistance and linear resistance measurement.....	88
5.1.10 Conductance atomic force microscopy (CS-AFM).....	94
5.1.11 Cyclic Voltammetry measurements.....	94
5.1.12 PEDOT:PSS coated wool fabric electroconductivity demonstration.....	97
5.1.13 FTIR-ATR mode measurement.....	98
5.1.14 VIS-NIR absorption spectra.....	105
5.1.15 XPS surface analysis.....	107
CONCLUSION.....	113
REFERENCES.....	115
SANTRAUKA/SUMMARY.....	143
ACKNOWLEDGEMENTS.....	157
LIST OF PUBLICATIONS.....	158
DESCRIPTION OF THE LIFE, SCIENTIFIC AND CREATIVE ACTIVITIES.....	159

## INTRODUCTION

The next big advances in modern technology are likely to be conductive materials and wearable electronics, which are expected to surpass portable devices. Conductive materials enable the integration of sensors that detect and respond to external stimuli [1-5]. Stimuli and responses can be triggered by a variety of causes, including chemical, thermal, magnetic and electrical [1]. The development of lightweight, flexible parts and fibrous structures with high electrical conductivity that can withstand the stresses of wear and textile maintenance is a major challenge for the successful deployment of wearable e-textile technology [2,6]. The development of electrically conductive textiles needs to take into account the properties of wearing comfort, breathability, flexibility, softness, resistance to multiple washings and mechanical elements during daily use. In order to develop lightweight materials as potential alternatives to metallic fabrics, higher conductivity must be combined with good mechanical properties [7].

Conductive textiles are fabricated using natural and chemical fibers with conductive additives, such as conductive polymers, metals, oxides, and carbon. ICPs as polyaniline (PANI), polypyrrole (PPy) and PEDOT:PSS are employed to create conductive coatings or tracks on textiles [8]. ICPs are particularly valued for their flexibility, electrical conductivity, and optical properties, which render them highly relevant for advanced applications. These ICPs can be applied to textiles through conventional methods, such as exhaust dyeing, coating, screen printing or digital printing, and can be fixed using a binder or by directly reacting with the functional groups of the fibers [8-14]. Conductive polymer PEDOT:PSS is lightweight, forms flexible film and can be applied onto the textile without affecting its flexibility and softness. The electrical properties of textiles coated with conductive polymers are influenced by many factors during the finishing process, such as the concentration of chemicals used, the thickness of the coating layer, the fiber content of the textile and the adhesion of the coating to the substrate [10, 15]. The resulting materials are mainly used in the development of electronic, conductive, smart and other textile materials.

The resulting conductive polymer coating often lacks sufficiently strong adhesion between the textile and the conductive polymer layer. Due to the poor adhesion between the textile material and the polymer, the coating delaminates during wear or after washing. One approach to enhancing the properties (resistance to washing, delamination, and rubbing off) of the PEDOT:PSS coating applied on wool fabric without reducing its electrical conductivity by introducing as a crosslinker a commercially available



combination of low formaldehyde content melamine resins into the printing paste could be used.

Adhesion can be improved by cleaning the surface of the material with a low-pressure plasma. For surface modification of heat-sensitive polymeric and textile materials, low-pressure plasma is suitable. Plasma processing generates numerous electrons, free radicals, ions, and metastable species, which can break the molecular chain on the surface within a short time, increase the number of active groups and unsaturated bonds and play a specific etching effect [16]. The plasma not only changes the morphology of the substrate surface, but also binds the active sites to the surface, making the surface active for further reactions [17]. This method also enables the incorporation of functional groups into the material's surface without altering its intrinsic properties [18], with the advantages of convenience and eco-friendliness, and, more importantly, of being capable of activating the surface of the substrate and hydrophilicity for penetration of the polymer into the textile [19, 20].

### **Goal of the thesis**

The aim of this study is to develop a wear-resistant, electrically conductive textile technology using the PEDOT:PSS polymer.

This aim will be achieved by:

1. Develop functional textile materials using sustainable modification and coating methods.
2. Analyze samples coated with the PEDOT:PSS composition using innovative microscopic, physicochemical, and spectroscopic methods to assess their structural, morphological, and electrical properties.
3. Evaluate the electrical conductivity and surface color stability of coated textile materials after rubbing and washing cycles, considering the impact of different coating compositions and fixing agents.
4. Investigate the resistance of electrically conductive textiles to mechanical rubbing and washing durability.

The novelty of this doctoral research lies in the development of a sustainable textile coating technology that enables the formation of a wear-resistant and electrically conductive PEDOT:PSS composite layer on wool fabric without altering its inherent textile properties. This work addresses a significant gap in the integration of conductive polymers into textiles, where durability under mechanical stress remains a key limitation. By systematically evaluating and comparing multiple deposition methods, the study identifies an environmentally friendly approach that ensures both high electrical performance and enhanced wear resistance. Furthermore, comprehensive

characterization using advanced analytical techniques provides new insights into the structure–property relationships of PEDOT:PSS coatings on textile substrates, supporting their potential use in next-generation smart textile applications.

### **Relevance of the work**

In modern materials engineering, increasing attention is being paid to smart textiles capable of performing additional functions, such as electrical conductivity or signal transmission. Environmentally friendly and sustainable textile technology solutions are also becoming increasingly relevant. PEDOT:PSS is a conductive polymer widely used in the development of wearable electronics. However, integrating these materials into textiles poses challenges due to their resistance to wear. This work analyzes the electrical and wear resistance properties of textiles coated with PEDOT:PSS polymer. More sustainable coating methods are also explored, as they are essential for developing reliable, sustainable, and practically applicable smart textile solutions.

### **Key statements for the defence**

- The N<sub>2</sub> gas low-pressure plasma modification increased the hydrophilicity and reactivity of the wool material, the conductive polymer PEDOT:PSS penetrated deeper and more evenly into the wool fibre without altering textile properties.
- The application of the electrically conductive polymer PEDOT:PSS to wool fabrics can be achieved by exhausting, coating and printing techniques, giving the wool fabric an electrically conductive properties without sacrificing flexibility.
- Low-formaldehyde melamine resins enhance the adhesion between wool fibers and PEDOT:PSS, improve certain wear properties such as washability and abrasion resistance, while maintaining electrical conductivity.

## THESIS DESCRIPTION

This thesis investigates the creation of electrically conductive textile using the intrinsically conductive polymer (ICP) poly(3,4-ethylenedioxythiophene) poly(styrene sulfonate) (PEDOT:PSS). Two PEDOT:PSS commercially available products named Clevios F ET and Clevios SV 3 (Heraeus Holding GmbH, Hanau, Germany) were selected due to their technical characteristics - high conductivity, chemical composition, viscosity and suitability for the printing/coating and dyeing methods. Wool fabric was processed using eco-friendly low-pressure nitrogen ( $N_2$ ) gas plasma and coating with PEDOT:PSS products by exhaust dyeing, flatbed screen printing, and digital printing methods were used in this work. The development of electrically conductive, flexible, and wearable textiles is structured into three main phases in this study.

In the first part wool fabric was treated using these two commercially available PEDOT:PSS dispersions with different viscosity, one for exhaust dyeing Clevios F ET and the other Clevios S V3, for flatbed screen printing. Prior to exhaust dyeing with Clevios F ET at 90 °C, the wool fabric, which contains basic groups of amines ( $-NH_2$ ), was preactivated using a low-pressure non-polymer-forming  $N_2$  gases plasma. This treatment enhanced the hydrophilicity, reduced felting, increased adhesion between the coating and wool fibre, and enhanced the electrostatic bonding between PEDOT:PSS's negatively charged sulfonate groups and the wool's protonated amino groups with the cationic protonated amino groups of wool. In addition to ensuring that more PEDOT:PSS negatively charged  $SO_3^-$  counter ions would be electrostatically bonded with the cationic protonated amine groups of the wool fiber. Initially, the surface morphology of pre dyed wool fabric with and without plasma treatment was studied using scanning electron microscopy (SEM). Fabrics were evaluated before and after  $N_2$  plasma treatment, the fabrics were tested for aqueous liquid repellency. By using Fourier transform infrared spectroscopy with attenuated total internal reflection (FTIR-ATR) spectroscopy and X-ray photoelectron spectroscopy (XPS), the newly formed functional groups that formed on the surface of the wool fabric after low-pressure  $N_2$  plasma treatment were identified. Surface color measurements of Clevios F ET dyed wool fabric showed that samples treated with  $N_2$  plasma exhibit greater color depth compared to untreated samples. Since color depth is primarily associated with an increased quantity of colorant, it can be stated that plasma-treated samples have a higher deposition of conductive dye, leading to improved conductivity. A strong correlation has been established

between the instrumentally measured color change (primarily driven by an increase in color depth) and surface resistance, allowing us to conclude that greater color depth corresponds to increased conductivity.

In the second part of this research, a commercial low formaldehyde content melamine resin product Tubicoat Fixing Agent HT (CHT Group, Germany) was used to develop wear-resistant textiles without electrical conductivity reducing. This crosslinker was used to improve the wear properties (resistance to washing and rubbing) of PEDOT:PSS coated wool fabric without reducing the electrical conductivity. Wool fabric dyed and printed with PEDOT:PSS in various shades of blue was subjected to spectrophotometric measurements of the surface colour including - color difference ( $\Delta E^*ab$ ), K/S value (Kubelka-Munk function) and other surface colour parameters. The color of coated samples also was evaluated visually. It was also determined how melamine formaldehyde (MF) resins affected electrical properties, washing and rubbing resistance of wool fabric treated with PEDOT:PSS. The electrical conductivity of the textile samples containing melamine-formaldehyde resins as an additive to increase wearing performance did not significantly diminish, as demonstrated by the resistivity measurement, and their electrical conductivity persisted following the washing and rubbing tests.

In the final part of the work, the plasma-treated wool fabric was coated with PEDOT:PSS via an environmentally sustainable digital printing technique. The application of a melamine-based resin system resulted in highly durable coatings that improved wash and abrasion resistance. The surface morphology and a cross-sectional view of wool fabric that has undergone several alterations were examined using SEM. The surface morphology and a cross-sectional view of wool fabric that has undergone several alterations were examined using SEM. The SEM image demonstrated that in the plasma-treated fabric after dyeing and coating with PEDOT:PSS, the polymer penetrates more deeply into the wool fibers. Additionally, with coating appears more consistent and homogenous when using a Tubicoat fixing agent HT. Using FTIR-ATR analysis, the chemical structure spectra of wool fabrics coated with PEDOT: PSS were examined. The structure of the wool fabric is depicted in the SEM image, along with the extent to which the coating penetrates it when different Clevios F ET/Clevios S V3 products composition are printed. The functional groups of PEDOT:PSS introduced onto the surface after coating of wool fabric were characterized by XPS, FTIR-ATR spectroscopy. The optical properties of fabrics coated with used PEDOT:PSS products and different coating methods were also investigated

using Visible-Near Infrared (Vis-NIR) spectroscopy in the wavelength range of 600-1200 nm. Cyclic voltammetry (CV) has been used to test the electrochemical properties of textiles with used PEDOT:PSS polymer coatings. At the beginning of a capacitor development, CV provides basic information about the capacitive electrochemical cell including: voltage window, capacitance, cycle time. Current-sensing atomic force microscopy CS-AFM was utilized to simultaneously investigate the nanoscale electrical properties and surface topography of the sample, enabling the identification of conductive regions, uniformity of the PEDOT:PSS coating, and potential defects affecting performance. This method was applied for the first time to wool fabrics coated with the conductive polymer PEDOT:PSS.

The results of electrical and wearing resistance showed that after N<sub>2</sub> low-pressure plasma treatment, digital printing with the Clevios F ET, Clevios S V3 and 3 % Tubicoat fixing agent HT mixture provides more intense color on wool fabric after rubbing and washing cycles also retain its electrical conductivity better than other coating methods.

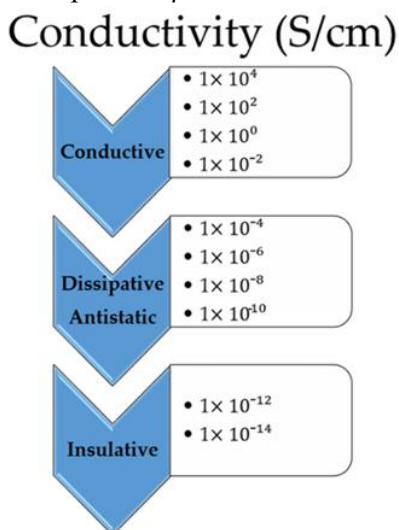
# LITERATURE OVERVIEW

## 1. CONDUCTIVE MATERIALS FOR TEXTILE APPLICATION

### 1.1 Definition of the concept

Evaluating the conductivity of textiles is crucial for determining their suitability for various applications, particularly in smart textiles, anti-static materials, and EMI shielding fabrics. The evaluation of conductivity involves quantifying a textile's ability to conduct electrical current. This process requires precise methodologies to ensure accurate and reliable results, as the conductivity characteristics influence the performance and effectiveness of the textile in its intended application [21, 22].

Electrostatic discharge (ESD) is a very common and easily attainable phenomenon in the realm of alternative nonmetal-based conductive fabrics [23-26]. Components for smart textiles need to have a conductivity that is significantly higher than the electrostatic discharge range to replace metallic conductors in fabrics that effectively transmit information and support computing. According to the ESD Association standard [23], dissipative materials have conductivities between  $1 \times 10^{-11}$  S/cm and  $1 \times 10^{-4}$  S/cm. Conductive materials are those that have conductivity greater than  $1 \times 10^{-4}$  S/cm (Figure 1). Each resistivity value ( $\rho$ ) corresponds to a conductivity value ( $\sigma$ ) based on the relationship:  $\sigma = 1/\rho$ .



**Figure 1.** Conductivity ranges for different applications [23,7].

Conductive fabrics are electrically functionalized fabrics with the advantages of flexibility, elasticity, and wearability [27, 28]. In fact, there are several obstacles to be overcome in the quickly expanding field of electronic textiles, or E-textiles, due to the rigidity and weight of metallic conductors [2, 29]. Electrostatic discharge terminology glossary (ESD ADV1.0) defines conductive materials as “a material that has a surface resistance of less than  $1.0 \times 10^4 \Omega$  or volume resistance of less than  $1.0 \times 10^4 \Omega$ .”

The process of creating conductive textiles involves incorporating conductive materials, including carbon, conductive polymers, or metals (such as copper, gold, or silver), into conventional fabrics. Polymers that are intrinsically conductive, PPy, PANI and PEDOT:PSS, are composed of organic molecules that have extended  $\pi$ -orbital systems along their conjugate backbones that allow electrons to flow through [30]. Conductive polymers have a special structure that makes them lighter and more resistant to wearing as opposed to metals [31]. Because of these polymer's characteristics, conductive fabrics are used for wearable sensors [28–32, 40], antennas [32,33], textile-integrated batteries [34–37], and fabric-based energy storage devices [38]. Conductive fabrics can be produced by synthesizing conductive polymers onto the fabric material [39], coating or by knitting and weaving conductive threads [40].

## 1.2 Electroconductive additives

Several common techniques exist for creating electroconductive textiles, such as metal coating, incorporating metal wires and fibers into the fabric's structure, and combining metal fibers while spinning or weaving. In addition to these metalized textiles, conductive polymers, carbon black, graphite, graphene, carbon nanotubes, and a class of two-dimensional (2D) inorganic compounds MXene are examples of non-metallic electroconductive materials that are used to create electroconductive fabrics that have far superior mechanical and functional qualities. In a nutshell, there are several types of electroconductive textiles: those based on metal, those based on graphene (G), those based on MXene, carbon nanotubes (CNTs), or ICPs. By combining metal fibers with regular textile fibers during spinning, metal-based electroconductive textiles can also be created, offering additional benefits such as shielding against EMI and dispersing electrostatic charges. When there is a high conducting material composition and little porosity, the shielding efficiency rises. Metallic yarn/fabric are produced in a traditional set up by a weaving or knitting procedure, however the prepared fabrics don't have the comfort, drape, or flexibility of textiles [41]. By applying conducting materials

to textile fibers, yarns, and fabrics, it is possible to effectively overcome these limitations associated with metallic electroconductive textiles. Among these are conducting polymers including polyacetylene (PA), polyphenylene (PP), (PPy), (PTh), polyphenylene sulphide (PPS), (PANI), as well as a variety of carbonaceous materials such carbon black (CB), graphite (Gr), G, CNTs. Carbon black (CB) has shown limited effectiveness in rendering textiles electrically conductive because of their lack of affinity for textiles. G on the other hand, has superior optical, mechanical, electrical, and thermal conductivity due to its two-dimensional honeycomb lattice structure made of carbon atoms [42-43]. However, because to *van der Waals* interactions, G has a tendency to clump together and even restack to create Gr, making it challenging to work with. Due to their negative surface charge and excellent colloidal stability, these derivatives offer higher yield, and excellent dispersibility in a variety of solvents, its oxide derivatives, such as nonpolar G quantum dot, graphene oxide (GO), and reduced GO, are currently the most popular for producing scalable quantities of graphene materials through wet chemical processing [44]. The fibers functional groups can interact with each other more effectively, better bind to the fabric, and become more flexible, washable, and long-lasting due to the negative surface charge. Numerous scientific articles have claimed that treating textiles in conductive polymeric solutions with graphene or graphene derivatives can enhance their durability and conductivity (at least initially). Textiles have been coated with G materials using a variety of techniques, including vacuum filtration, electrophoresis, dip coating, brush coating, direct electrochemical deposition, kinetic trapping, wet transfer of monolayer, and screen printing [45-51]. Electroconductive textiles, which may have numerous potential uses, including energy-storing devices, drug delivery systems, flexible heating pads, electromagnetic interference (EMI) shielding, cooling and heating garments, sensors, actuators, antibacterial and antistatic clothing, and so forth, can be created by successfully and durably coating graphene onto textile substrates using the appropriate methodology [52]. In addition to these, MXenes, a class of novel 2D materials composed of transition metal carbides and nitrides, are also attracting a lot of attention in research these days because of their many applications, including biomedicine, wearable electronics, EMI shielding, conductive electrodes, and electrochemical and optoelectronic properties, as well as their high metallic conductivity, tuneable chemistry, and suitable surface termination groups [53]. MXenes are well dispersed in many common solvents such as water, ethanol, dimethylformamide, N-methyl-2-pyrrolidone, and dimethylsulfoxide, as well as in polymer solutions, MXenes can be applied to textile surfaces in a variety of ways, such as spraying, nip and dip,



spinning, coating and printing to transform conventional textiles into high-end smart and functional textiles [54].

### 1.2.1 Metal applications

The initial use of metal flakes and thin wires in textiles were decorative; nevertheless, it was not until the 1960s, with the advent of vapour deposition, that the textile industry began to use metals for their electrical conductivity. While the most conductive elements are copper, gold, steel, nickel, tin, and aluminium, conductivity can also be found in other materials. Metals are still the only workable option for applications requiring high conductivity, despite a variety of drawbacks such as their high cost, restricted versatility, and detrimental impacts on the environment. The four primary types of metal application processes are electroless plating, vacuum deposition, sputtering, and binder coating [55]. Similar to conventional textile coatings, the binder coatings employ polymer carriers and metal particles. The insulating polymer matrix will counterbalance the conductivity, hence various methods to increase the contact between the conductive particles without adding greater mass of metal are being explored. Most include optimizing surface area and experimenting with different sizes and shapes of metal particles, like mica particles coated in metal, oriented threads and flakes [56], and smaller like nano-particles [57]. Other coating properties will be greatly impacted by the binder polymer selection. The metal source (wire or powder) needs to be heated to a minimum of 1000° C and held under vacuum until it condenses onto a cold textile substrate to accomplish vacuum deposition.

There are advantages and disadvantages to using metallization methods, such as plating and sputtering. They result in materials that are stiffer and have reflective surfaces, but they also yield totally metalized fabrics [58, 59]. Metal particles such silver (Ag) and cuprum (Cu) may also leak out and harm the environment when these materials are used in applications where washing or direct wear (abrasion) is a part of the life cycle [60, 61].

### 1.2.2 Carbon and its derivatives applications

A vast spectrum of conductivities can be found in materials made entirely of carbon atoms, ranging from the insulator diamond to conductors like CB, G, and CNTs. The degree of delocalized electrons will determine the conductivity level, making graphitization and carbon compound purity crucial variables. The most popular technique for applying conductive polymer composite (CPC) coating for textile surface deposition is combining

conductive carbon particles typically CB or CNTs with a thermoplastic or thermoset polymer binder. Although carbon sputtering is another option, it has primarily been used as a finishing step before scanning electron microscopy imaging. Moderate to good conductivity is provided by CPC coatings, depending on the kind of carbon particle, loading level, and dispersion level. In theory, CPCs based on CNTs should have lower percolation thresholds than those based on CBs due to geometry; however, in practice, this is not necessarily the case due to the CNTs' frequently encountered fragility and processing challenges. On the other hand, CB are almost often grouped together, which may work to their favour in creating conductive networks. Carbon coatings come in various tones of black, and to maintain a steady conductivity, the carbon fillers need a stiff coating to prevent drifting away during operation. However, this shift in conductivity can also be employed as a resistive strain sensor [62] when the coating is less hard. However, carbon coatings are typically applied in thick layers, which significantly changes the textile's mechanical characteristics.

### 1.2.3 Intrinsically conducting polymers for textile

Historically, polymers were viewed as insulators until the 1970s when Shirakawa and colleagues demonstrated that polyacetylene could become conductive through iodine doping [63]. The discovery of conductive polymers started with the path breaking discovery that halogen doped polyacetylene ( $-\text{CH}=\text{CH}-$ )<sub>n</sub> show high electrical conductivity, which led to the 2000 Nobel Prize in Chemistry award [64]. Since then, there have been several fundamental studies and applications of conductive polymers. The carbon atom in saturated polymers, such as polyethylene, form four covalent  $\sigma$ -bonds (saturated  $\text{sp}^3$ -carbon). Whereas the carbon atom in conjugated polymers possess  $\text{sp}^2$ -p<sub>z</sub> ( $\pi$ ) orbitals, with three bonding electrons, while the remaining p<sub>z</sub> orbitals contribute to the  $\pi$ -conjugated system. The common feature in conductive polymers is conjugation, i.e., the alternation of single and double bonds, and hence the synthesis of  $\pi$ -conjugated chains is central to the science and technology of conductive polymers. The charge carriers are delocalized in conjugated systems and provide the “highway” for charge mobility along the backbone of the polymer chain. The conductivity of conjugated polymers can be significantly enhanced through doping, typically involving oxidation or reduction processes [65]. The conductivity of doped polyacetylene (PA) can reach  $10^5$  S/cm which is comparable to that of copper [32]. However, PA is difficult to synthesize and is unstable in air which prevented its commercialization. The most important conductive polymer candidates

currently are PPy, PANI, and PTh, whose ICPs comparison are shown in Table 1, Poly(3,4-ethylenedioxythiophene) (PEDOT), is the most studied and successful PTh derivative polymer due to its higher electrical conductivity and chemical stability which make it suitable in the development of smart textiles [33, 65-68]. In contrast to PPy and PANI, the exploration on PEDOT is comparatively recent.

**Table 1.** Comparison of intrinsically conductive polymers (ICPs) for textile applications

Conductive Polymer	Conductivity (S/cm)	Properties	Applications in textiles	References
<b>PEDOT:PSS</b>	4700	High electrical conductivity	Wearable electronics	[64]
		Excellent stability	Sensors	
		Water processable	Antistatic coatings	
<b>PANI</b>	112	Tunable conductivity	pH sensors	[69]
		Low cost	EMI shielding	
		Moderate stability	Flexible electronics	
<b>PPy</b>	2000	High conductivity	Biomedical textiles	[70]
		Biocompatibility	Actuators	
		Good stability	Antistatic materials	
<b>PA</b>	10 <sup>5</sup>	Extremely high conductivity	Experimental conductive coatings	[63]
		Poor environmental stability	Rarely used in textiles	
		High conductivity	Flexible sensors	
<b>Polythiophene (PTh)</b>	560	Excellent flexibility	Wearable devices	[71]
		Stability with doping	Energy storage	

This discovery extended to other polymers like PANI and PPy, sparking interest in all-plastic electronics. However, early challenges, including instability, complex processing, and unfavorable color properties, slowed the progress of ICPs. Continuous research into synthesis methods and material modifications eventually led to more practical applications [15].

In recent years, the focus of smart textile research has shifted toward improving the practical attributes of fabrics, such as wearability and durability. Wearable technologies have evolved from incorporating devices such as LEDs and mobile phones into garments, as seen in prototypes from companies like Philips, Levis, and Nokia [71-72]. However, integrating gadgets directly into textiles often results in bulky, impractical clothing. Consequently, there is growing interest in developing lightweight, flexible, fully conductive fabrics that resemble conventional textiles while offering electronic functionalities [73, 74]. Conductive polymers are especially suited to this task due to their flexibility, stability, and relative ease of processing [74, 75]. The discovery of ICPs opened up new possibilities for smart textiles [76, 77]. Upon doping, these polymers exhibit electrical conductivity due to the delocalization of  $\pi$ -electrons along the polymer backbone, similar to conduction in semiconductors, similar to the mechanism in semiconductors [77, 78]. As a result, textiles coated with these materials exhibit electrical properties that can be harnessed for applications like sensors, energy storage, or heat generation [78]. In particular, the polymerization of PPy and PANI on fabric substrates has gained traction in the textile industry [79]. For instance, PPy coated polyester has been used to create heat-generating textiles [80].

Further advancements include reports of PPy and PEDOT coatings on polyester fibre through chemical and electrochemical oxidation, which resulted in conductive textiles that could function as strain sensors [81]. These innovations highlight the potential of conductive textiles in various sectors, though challenges remain, such as ensuring air stability and overcoming the need for highly acidic conditions in the polymerization process [82, 83]. Commercially available products, such as EeonTex [84], demonstrate the growing feasibility of these technologies, despite ongoing issues like the complexity of production and post-treatment processes. In addition to in situ polymerization, fully polymerized PANI, PPy, and PEDOT dispersions are available commercially and offer alternative approaches for creating conductive fabrics [85, 86]. These materials, along with innovations like ICPs coated latex particles, present promising solutions for the future of conductive textile development [15].

Intrinsically conducting polymers (ICPs) have emerged as key materials for developing advanced functional textiles. Their unique electrical, thermal,

and mechanical properties enable a wide range of applications in wearable electronics, smart fabrics, and energy systems. The Table 2 below highlights major applications of ICPs in textiles, along with relevant studies for further exploration.

**Table 2.** Applications of intrinsically conducting polymers (ICPs) in textiles.

<b>Application</b>	<b>Description</b>	<b>Reference</b>
<b>Electrically Conductive Textiles</b>	Integration of ICPs to create textiles with electrical conductivity for applications in sensors, actuators, and energy storage devices.	[87]
<b>Flexible and Stretchable Strain Sensors</b>	Utilization of ICPs in developing flexible and stretchable strain sensors for wearable electronics.	[88]
<b>Smart Textiles</b>	Application of conductive polymers in smart textiles for medical, protective clothing, and interactive displays.	[89]
<b>Energy Harvesting and Storage</b>	Development of textiles integrated with ICPs for energy harvesting and storage applications.	[90]
<b>Electromagnetic Interference (EMI) Shielding</b>	Use of ICP-coated textiles for EMI shielding in electronic applications.	[91]

## 2. INTRINSICALLY CONDUCTIVE POLYMER PEDOT:PSS

### 2.1 PEDOT:PSS properties

The PEDOT was developed in the late 1980s by Bayer AG and found to have the then rare combination of high conductivity, transparency and environmental stability [92]. PEDOT:PSS is a conjugated polymer system in which PEDOT is a stable conjugated polymer that, when combined with PSS, remains oxidized, highly conductive, and water dispersible [93]. Its insolubility still posed a problem but was later circumvented by pairing it with PSS, a water soluble polyelectrolyte that also functions as a charge balancing dopant. In Table 3, the chemical structure [94] of the PEDOT:PSS complex is shown to the left and its secondary structure indicated to the right.

In the chemical structure, the upper structure is the PEDOT and it is interesting to notice the positions of the dioxy rings and how they uphold the

regioregularity of the thiophene. It is also worth noticing the oligomeric, rather than polymeric, lengths of the PEDOT molecules from the secondary structure. The addition of PSS to the structure made it possible to commercially offer PEDOT:PSS dispersions, but also resulted in a high amount of water, 90 – 95%, adsorbed to the PSS in the products; in spite of this, dried PEDOT:PSS films have exceptional stability to humidity and pH. PEDOT:PSS is inherently blue and films made from it tend to have a bluish tint. If, however, they are thin enough, corresponding to  $\leq 200$  nm pure PEDOT:PSS, the visible light transmission through the film will be at least 85% [95, 96]. The coatings in this work were all in different shades of blue.

**Table 3.** Summarizing the properties of PEDOT: PSS [97, 98]:

Properties	Description
<b>Electrical Conductivity</b>	Ranges from 0.1 to 1000 S/cm depending on formulation and processing
<b>Transparency</b>	Can form thin, transparent films
<b>Mechanical Flexibility</b>	Suited for flexible electronic applications
<b>Environmental Stability</b>	Resistant to oxidation and deterioration in natural environments
<b>Processability</b>	Can be easily processed via various deposition methods from aqueous solutions

**Table 4.** Synthesis process of PEDOT:PSS [97, 99]:

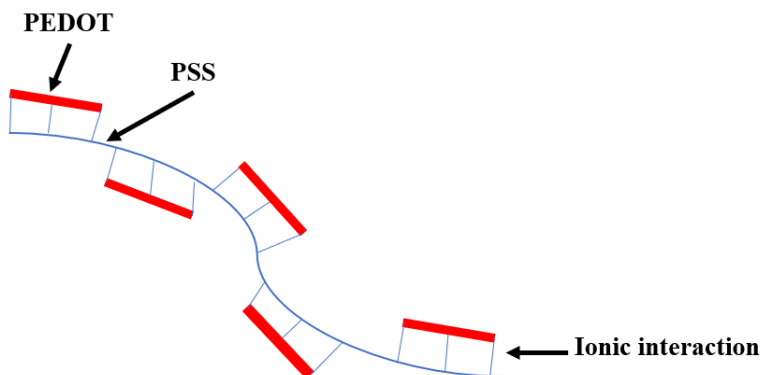
Synthesis process	
<b>Polymerization</b>	EDOT monomers are polymerized using an oxidizing agent in the presence of PSS.
<b>Dispersion</b>	PSS stabilizes the PEDOT chains in aqueous solution, creating a colloidal dispersion.

While PSS is a sulfonated polystyrene that interacts with PEDOT by electrostatic interactions, PEDOT is a conjugated polymer with alternating single and double bonds along its backbone. Depending on the processing conditions, the PEDOT:PSS complex can generate different morphological shapes that impact its mechanical and electrical properties. PEDOT:PSS, by varying the PEDOT to PSS ratio, doping concentration, and processing parameters, PSS high electrical conductivity can be optimized. It can therefore be used in situations where conductive routes in textiles are necessary. There are several advantages for the PEDOT:PSS water-soluble polyelectrolyte system for textile applications, including electrical conductivity, applicability with traditional textile technologies, commercial availability, water solubility,

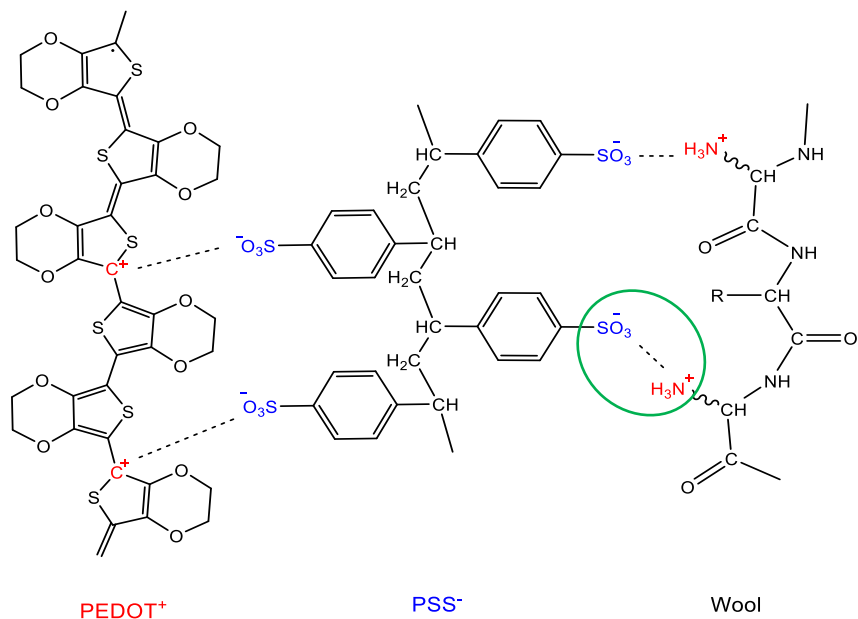
stability, and high visible light transmittance (Table 3) [98]. A disadvantage influenced by the solubility of the conductive polymer component PSS in water causes the formed coating to peel off from the textile, thus decreasing its resistance [100-102] to wet treatments. It is also important to evaluate the ability of the PEDOT:PSS coating on wool fabric to retain its conductivity and resistance to rubbing and washing [103-107].

### 2.1.2 PEDOT: PSS as “conductive acid dye”

Various functional finishing of textile materials can be achieved through conventional dyeing and coating processes by applying chemical compounds that carries ionisable groups, which are a common feature of acid dyes [108]. Most acid dyestuffs acquire their acidity from the present of sulfonic acid functional groups ( $-\text{SO}_3\text{H}$ ) or nitro ( $-\text{NO}_2$ ) groups in the molecule [11, 109]. These dyes being water soluble anionic dyes are used primarily to nitrogenous fibres such as wool, silk and nylon, all of which contain basic groups. Wool is a natural protein fiber composed of 18 amino acids with basic amino ( $-\text{NH}_2$ ) and acidic carboxyl ( $-\text{COOH}$ ) groups and sulphur, linked adjacent macromolecules to each other by cross disulphide bonds [11]. Nitrogen containing fibers such as wool fibers are usually dyed with acid dyes of which contain basic groups. Researches assigned PEDOT:PSS to a “conducting acid dye” which can also tightly bind to protein fibres through electrostatic interaction of PSS chain negatively charged sulfonate ( $-\text{SO}_3^-$ ) ions to protein fibre cationic sites (Figure 2, 3) and to dye them in various shades of blue [11,110,111].



**Figure 2.** PSS-chain with PEDOT-oligomers.



**Figure 3.** PEDOT:PSS negative charged sulfonate ions ( $-\text{SO}_3^-$ ) interaction with the cationic amine groups of the wool fiber.

### 2.1.3 PEDOT:PSS crosslinking materials

The process of chemically joining polymer chains to create a network structure is known as crosslinking. Crosslinking in the context of PEDOT:PSS can be accomplished in a number of ways that add covalent connections between the chains of PEDOT and PSS or between PEDOT:PSS and other polymeric materials [112, 113]. PEDOT:PSS with crosslinking material can increase stability, and mechanical strength, which will make it more suited for incorporation into flexible and wearable electronic devices [114, 112, 115].

PEDOT:PSS film is prone to delaminate and disperse due to a presence of a water-soluble PSS chain and this limits their use for textile. Most approaches involve cross-linking PEDOT:PSS with different agents, such as silanes [116], poly (ethylene glycol) [117], or divinylsulfone (DVS) [118, 119]. Researchers [120] found that after introducing of DVS crosslinking of the PEDOT: PSS occurs at a room temperature without reduction of its electronic conductivity. DVS having two *S*-vinyl substituents with two reactive groups at opposite ends of the molecule that are capable of reacting with and thereby forming bridges between macromolecules can react as a crosslinking agent. Study performed by D. Mantione et al. [120] identified that the reaction between PEDOT: PSS and DVS possibly are a physical



crosslinking. By introducing the DVS crosslinker, the PEDOT electrodes show remarkable stability in water, without reducing its conductivity. PEDOT:PSS/DVS electrodes maintain their elasticity and therefore their resistivity is little affected when stretched in water. PEDOT:PSS/DVS textiles can be developed as mechanically robust wearable electronic garments that can be widely applied health monitoring [115].

To enhance washability, PEDOT can be combined with fixers such as self-cross-linking silicones. This strategy secures the PEDOT layer to the textile, making it resistant to washing while maintaining conductivity. Fixers like silicone-based agents have shown strong adherence and wash durability on polyester, proving useful for applications in wearable technologies [121, 122]. In general, in PEDOT coatings, a epoxy silane coupling agent ((3-glycidyloxypropyl) trimethoxysilane (GOPS) crosslinker is commonly used. GOPS presented some important drawbacks such as its high curing temperature (140° C) and negative effect on the conductivity values. Due to the natural insulating properties of the siloxane network, this cross-linker is normally used together with doping agents such as ethylene glycol or dimethyl sulfoxide (DMSO) to reduce the loss of conductivity generated by GOPS [112]. Careful studies of the mechanism and effects of cross-linking PEDOT:PSS with GOPS revealed that the epoxy group at one end of GOPS reacted with the free sulfonic acid moiety of PSS [123]. GOPS has proven effective in successfully suppressing dissolution and delamination of PEDOT:PSS films in aqueous solutions [124-126].

Low molecular weight poly (ethylene oxide) (PEO) also reported as secondary dopant. The addition of small amount of low molecular weight PEO can lead to an increase in conductivity of PEDOT:PSS by two orders of magnitude [124]. Unlike other dopants, such as dimethyl sulfoxide (DMSO) and ethylene glycol (EG), the PEO stays within the PEDOT:PSS film after film processing. Hopkins et al. compared the conductivity of hybrid PEO/PEDOT:PSS and poly(vinyl alcohol)(PVA)/PEDOT:PSS, and found the hybrid PEO/PEDOT:PSS film has higher electrical conductivity than the PVA/PEDOT:PSS film because the crystallization of high molecular weight PEO drives the formation of the conducting polymer networks in solution-cast phase-segregated PEO/PEDOT:PSS film [125]. Although the incorporation of considerable amount of insulating high molecular weight PEO into PEDOT:PSS film shows lower electrical conductivity than pristine PEDOT:PSS, the addition of high molecular weight PEO into aqueous PEDOT:PSS solution can help improve its spin ability to produce conducting electrospun PEDOT:PSS nanofibers [127] (Table 5).

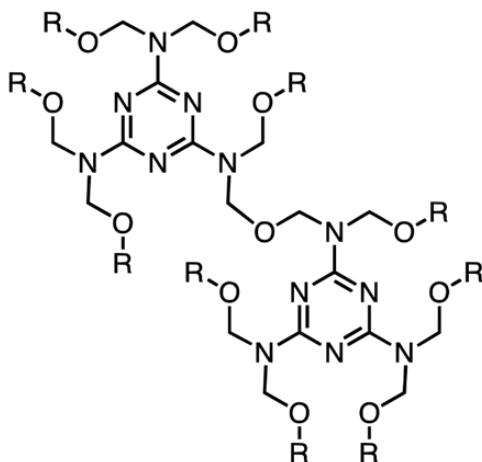
**Table 5.** Most useable crosslinking agents advantages and disadvantages

Crosslinker	Advantages	Disadvantages
<b>Divinyl sulfone (DVS)</b>	Forms strong covalent bonds with fibers;	Excessive crosslinking can reduce fabric flexibility;
	Enhances mechanical durability and washability;	Requires careful handling (hazardous);
	Good moisture resistance;	
	Improves adhesion and water resistance;	Can reduce conductivity if used in excess;
<b>Glycidoxypropyltrimethoxysilane (GOPS)</b>	Widely used in e-textile applications;	Increases fabric stiffness;
	Stable under environmental conditions;	
<b>Zirconium acetate</b>	Mild crosslinking agent, maintains flexibility;	Less effective for very high durability needs;
	Enhances adhesion without reducing conductivity;	May require higher curing temperatures;
	Enhances electrical conductivity by reducing phase separation;	Less effective in improving long-term mechanical stability;
<b>Ethylene glycol (EG)</b>	Maintains fabric flexibility;	Conductivity can degrade with washing;
	Easy to apply, inexpensive;	
	Improves conductivity significantly by modifying PEDOT structure;	Does not improve mechanical adhesion to textile;
<b>Dimethyl sulfoxide (DMSO)</b>	Simple post-treatment;	Limited impact on durability or washability;
	Improves flexibility and reduces brittleness;	Can reduce conductivity if not optimized;
<b>Polyethylene glycol (PEG)</b>	Can be used to tune mechanical properties;	Limited water resistance without additional treatment;
	Strongly enhances conductivity;	May degrade textile fibers over time if not carefully controlled;
<b>Methanesulfonic acid (MSA)</b>	Can be used in combination with other crosslinkers;	Limited improvement in adhesion;
	Improves processability;	
<b>Dodecylbenzenesulfonic acid (DBSA)</b>	Improves conductivity and flexibility;	Lower mechanical strength improvement;

<b>Formaldehyde melamine resin</b>	Helps in dispersion of PEDOT;	Limited water resistance, requires additional treatment;
	Compatible with various fabrics;	
	Creates a highly durable crosslinked network;	Can be toxic or irritant if not handled properly;
	Excellent mechanical and chemical resistance;	May increase stiffness and reduce fabric flexibility;
	Good washability;	

### 2.1.3.2 Melamine resin as PEDOT:PSS crosslinkers

Melamine resin or melamine formaldehyde is a resin with melamine rings terminated with multiple hydroxyl groups derived from formaldehyde. The molecular formula of melamine-formaldehyde depends on the degree of polymerization. Its main components are: melamine ( $C_3H_6N_6$ ) and formaldehyde ( $CH_2O$ ). During the reaction between melamine and formaldehyde, a melamine-formaldehyde resin is formed, whose composition depends on the reaction conditions and polymerization degree. The general repeating structure can be represented as:  $(C_3H_6N_6) \cdot (CH_2O)_n$  [128] (Figure 4). In the textile industry, melamine formaldehyde resin and derivatives are important raw materials for preparing fabric printing and dyeing finishing agents. Its mechanism of action is mainly to serve as a surface modifier and coupling agent for fabrics, thereby improving the anti-shrinkage, anti-wrinkle and washability properties of fabrics. However, due to poor storage stability, rough fabric feels after treatment and easy absorption of chlorine and yellowing, there are more and more studies on its modification. Currently, melamine resin is etherified with methanol, and formaldehyde modifiers such as cyclovinylidene urea and borax are added to obtain an ultra-low-aldehyde and high-stability modified melamine-formaldehyde resin finishing agent [128].



**Figure 4.** Melamine-formaldehyde resin (R - H, alkyl)

MF is one of the hardest and stiffest thermosetting polymers, which provides good properties and performance. It is an amino resin and has various material advantages, such as transparency, better hardness, thermal stability, excellent boil resistance, scratch resistance, abrasion resistance, flame retardant, moisture resistance and surface smoothness, which lead MF to large industrial applications [128]. These polymers were originally used as wood adhesives and have now found applications in flooring and decorative laminates, molding compounds, coatings and adhesives. MF resins are incorporated in wide variety of products that are valued for its toughness and relative ease of manufacture. The curing behavior and the degree of crosslinking of MF resin determine the tailored product properties such as mechanical, thermal and electrical properties. Cured MF polymers are sufficiently hard and exhibit high resistance against temperature, chemicals and hydrolysis, making them suitable for interior working surfaces. If the resin is not cured properly, MF will lack mechanical strength and surface finishes [129,130].

A popular thermosetting polymer with good adhesion, durability, and resistance to heat and chemicals is MF resin (Table 6). Utilizing PEDOT:PSS as a fixing agent on wool textiles can greatly enhance the stability and integration of the conductive coating. Wool fiber functional groups and PEDOT:PSS form covalent bonds with the melamine-formaldehyde resin. The crosslinked structure improves mechanical strength and conductivity by forming interpenetrating polymer networks.

The allowable limit of formaldehyde in textiles is regulated by various standards and agencies worldwide, as formaldehyde can pose health risks, especially in close contact with skin. By European Union (EU) formaldehyde

limits regulations for direct skin contact textiles (e.g., clothing) to 75 ppm, for non-skin contact textiles (e.g., furniture fabric) 300 ppm, Eco-labels (like OEKO-TEX® Standard 100) have stricter limits, with 16 ppm for products intended for babies and 75 ppm for adult textiles in direct skin contact [130]. In our tests, free formaldehyde was around 300 ppm.

**Table 6.** Advantages and disadvantages of formaldehyde melamine resin in textile applications [131-132]:

Aspect	Advantages	Disadvantages
<b>Durability</b>	Increases the durability of fabrics by improving resistance to wear and tear.	May affect fabric softness, making it feel stiffer or less comfortable against the skin.
<b>Wrinkle resistance</b>	Provides wrinkle resistance, reducing the need for ironing and enhancing appearance retention.	Overuse can lead to a loss of flexibility, making the fabric feel brittle over time.
<b>Shrinkage control</b>	Reduces fabric shrinkage, helping textiles maintain their shape after washing.	Can contribute to fabric stiffness, affecting drape and flexibility.
<b>Water and stain resistance</b>	Improves water and stain resistance, making fabrics easier to clean and maintain.	High resin content can compromise breathability, making textiles less suitable for wearable items.
<b>Heat resistance</b>	Adds heat resistance, making fabrics less likely to degrade when exposed to high temperatures.	Requires precise processing conditions; improper curing can affect fabric quality.
<b>Flame retardancy</b>	Enhances flame-retardant properties, making it useful in protective fabrics and industrial applications.	May release formaldehyde over time, posing potential health risks.
<b>Easy maintenance</b>	Reduces pilling and helps fabrics maintain a fresh look after multiple washes.	May require specific washing conditions to maintain resin properties, adding maintenance complexity.
<b>Cost efficiency</b>	Provides an affordable solution to enhance fabric properties, ideal for commercial and industrial textiles.	Non-biodegradable and difficult to recycle, contributing to environmental concerns in textile waste.

Our studies have shown that melamine formaldehyde resin crosslinking PEDOT:PSS with wool textiles offers a reliable technique for producing

conductive and long-lasting wool textiles (Figure 5). With this method, the conductive layer is applied uniformly and has increased adhesion and endurance, which makes treated wool appropriate for a variety of smart textile applications. The choice of MF resin and process parameters can be tailored to meet specific performance requirements, enabling the development of advanced functional textiles [133,].

In this work MF resin systems were chosen to use for textiles to produce highly durable coatings, especially for impregnation against moisture [133]. For this reason, some of the investigated samples were treated with a low formaldehyde content melamine resin named Tubicoat fixing agent HT, which does not require high curing temperatures and can improve the properties of PEDOT:PSS coatings on wool fabric, such as resistivity to washing, delamination and mechanical effecting, without compromising its electrical conductivity [129, 134-142].

## 2.2 PEDOT: PSS applications

The conjugated polymer system PEDOT:PSS was first used for antistatic films in the photographic industry but soon found other applications as PEDOT:PSS dispersions became commercially available. Commercially available PEDOT:PSS aqueous dispersions have coating formulas recommended for glass, plastic, and ceramic surfaces [143]. It is well known for its superior electrical conductivity, environmental stability, and processability, which make it ideal for a range of uses in wearable electronics and smart textile applications like sensors, heating elements, and EMI shielding [72].

Due to their organic nature, conducting polymers present many advantages in the development of flexible, conformable, stretchable, as well as wearable electronics [9, 114]. In the field of bioelectronics, traditional metal electrodes are actually being replaced by conducting polymer electrodes based on PEDOT derivatives, which have shown many benefits in recording electrophysiological signals [8, 114]. When PEDOT:PSS is used in cutaneous electrode coatings, these electrodes have low impedance when in contact with the skin, improving thus the signal-to-noise ratio [114, 115]. The development of electronics that can be embedded in our clothing or body is of extreme interest for the development of the next generation of medical devices that can continuously monitor our health [114, 8]. There are currently many examples highlighting the potential of conducting polymer-based electrodes for such applications. For instance, it is possible to make conformable self-supporting tattoo electrodes with PEDOT:PSS that compliantly adhere to the skin,

providing a seamless communication channel with the human body [114, 112]. Electronic textiles integrating PEDOT electrodes equally appeared as another type of technology facilitating. The fabrication of wash-and-wear resistant conductive silk threads dyed with conjugated polyelectrolytes has been extensively studied by Müller and Ryan [144-148]. The interaction between protein-based fibers and ICPs, such as PEDOT:PSS and poly(4-(2,3-dihydrothieno[3,4-b][1,4]dioxin-2-yl-methoxy)-1-butananesulfonic acid) (PEDOT:S), under varying pH conditions, and the imparted conductivity to protein fibers, was investigated in a separate study [147].

Synthetic polyamides, which are long-chain polymers containing recurring cationic amide (-CONH-) groups, exhibit similar properties to protein fibers, enabling ionic bonding with ICPs. Plasma treatment, applied prior to coating with glycerol-doped PEDOT:PSS polymer, was shown to enhance adhesion on polyamide fibers [148]. M. R. Moraes [148] also conducted trials on dyeing cotton yarns with PEDOT:PSS formulations.

Due to the neutral substantivity of anionic dyes to regular PET and cotton fibers, these materials cannot be dyed effectively with acid dyes. However, Y. Guo et al. [114] demonstrated the fabrication of all-organic conductive wires by using patterning techniques, such as inkjet printing and sponge stenciling, to apply PEDOT:PSS onto nonwoven PET fabrics. Additionally, it is well-documented that cationization can improve the substantivity of anionic dyes on cotton by introducing positively charged sites on the fiber [149].

The thermoelectric performance of PEDOT:PSS can be optimized by adjusting its conductivity through different treatments. For thermoelectric materials to sustain a temperature differential, lower thermal conductivity is preferable. Furthermore, for the electrochromic fabric prototype, PEDOT:PSS was utilised by simply immersing commercially available Spandex in a PEDOT: PSS solution. They can be employed as flexible and deformable substrates because the coating has no effect on the substrate's mechanical qualities [13,75].

PEDOT:PSS is appropriate for thermoelectric applications since it typically has a low thermal conductivity. Because of PEDOT: PSS flexibility, fabrics can be treated with it without noticeably losing their softness or drapability. Its longevity also guarantees that the conductive qualities endure even in the face of mechanical deformation. PEDOT:PSS is appropriate for wearable and outdoor applications where environmental exposure is a concern since it is stable in ambient circumstances (Table 7). The table below summarizes the key applications of PEDOT:PSS in textiles, highlighting its role in enabling advancements such as wearable electronics, smart fabrics, and flexible conductive materials. Each application is linked to relevant studies,

providing insights into the latest developments in this field. It is observed that the wash and wear resistance of PEDOT:PSS coated fibers and textiles remains a challenge [148, 150, 151]. Notwithstanding the difficulties, more study and development should improve the scalability and performance of PEDOT:PSS integrated textiles, opening the door for cutting edge functional fabrics in the future.

**Table 7.** Applications of PEDOT:PSS in textiles

Application	Description	Relevant Article
<b>Wearable electronics</b>	PEDOT:PSS-coated fibers for flexible and conductive wearables, enabling smart clothing applications.	[90]
<b>Smart fabrics</b>	Integration of PEDOT:PSS for developing textile-based sensors, circuits, and interactive garments.	[64]
<b>Conductive patterns</b>	Use of PEDOT:PSS in inkjet and screen printing to create conductive patterns on fabric surfaces.	[152]
<b>Flexible electronics</b>	Development of PEDOT:PSS composite textiles for wearable energy storage and flexible circuits.	[64]
<b>Thermal management in textiles</b>	Creation of thermoelectric fibers with PEDOT:PSS for temperature regulation and Joule heating effects.	[153,154]

Research on the electrical conductivity and surface resistance of PEDOT:PSS-coated textiles has examined various fabric types and coating methods (Table 8). Cotton was impregnated with a PEDOT:PSS solution containing silver nanoparticles (Ag NPs) and dimethyl sulfoxide (DMSO), achieving a surface resistance ranging from 42.3 to 47.7  $\Omega$  depending on immersion duration [152]. Polyester, coated with PEDOT:PSS using a dip-coating method, exhibited conductivity between 30 and 200 S/m, making it suitable for sensors and wearable electronics [8]. Non-woven PET fabric, coated using a spraying method, achieved a surface resistance below 2  $\Omega$ /sq, which is promising for flexible electrodes and antennas [8]. Nylon/Spandex fabric, coated with a PEDOT:PSS and polyurethane (PU) mixture, maintained a surface resistance of  $\sim 1.7$   $\Omega$ /sq even after stretching up to 650% and undergoing multiple washing cycles, demonstrating its suitability for stretchable wearable devices [153]. Polyurethane non-woven fabric, coated with PEDOT:PSS and PU layers, exhibited a surface resistance between 35 and 240  $\Omega$ /sq, depending on the number of coating layers, making it suitable



for flexible sensors and energy storage applications [8]. Silk threads, dyed with a PEDOT:PSS solution, achieved conductivity of approximately 14 S/cm, which remained stable after washing, demonstrating their potential for wearable electronics [8]. Knitted cotton fabric, coated with a PEDOT:PSS composite via screen printing, showed a surface resistance of 24.8 k $\Omega$ /sq, making it applicable for textile-based sensors [8]. Additionally, PEDOT:PSS fibers, produced using a wet-spinning process, exhibited high conductivity (up to  $3663 \pm 326$  S/cm), a Young's modulus of up to 22 GPa, and a tensile strength of 550 MPa, making them suitable for electronic textiles [154]. These findings highlight how different coating techniques and modifications can significantly enhance the electrical properties of textiles, enabling new applications in wearable electronics, sensors, and energy storage systems.

**Table 8.** Electrical conductivity and surface resistance of PEDOT:PSS-coated textiles [155, 156, 157].

Textile Fiber	Coating Method	Electrical Properties	Application
Cotton	Dip-coating	Surface resistance: 42.3–47.7 $\Omega$	Flexible electrodes
Polyester	Dip-coating	Conductivity: 30–200 S/m	Sensors, wearable electronics
Nylon/Spandex	Dip-coating	Surface resistance: $\sim 1.7$ $\Omega$ /sq	Stretchable wearable devices
Polyurethane (PU)	Dip-coating	Surface resistance: 35–240 $\Omega$ /sq	Flexible sensors, energy storage
Silk	Dyeing	Conductivity: $\sim 14$ S/cm	Wearable electronics
Knitted cotton fabric	Screen printing	Surface resistance: 24.8 k $\Omega$ /sq	Textile sensors
Polyester (PET)	Spraying	Surface resistance: $< 2$ $\Omega$ /sq	Flexible electrodes, antennas
PEDOT:PSS fibers	Wet spinning	Conductivity: up to $3663 \pm 326$ S/cm	Electronic textiles components

### 2.3 Methods of inserting ICPs into textiles

Various techniques such as immersing, dipping, printing, dyeing, *in situ* polymerization, and coating are employed for integrating PEDOT:PSS into textile substrates. Each method offers unique advantages and can be selected based on the desired properties of the final textile product, including conductivity, flexibility, durability, and pattern precision. The choice of

method depends on the specific application and performance requirements of the smart textile.

One of the simplest and most accessible methods for embedding PEDOT into textiles is immersing and dipping. In this approach, the fabric is immersed in an aqueous PEDOT solution, allowing PEDOT particles to penetrate and diffuse through textile fibers, forming a conductive network. Repeated dipping cycles, often combined with additives such as d-sorbitol, significantly enhance conductivity and durability. For instance, cotton fabrics treated with PEDOT and additives have demonstrated durable conductive coatings that remain effective even after washing [8, 122].

Dyeing is another method for integrating PEDOT:PSS into textiles, utilizing existing industrial infrastructure for scalability. For example, PEDOT:PSS can be applied in dyeing machines at elevated temperatures, such as 90 °C. This method is highly efficient for producing conductive textiles on a large scale while retaining the traditional feel and functionality of fabrics. However, optimization of solution formulations, machine settings, and post-processing is essential to achieve high conductivity and durability [15].

Coating methods are widely used for applying PEDOT:PSS to textiles. These include dip coating, spray coating, and roll-to-roll coating. Dip coating involves immersing the textile in a PEDOT:PSS solution and gradually withdrawing it, allowing a homogeneous coating to form as the solvent evaporates. Spray coating applies a thin, even layer of PEDOT:PSS as a mist, while roll-to-roll coating is particularly suitable for continuous and large-scale production. Coating processes are versatile and can be tailored to add or modify functionalities, such as hydrophobicity or rigidity, depending on the intended application [121, 9, 158].

Spray coating is a technique that evenly applies PEDOT solutions to textiles, forming thin, uniform conductive layers. This method has demonstrated significant improvements in conductivity. For instance, spraying DMSO-doped PEDOT on polyester has been shown to reduce sheet resistance from 76.5  $\Omega/\text{sq}$  to approximately 12.1  $\Omega/\text{sq}$ , enabling effective conductivity without sacrificing the flexibility of the fabric [134,159].

*In situ* polymerization is a robust method that involves polymerizing PEDOT directly on textile fibers. This process is performed by immersing the fabric in a monomer solution and subsequently oxidizing it, resulting in a well-bonded conductive coating. This approach ensures high durability and wash resistance, making it suitable for applications such as wearable electronics. For instance, fibers like Spandex and PET have been successfully treated using this method to achieve long-lasting conductivity [103,159].

Electrospinning and wet spinning are advanced techniques that allow the production of PEDOT fibers, which can then be woven into textile structures. Electrospinning involves using high voltage to create fine fibers, while wet spinning enables the production of continuous conductive fibers. Post-treatment with sulfuric acid has been shown to improve fiber conductivity by reorganizing polymer chains and removing excess PSS. These techniques are particularly valuable for creating stand-alone conductive fibers without the need for a textile substrate [159, 160].

Chemical vapor deposition (CVD) is another method used to integrate PEDOT into textiles. This technique involves vapor-depositing PEDOT onto textile surfaces, creating thin, conformal layers. CVD offers precision and is particularly suited for high-performance textiles where minimal weight and high flexibility are required. However, due to its complexity and cost, CVD is less commonly applied on a large scale [10].

Printing techniques, including screen printing (Figure 6), rotary printing, and inkjet printing, allow the precise deposition of PEDOT:PSS onto textiles. Screen printing is widely used in the textile industry for applying thick, opaque layers, while inkjet printing offers high resolution and precise control over patterning. The digital printing method refers to the use of compact, desktop-sized digital printers designed for laboratory printing directly onto textiles or other materials. This method leverages advanced inkjet printing technology to apply designs or coatings with precision and efficiency. Inkjet printing, for instance, has been successfully employed to deposit DMSO-doped PEDOT on PET fabrics, achieving flexible, low-resistance conductive patterns. These methods are ideal for creating intricate designs and functional areas on smart textiles, making them suitable for applications like wearable sensors [161, 135, 162]. Guo et al. demonstrated a fabrication of all-organic conductive wires by utilizing patterning techniques such as inkjet printing and sponge stencil to apply PEDOT:PSS onto a nonwoven polyethylene terephthalate (PET) providing a wide range of resistance, i.e., tens of kW/sq to less than 2 W/sq that allows the resistance to be tailored to a specific application [10]. Sinha et al. demonstrated the integration of screen-printed PEDOT:PSS electrocardiography (ECG) circuitry on finished textiles and recorded an ECG signal comparable to Ag/AgCl connected to copper wires [163]. Zhao et al. also used screen-printing to produce a PEDOT:PSS and carbon-based disposable electrochemical sensor for sensitive and selective determination of carmine [164]. Tseghai et al. used a flat screen printing to coat a PEDOT:PSS conductive polymer composite on to a knitted cotton fabric and obtained a sheet resistance of 24.8 kW/sq [64]. The conductive textile fabric stays

conductive until its inflection point of stretching. The picture of screen printing is shown in Figure 5.



**Figure 5.** Picture illustration of manual flat-bed screen printing (AI generated, 2025).

Post-treatment with acids, such as sulfuric acid, is often employed to enhance the conductivity of PEDOT:PSS films by removing excess PSS. This step improves polymer alignment and charge transport properties, resulting in higher conductivity for e-textile applications. Acid post-treatment is a critical step for optimizing performance in high-conductivity applications [8].

The uniformity as well depth of dyeing/coating depends on the functional group of the textile. Ding et al. treated cotton, cotton/polyester, polyester and nylon/spandex fabrics by impregnating with PEDOT:PSS and showed that conductivity is higher for fabrics which swell well in water [13]. Ryan et al. dyed up to 40 m long silk yarn with PEDOT:PSS with conductivity of  $\sim 14$  S/cm which was durable to machine washing [103]. The reason to wash durability of PEDOT:PSS on silk is due to the dyeing and the presence of a fluorosurfactant Zonyl FS-300 used during dyeing. When cotton was dyed by the same method, it was too fragile due to hydrolysis of the cellulose by the strong acidic PEDOT:PSS. The same group further demonstrated a continuous dyeing process to produce more than 100 m of silk thread dyed with PEDOT:PSS for a wash and wear resistant functional thread with a conductivity of about 70 S/cm [11]. Ding et al. produced PU fibrous nonwoven and treated it with PEDOT:PSS by dip-coating [2]. The PEDOT:PSS/PU nonwovens showed sheet resistance of 35–240  $\Omega/\square$  (electrical conductivity of 30–200 S/m) by varying the number of dip-coating times. This conductive nonwoven maintained its surface resistance up to 50% strain, promising for wearable application. Tadesse et al. also treated polyamide/lycra elastic fabric with PEDOT:PSS by dipping only once and showed a sheet resistance of  $\sim 1.7$

W/sq [165]. The fabric was stretchable up to  $\sim 650\%$  and maintained reasonable conductivity up to washing cycles. The durability to washing in this case is also due to dyeing where there is some kind of chemical interaction between the fiber and PEDOT:PSS.

These diverse methods for integrating PEDOT:PSS into textiles highlight the adaptability of the material for various applications. Each technique offers unique advantages, whether in scalability, precision, or durability, enabling tailored solutions for the development of innovative smart textiles.

### 3. CONDUCTIVE TEXTILES

#### 3.1 Antistatic textiles

Specialized textiles designed to reduce the build-up of static electricity are known as anti-static textiles (conductivity:  $10^{-5}$ – $10^{10}$  S/cm). Friction or material separation can cause static electricity to accumulate on the surface of materials, especially textiles. This can lead to pain, harm delicate electronic components, and ignite flammable materials. Antistatic fabrics are therefore necessary in a variety of industries where regulating static charge is vital for both functioning and safety. The term "antistatic textile" generally refers to materials that reduce or eliminate static electricity. In a variety of applications, the antistatic textiles reduce and eliminate static electricity, they improve functionality, safety, and comfort [166, 167, 168].

These textiles offer practical solutions for stopping static build up, guaranteeing the security of electronic components, lowering contamination in cleanrooms, and safeguarding personnel in dangerous situations by incorporating conductive fibers and antistatic finishes. Research and innovation efforts are still focused on creating more effective and environmentally friendly antistatic materials as technology develops.

##### 3.1.1 Guidelines and policies

In order to guarantee the efficacy and safety of antistatic fabrics, a number of standards and laws control their manufacturing. Most important standards are IEC 61340 [169], ISO 6356 [170] EN 1149 [171]. According to European Union regulations, antistatic properties are strictly regulated, especially concerning protective clothing. For example, antistatic textiles must comply with the EN 1149 series of standards, which cover various requirements [172, 173, 174]. These standards define how textile products

must be tested and what results must be achieved for the product to be considered antistatic. Therefore, an antistatic textile product, according to the regulation, should be tested in accordance with the relevant standard (e.g., EN 1149) and must meet the requirements to be considered antistatic and suitable for use in the specified areas.

Conductive fibers and antistatic finishing are the two main methods used to impart antistatic properties to textiles. It can be achieved by coating conventional fibers with conductive materials or by blending of non-conductive fibers with conductive additives, such as carbon, stainless steel, or silver. Conductive fibers serve as a pathway to assist in dispersing static charges. Chemical treatments are applied to textile surfaces to prevent static electricity. Frequently, these finishes have polar or ionic groups that draw moisture from the air, increasing the surface conductivity of the fabric and aiding in the dissipation of static charges. Quaternary ammonium compounds and derivatives of polyethylene glycol are common anti-static agents [175, 176].

Antistatic fabrics can regulate and disperse static charge. They are widely used in a variety of industries such as in:

- Electronics manufacturing to avoid ESD, which can harm delicate components, antistatic clothing, gloves, and matting are essential in areas where electronic components are handled.
- Cleanrooms to reduce particulate attraction and contamination, antistatic textiles are utilized in cleanrooms. In sectors like biotechnology, pharmaceuticals, and semiconductor manufacturing, they are indispensable.
- Medical settings to protect patients and healthcare professionals from static accumulation that could harm delicate medical equipment, antistatic textiles are used in medical settings
- Industrial workwear to lessen the possibility of sparks from static electricity causing explosions or fires, employees in industries that handle volatile materials, such the mining and petrochemical sectors, wear anti-static apparel.
- Consumer products carpeting, furniture, and clothing that benefit from antistatic qualities, which also increase comfort and lessen shocks and static cling.

Several test techniques are used to assess the efficacy of antistatic textiles:

- Surface resistivity determines the fabric's resistance to electrical flow on its surface. Better anti-static effectiveness is indicated by lower resistance.

- Charge decay time evaluates the rate at which a static charge can be released from a fabric. More efficient static dissipation is shown by shorter decay durations.
- Series triboelectric testing ascertains whether the fabric has a tendency to absorb or release electrons when it comes into touch with certain substances. This test aids in predicting the fabric's potential for static accumulation.

### 3.2 Electromagnetic interference shielding (EMI) textiles

Electronic equipment and systems are shielded against electromagnetic radiation that may result in malfunctions or data corruption by EMI shielding fabrics. Electromagnetic interference is a serious threat that affects both the normal function of sensitive apparatus and human health. Usually, conductive elements like metal strands or conductive coatings are woven into the fabric to create these textiles. Applications include shielding parts in electronic systems, containers for electrical devices, and protective apparel. Textiles designed to shelter electronic systems and devices from electromagnetic radiation, which can lead to interference, malfunctions, and data corruption, are known as electromagnetic interference (EMI) shielding textiles. The reduction of electromagnetic radiation (EMR) impact is extremely important for the protection of people frequently using electrical and electronic devices which are capable of emitting electromagnetic waves with frequencies that are potential hazards to health.

The most common type of electromagnetic interference occurs in the radio frequency of electromagnetic radiation (EMR) spectrum from  $10^4$  to  $10^{12}$  Hz. This energy can be radiated by computer circuits, radio transmitters, fluorescent lamps, electric motors, over-head power lines, lightning, and many other sources [177]. The most utilized microwave range can be defined as 1–40 GHz, as modern point-to-point, wireless, and satellite communications occupy this range. EMR shielding refers to the reflection, absorption and successive internal reflections (usually neglected) of EMR by a material, which may act as a shield against the penetration of the radiation [178]. Electrically conductive woven or knitted fabrics with particular EMR shielding properties due to their structure and flex ability, offer an opportunity to counter these threats. Furthermore, textile materials can be subjected to a number of dyeing and finishing processes for providing additional functionality such as electrical conductivity and EMR shielding.

The desired property of EMR shielding textile materials is low transmission that means high shielding effectiveness – SE (dB) [179, 180]. According to the requirements of EMR shielding textiles on general use [9], conductive textiles can be classified in five grades from a fair grade to an excellent one:

- (a) fair –  $7 \text{ dB} \geq \text{SE} > 5 \text{ dB}$ ;
- (b) moderate –  $10 \text{ dB} \geq \text{SE} > 7 \text{ dB}$ ;
- (c) good –  $20 \text{ dB} \geq \text{SE} > 10 \text{ dB}$ ;
- (d) very good –  $30 \text{ dB} \geq \text{SE} > 20 \text{ dB}$ ;
- (e) excellent –  $\text{SE} > 30 \text{ dB}$  [9].

For EMR shielding applications, typically SE of at least 20 dB (indicates that 99% of the electromagnetic energy is reflected or absorbed by the material) is needed. SE of 30 dB indicates that 99.9% of the EM energy is reflected or absorbed by the material, with only 0.1% exiting the shielding material [181,182]. For EMR shielding applications, typical shielding effectiveness - SE (dB), of at least 20 dB is needed [183, 184]. Emitting electromagnetic radiation inadvertently might result in EMI. The spectrum's radio frequency range, which runs from  $10^4 \text{ Hz}$  to  $10^{12} \text{ Hz}$  is the most prevalent kind of EMI occurs. Computer circuits, radio transmitters, fluorescent lights, electric motors, overhead power lines, lightning, and many more devices can emit this energy [185]. The microwave range, which is 1 GHz – 40 GHz, is the most commonly used range [186]. This range is occupied by the majority of contemporary point-to-point, wireless, and satellite communications [187]. Because of their structural order and elasticity, conductive knitted or woven materials with specific EMR shielding qualities present a chance to address these threats. Electrical conductivity or reciprocal value of its surface resistivity, is a key parameter of conductive textiles, which often determines the scope for application of a given material.

Applications involving the transport of electrical data, EMI shielding and heating textiles call relatively low resistivity levels less than  $10^3 \Omega/\text{sq}$ . [188, 189], while the materials for electrostatic dissipative protective clothing should have the performance of around  $10^9 \Omega/\text{sq}$ . [190].

There are various techniques to improve the conductivity of textiles:

- introduction of electrically conductive yarns (carbon fibres, metal fibre) [190, 191];
- metallization of fabrics or yarns (voltaic, vacuum vaporisation) [192, 193];



- lamination or coating of conductive layers onto the fabric surface with: metal particles, transparent organic metal oxides, carbon, ICPs [194-198].
- PEDOT:PSS as ICP is often chosen due to its commercial availability, stability, easy processing during film formation on various substrates and high conductivity comparing to other ICPs [199].

The ICPs are an attractive material for EMR shielding. Comparing with some commonly used metallic shielding materials ICPs are not only reflecting but also absorbing EMR in the microwave frequency range [200, 201], combine high conductivity, flexibility, good process ability, relatively low mass, low density and corrosion resistance comparing with metals [202]. The effects on the EMR shielding of the surface of electrostatic properties, the distribution of coating and coating deposit were investigated and compared with textile containing metalized yarns [203]. The studies of textiles coated with conductive polymers showed that they are not highly effective as EMR shielding materials owing to their medium-level conductivity and therefore large skin depth. Combined with the fact that coatings are naturally thin, they cannot act as effective reflective barriers to EMR [204-207]

The shielding efficiency of metalized textile fabrics mainly derives from energy reflection, but not from its absorption [86-88]. The past works concerning EMR shielding with ICPs on textile fabrics are focused mainly on PANI and PPy applications [208-213]. However, increasingly appears publications about application of other ICPs such as PEDOT:PSS, for development of EMR shielding textiles [9]. Conductive polymers may be used as alternatives to some commonly used metallic shielding materials. In contrast to metallic shielding materials, conducting polymers not only reflect but also absorb electromagnetic radiation in the microwave frequency range [210, 212]. ICPs are innovative materials, and are good materials to obtain conductive coating systems for fabrics. Mainly for these purposes such polymers as PANI, PPy and their composites are used [214]. There are some papers in the literature, where it is stated that conductive polymers, have a significant advantage over the shielding textile materials with metalized yarns [195,214], but also occur studies which claim higher EMR shielding effectiveness of metalized fabrics compared with ICPs coatings. That could be explained that in different studies the fabrics with different quantity of conductive additives, types of coatings and structural homogeneity are investigated. The conjugated polymer system, used in this study PEDOT:PSS is today most promising and widely used in research and development of conductive coatings. The literature contains few papers [215, 216] regarding

the electrically conductive textile coatings by the addition of a dispersion of PEDOT:PSS to a coating formulation. In both studies the influence of PEDOT:PSS concentration in coating formulation on the surface resistivity was investigated. In the study [215] also the effect on the surface resistivity of the addition of a conductivity enhancer, such as ethylene glycol, as well as the influence of drying procedure during the coating have been investigated. However, the evaluation of EMR shielding properties of such coated fabrics were not included in either of the papers. Also, in these studies the influence of washing on electrical properties of PEDOT:PSS coated fabrics as not examined. Another interesting way of obtaining the materials with greater capability of absorbing EMR radiation is application of coatings with absorbers of EMR fields, such as carbon, ferrite [217,189,218].

In purpose properly to evaluate the shielding properties of developed fabrics it is very important to select a relevant parameters and methods of their measurement, to obtain the reliable results. A parameter that characterises any shield is the SE and is defined as the ratio of the electromagnetic field strength measured without and with the tested material when it separates the field source and the receptor [195,219,220]. The same relationships are valid in relation to the conjugated field (far field—where the distance from EMR source is higher than  $\lambda/2\pi$ ) or electric component (near field) [220]. There are several methods used for evaluating the SE of flat shielding structures [194,219,221, 222]. There are developed particular methods of electromagnetic shielding investigation for far-field and near-field measurements [223,224]. Currently known methods differ in frequency range, sample dimensions, measurement conditions, the geometry of the test setup. Therefore, it is not possible to compare the results of shielding effectiveness obtained by so diverse test methods. There is also a lack of generally accepted standardised methods for measuring shielding effectiveness [206]. Currently these fabrics are essential in settings including the military, aerospace, medical, and consumer electronics industries where electrical performance and dependability are crucial.

U.S. Patent No. 0258110 discloses a method of making an electrically conductive cotton material by incorporating conductive PEDOT:PSS film into a base cotton substrate by drop casting or dip coating. The amount of PEDOT:PSS used in the fabrication process controls the conductivity and sheet resistance of the conductive cotton material, and can be varied by the number of repeated drop casting or dip coating cycles. In this patent application declares that it can be customized for protection from ESD as well as EMR, however the electromagnetic shielding effectiveness of this conductive cotton material therein was not evaluated and specified. Also, this

patent application's disadvantage is that the values of parameters such as the ICP content, resistance and sheet resistance in a conductive cotton material are dependent on how many times the drop casting or dip coating and drying at 90 - 110° C cycles were performed and as a substrate only fabrics made from cotton are suitable. For EMR shielding textiles the sheet resistance should be around 1000  $\Omega$ /sq. [225,226]. However, EMR shielding effectiveness depends not only on resistance, but also on other parameters. Such parameters as shield thickness, structural parameters of fabric, skin depth of shield used, etc. are affecting the performance of shielding materials. As explained in this method of making conductive cotton, not less than 3 times of drop casting or dip coating and drying cycles are required to fulfil this requirement. After this triple treatment with PEDOT:PSS the sheet resistance value in the network cotton fabric was 148.2621  $\Omega$ /sq. It means that in this patent application disclosed method of making an electrically conductive cotton material using organic conductive polymer such as PEDOT:PSS is time consuming and energy-intensive.

Research on knitted or woven fabrics for camouflaging objects or people involves coatings with conductive polymers (e.g., PEDOT). These radar-shielding textiles use synthetic fiber fabrics and require complex production, including ICP coatings and metal thread insertion. Silver-coated threads, though effective, are costly. The fabrics, intended for clothing like camouflage suits, prioritize durability (resistance to washing, abrasion, etc.) [227].

In patent [228] EMR shielding fabrics made from wool, polyamide, and cotton, as well as blends of these fibers coated with conductive polymer PEDOT:PSS formulations, were developed and characterized. One of the objectives of the work was to create a water-resistant conductive crosslinked PEDOT:PSS layer on the mentioned fabrics to improve the durability of the coated fabrics. The idea of the work was partly based on the electrostatic interaction theory between the negatively charged sulfonate ions of the water-soluble conjugated polyelectrolyte PEDOT:PSS and the protonated amino groups in wool, the amide bonds in polyamide, and the positively charged sites in chemically modified cotton. Another aspect of the work was the creation of a non-dispersible and non-delaminable conductive polymer coating on the textile material through the physical crosslinking of PEDOT:PSS and DVS, which can cause the coagulation of conductive polymer dispersion and reduce its solubility in water without affecting its conductivity. The coating of the fabric with conductive polymer formulations could have been done using successive dyeing in an exhaust process and at least one of the following roll-to-roll processes: air knife coating, knife-over-roll coating, gap coating, flat screen printing, or rotary printing methods.

### 3.2.1 Mechanisms of EMI shielding

Electromagnetic waves can be reflected, absorbed, or conducted by EMI shielding textiles. The materials utilized, the way the textile is made, and the electromagnetic wave frequency all affect how effective EMI shielding is important mechanisms consist of:

- Reflection – electromagnetic waves are reflected by the textile's conductive properties, keeping them from passing through. Because of their excellent conductivity, metals including copper, silver, nickel, and aluminium are frequently employed [229]
- Absorption – electromagnetic waves are absorbed by the cloth and safely evaporate as heat. High magnetic permeability materials, such as ferrites and conductive polymers, are used to accomplish this [230].
- Conduction – electromagnetic waves can be deflected and neutralized by the textile's conductive pathways. Integrating conductive fibers or coatings makes this easier [231].

### 3.2.2 EMI shielding textile application

There are many uses for EMI shielding textiles: Military and aerospace to protect delicate equipment from electromagnetic interference and ensure dependable communication and operation, these materials are employed in tents, enclosures, and protective clothes. Electrically conductive woven or knitted fabrics with particular EMR shielding properties not only offer an opportunity to counter these threats, but also can be applicable to develop radar absorbing materials (RAM), for use in the field of stealth technology to disguise a vehicle or soldier from radar detection [232].

Medical devices to ensure that therapeutic and diagnostic equipment operates accurately, medical devices and implants are shielded from electromagnetic interference using EMI shielding materials.

Consumer electronics to reduce interference and enhance device performance, EMI shielding fabrics are used in the casings of electronic gadgets including laptops, tablets, and smartphones. The International Agency for Research on Cancer (IARC) [233]. Classifies radio frequency electromagnetic fields as group 2B, which includes factors probably carcinogenic to human.

Automotive industry to shielding electronic systems like entertainment and navigation from electromagnetic interference; these textiles are utilized in automobiles to improve their dependability and safety.

Architectural applications to construct shielded rooms or enclosures that shield delicate electronics from outside electromagnetic interference EMI shielding fabrics are incorporated into architectural materials.

The SE, which is measured in decibels (dB), is a measure of how well EMI shielding textiles work. Important testing techniques include of:

- Transmission Line Method gauges the quantity of electromagnetic radiation that passes through fabric.
- Shielding Chamber Test the fabric's functionality in a regulated setting that mimics actual circumstances.
- Surface and Volume Resistivity Test evaluates the fabric's electrical conductivity and to determine how well it shields [234].

A number of standards such as IEEE 299 [235], MIL-STD-285 [236] and ASTM D4935 [237] guarantee the effectiveness and calibre of EMI shielding textiles. Textiles designed to guard electrical systems and gadgets from EMI are crucial. These textiles offer efficient solutions for a variety of applications, from the consumer electronics and automotive industries to the military and medical fields, thanks to the utilization of conductive materials and creative construction techniques. Research and development in this area are being driven by the growing need for effective and dependable EMI shielding textiles as electronic gadgets become more and more integrated into daily life.

### 3.3 Electroconductive additives and application for Smart/E-Textiles

Electrical conductivity is a crucial performance attribute for e-textiles, as it enables them to collect, store, and send signals and data to fulfil their primary purposes. Because they prevent the passage of electric charges, textile fibers and polymers are naturally insulators [238,239]. However, fabrics are altered to provide electrical conductivity to have a wider range of applications beyond clothing. Conductive textile materials are considered smart or intelligent by standards [240], but not Ultra-Smart, because they cannot respond to their surroundings. Nevertheless, they enable a wide range of smart textile applications, particularly those that monitor bodily functions and include sensors, actuators, communication, heating fabrics, and static electricity-free clothing [241-243]. Conventional textiles without conductive materials (e.g., natural or synthetic materials such as cotton, wool, polyester) have very high resistance. The electrical resistance of this textiles can be from  $10^9$  to  $10^{15} \Omega/\text{cm}^2$ . This leads to unappreciated static cling and ESD. To avoid these features, the conductivity of textiles is increased by adding metals and carbon compounds either as particles, fibres or yarns [244,245].

### 3.3.1 Smart textiles past, present and future

The interest in electro-active textiles took on about fifteen years ago with the dawn of smart textiles. Initially, smart textiles were primarily design projects, achieved by simple addition of electrical components to textile products. The bulkiness of the electrical components and their incompatibility with textile use (e.g., washability) soon evolved the research towards the integration of smart functions to the textiles themselves [158]. Electronic textiles, sometimes referred to as smart textiles or E-textiles, are textiles that have sensors, actuators, and microcontrollers built in them. These textiles offer interactive features beyond ordinary materials by sensing, responding, and adjusting to environmental stimuli. Without textiles, which we need for protection, clothing, and decoration, our lives would be incomplete. These days, phrases like "wearable computing," "intelligent textile," and "smart textile" are frequently employed in casual conversations [246-251].

The research and innovation priorities of Europe's textile and clothing industry for the future were presented in a European Textile technology Platform (ETP) Document "Ready to transform" [252]. Herein, four strategic innovation themes such as Smart, high-performance materials; digitized textile materials; durable, circular and bio-based materials and processes; Safe, low footprint products and processes were singled out as particularly impactful for the successful and rapid transformation of the European textile ecosystem. In the field of Smart, high-performance materials, which includes e-textiles for smart wearable's an attention was focused on effective basic e-textile materials and components such as sensors and electronic circuits; on flexible substrates by 3D printing as well as to the reliability, durability, and safety of e-textiles such as integrated sensors/markers to measure and signal the lifetime or functionality of a smart textile function. Also, e-fabric solutions are becoming relevant, for instance, in energy harvesting and thermo-electricity, wireless key board fabrics, sensors for direction and speed of motion of a person, biosensors in healthcare as well as in fashion fabrics.

Today the textile industry is at the forefront of high-tech material using complex material property and process parameter simulation, advanced mechatronics and robotics, machine vision, self-adjusting or self-learning technology to enable efficient one-step or integrated production of complex, multi-layered, 3D shaped or multi-material/hybrid textile and composite structures. The research and innovation priorities of Europe's textile and clothing industry for the future were presented in a European Textile technology Platform (ETP) [252]. Herein, four strategic innovation themes such as smart, high-performance materials; digitized textile materials; durable,

circular and bio-based materials and processes; safe, low footprint products and processes were singled out as particularly impactful for the successful and rapid transformation of the European textile ecosystem. In the field of smart, high-performance materials, which includes e-textiles for smart wearable's an attention was focused on effective basic e-textile materials and components such as sensors and electronic circuits; on flexible substrates by 3D printing as well as to the reliability, durability, and safety of e-textiles such as integrated sensors/markers to measure and signal the lifetime or functionality of a smart textile function. Also, e-fabric solutions are becoming relevant, for instance, in energy harvesting and thermo-electricity, wireless key board fabrics, sensors for direction and speed of motion of a person, biosensors in healthcare as well as in fashion fabrics [253]. Various conductive materials, wires, and batteries were employed to enable these devices to function as "Wearable Computers" [254,255]. Making as many components as feasible out of textile materials presents a challenge for academics from the perspective of textiles. Thus, the development of electroconductive textiles is required. This can be accomplished in a number of methods, such as through the integration of conductive yarns or fibers, the application of conductive coatings, or the use of conductive inks [161,256-258].

However, as technology has advanced and needs have changed in recent years, have evolved, and the need for intelligent textiles and materials has grown worldwide. Functional textiles provide a basic purpose, but they also have built-in features that satisfy the needs of the final user. They can therefore be managed and changed. They can therefore be managed and changed based on the purpose for which they are intended. "Smart textiles" are fabrics that have the ability to determine the surroundings or stimuli, including mechanical, thermal, chemical, and electrical or magnetic. Intelligent and smart textiles have a wide range of applications, including from easy to extremely difficult applications, such as energy harvesting, sportswear, cars, military and defences, medical and healthcare, and protection. Thus, intelligent and next-generation textiles, or intelligent textiles, are regarded as such [169]. Technological and material breakthroughs in fibers, fabrics, chemicals and additives (polymer, functional nanomaterials, finishing chemicals, adhesives, etc.), and manufacturing processes are major forces behind the developments in the field of functional and smart textiles procedures. Textiles that are intelligent or smart are created by branch collaboration of technology and science, including electronics, design, nanotechnology, and material science as well as computer science [169].

### 3.3.1.1 Definition of smart textiles

Smart textiles, also known as intelligent textiles, are materials that have been engineered to have additional functionalities beyond traditional textiles. These functionalities can include the ability to sense environmental changes, respond to stimuli, and even communicate with other devices. The ISO/TR 23383:2020 standard [259] provides a clear and concise definition of smart textiles, helping to demystify this complex and exciting field. The standard offers a comprehensive categorization of smart textiles, breaking them down into various types based on their functionalities and applications. This categorization is crucial for manufacturers and designers as it helps in identifying the right type of smart textile for specific applications. Whether it's for healthcare, sports, fashion, or industrial use, the standard provides a roadmap for selecting and utilizing smart textiles effectively. These mechanical, thermal, or chemical input stimuli (such as variations in pH, electrical, magnetic, pressure, or temperature) can alter the output response's colour, shape, flow property, conductivity, and other characteristics. Stated differently, all functional textiles are smart, but not all smart textiles are functional. Smart textiles are made to provide the user with additional value, whether for performance, enjoyment, or safety. Applying definitions on textiles, a passive smart textile is thus a sensor, an active smart textile an actuator and a very smart textile is one that can adapt its response to the environment in a nonlinear fashion. Only the last definition corresponds to Kirstein's definition of a truly smart textile [24]. In some circumstances, the term smart textiles are used in a much more general sense; including advanced, functional and technical textiles [25,158] (Table 9).

**Table 9.** Applications of smart textiles [259]:

Sector	Applications
Healthcare	Wearable devices for monitoring vital signs, tracking activity, and administering medication.
Sports and Fitness	Real-time performance feedback for optimizing training and preventing injuries.
Fashion	Garments that change color, light up, or adjust to body temperature.
Industrial	Protective clothing, smart packaging, and safety enhancements.



### 3.3.2 Passive smart textiles

The earliest type of smart textiles is called passive ones, they are only able to detect inputs or ambient circumstances. Optical fibers, conductive materials, insulators, antimicrobial, self-cleaning, and waterproof, breathable textiles are a few examples. In summary, textiles loaded with silver nanoparticles on their surface have a strong antibacterial effect, and textiles loaded with titanium oxide ( $\text{TiO}_2$ ) have a self-cleaning feature. However, both types of textiles fall under the category of passive smart textiles because the textile is smart but not responsive due to the antibacterial effect of the silver and the photocatalytic property of the  $\text{TiO}_2$  [260-262].

### 3.3.3 Active smart textiles

Unlike passive smart textiles, active smart textiles can carry out interactive automatically and on their own in response to a given demand. In this setting, interactive are usually associated with receiving stimuli and providing feedback [26]. For instance, a crosslinked gelatine electrospun mat loaded with the antibiotic drug chlorhexidine functions as an active smart textile. When the mat expands in volume, the drug is released, killing both gram-positive (*S. epidermidis*) and gram-negative (*E. coli*) bacteria in response to pH changes in the environment caused by the presence of bacteria. In this case, the material's volume expands as the feedback response to pH changes, which act as input stimuli [263,264].

### 3.3.4 Ultra-smart or intelligent textiles

Ultra-Smart textiles, or third-generation smart textiles, are able to sense, respond, and adjust to stimuli and the environment around them [184]. They are composed of a unit that is fundamentally comparable to the brain in terms of cognition, reasoning, as well as the ability to make decisions. Nowadays, the creation of intelligent textiles is a reality, thanks to the effective fusion of traditional apparel technologies with several fields of science and technology, including communication, sensor and actuator technologies, artificial intelligence, biology, structural mechanics, material science, and advanced technology for processing.

The construction of smart/E-textiles involves the integration of various components. Some of them are:

Sensors – a variety of physical, chemical, or biological events can be detected by embedded sensors. Temperature sensors, pressure sensors,

moisture sensors, and biosensors that track vital indicators like respiration and heart rate are examples of common types [89].

Actuators – these parts give the textile the ability to react to detected stimuli by acting. Vibration motors, color-changing fibers, and heating components are a few examples [265].

Microcontrollers – these tiny computers interpret data from sensors and manage actuators. They enable complex capabilities and communication with external devices, acting as the smart textile's brain [266].

Conductive threads and fabrics – electrical pathways are made within textiles by using conductive materials, including carbon or silver-coated fibers, to facilitate the flow of power and data [267].

Power sources – to function, smart textiles need a power source, which can come from external power supply, energy-harvesting devices, or embedded batteries [89].

These advancements reflect the multidisciplinary nature of smart textile development and highlight the potential of ultra-smart textiles to revolutionize wearable technologies and everyday life.

### 3.3.5 Applications and testing methods for smart textile

Smart textiles and e-textiles find applications across diverse fields, demonstrating their versatility and innovative potential [247-249, 268]. Some of them can be mentioned:

Healthcare – patients' vital signs are regularly monitored by smart textiles. Healthcare professionals can receive real-time data from wearable health monitors that track vital signs like heart rate, body temperature, and breathing, alerting them to any irregularities.

Sports and Fitness – to track performance indicators like heart rate, muscular activity, and movement patterns, athletes wear smart apparel. This information aids in injury prevention and training regimen optimization.

Fashion – smart fabrics are used by designers to create clothing that can light up, change color or pattern, or react to the surroundings. These fabrics offer distinctive interactive experiences and improve visual attractiveness.

Military – through embedded communication systems, smart textiles are utilized in military gear and uniforms to monitor soldiers' physiological status, regulate body temperature, and improve situational awareness.

Safety and protection – during emergency operations, firefighters and other first responders wear smart textiles that monitor environmental parameters like temperature and dangerous gas levels, enhancing safety and situational awareness.

Consumer electronics – touch-sensitive controls and interactive features are made possible by the integration of e-textiles into commonplace products like headphones, gloves, and shoes.

The performance and reliability of smart/E-textiles are evaluated through various testing methods [265]. The following testing methods can be applied:

- Testing for durability – this method is used to determine how well a material can resist frequent washings, stretching, and use without losing its usefulness.
- Conductivity, resistance, and signal integrity of integrated electronic components are measured during electrical performance testing.
- Biocompatibility testing is applying to verify that the substances utilized, particularly for wearable health monitoring, are safe for extended skin contact.

### 3.3.6 Conductive textiles testing methods

Evaluating the conductivity of textiles is essential for ensuring their performance in various applications, from smart textiles [249] and antistatic materials [22] to EMI shielding fabrics [9]. Multiple measurement techniques, including four-point probe, surface and volume resistance, shielding effectiveness [9], and charge decay time, provide comprehensive insights into the electrical properties [133] of textiles (Table 10). Understanding and controlling factors that influence conductivity, along with adhering to standardized testing protocols, are critical for the development and optimization of conductive textiles in advanced applications.

**Table 10.** Methods of measuring textile conductivity

Method	Principle	Application	Advantages	Limitations
<b>Four-point probe method</b>	Uses four equally spaced probes; current is passed through outer probes, and voltage drop is measured across inner probes.	Measures fabric's sheet resistance, converted to conductivity.	High accuracy; reduced contact resistance errors.	Requires flat, uniform fabric surface for optimal results.

<b>Surface resistance measurement</b>	Measures resistance across the textile surface by placing electrodes at a fixed distance and applying voltage.	Common for evaluating anti-static properties.	Simple and quick method; suitable for many textiles.	Provides only surface resistance, not through-thickness conductivity .
<b>Volume resistance measurement</b>	Measures resistance through fabric thickness by placing electrodes on opposite sides and applying voltage.	Important for thorough conductivity applications like EMI shielding.	Gives complete picture of fabric's bulk conductivity.	More complex setup compared to surface resistance measurement.
<b>Electromagnetic shielding effectiveness (SE)</b>	Measures textile's ability to block/attenuate electromagnetic signals by comparing signal strength with and without textile barrier.	Crucial for EMI shielding textiles.	Direct assessment of shielding in real-world conditions.	Requires specialized equipment and controlled testing environments.
<b>Charge decay time</b>	Measures time for static charge to dissipate to a threshold after being applied to fabric.	Used for anti-static textiles to ensure quick neutralization of static charges.	Simple setup; relevant for static dissipation performance.	Less relevant for continuous conductive applications.

The conductivity of textile materials is influenced by various factors [9, 268, 250, 21]. One of the key factors is material composition, where the type and quantity of conductive elements, such as metal or carbon fibers and conductive polymers, play a significant role in determining the level of conductivity. The structure of the fabric also has a notable impact, as the weave, knit, or non-woven design affects the distribution and connectivity of

conductive pathways. Additionally, environmental conditions, including temperature, humidity, and mechanical stress, can alter the conductive properties of textiles. Furthermore, the processes and treatments applied to the material, such as coatings, finishes, and other modifications, can either enhance or diminish its conductivity. Together, these factors interact to shape the overall conductive behavior of textile materials.

The electrically conductive wool textile developed in this work exhibits a surface resistance of  $1 \times 10^3 \Omega/\text{sq}$ , making it suitable for various applications. Potential application areas include antistatic surfaces and garments ( $10^5$ – $10^{12} \Omega/\text{sq}$ ), where controlled dissipation of static charge is required (ISO 18080-4:2018) [269]. For instance, DuPont™ Tyvek® antistatic coveralls, made from a material with a surface resistance of approximately  $10^9 \Omega/\text{sq}$ , effectively prevent the accumulation of static charge, making them suitable for electrostatic discharge (ESD)-sensitive environments. Similarly, the wool-based conductive textile developed in this study could be applied to wearable antistatic garments, ensuring both conductivity and comfort.

Additionally, the material falls within the resistance range necessary for sensors and smart textiles ( $10^2$ – $10^4 \Omega/\text{sq}$ ), depending on the sensor type and sensitivity [89,267]. An example of such an application is Hexoskin smart shirts, which integrate sensors into textiles using conductive materials with a resistance of approximately  $10^3 \Omega/\text{sq}$ , allowing the monitoring of physiological parameters such as heart rate and respiration. The wool textile coated with PEDOT:PSS, possessing similar conductivity, has the potential for wearable sensor integration, particularly for flexible biosensing applications. However, the durability of PEDOT:PSS coatings under mechanical stress and washing remains a challenge.

Furthermore, the textile's conductivity makes it applicable in certain flexible electronic components ( $10$ – $100 \Omega/\text{sq}$ ), where electrical functionality must be maintained in deformable structures [271,272]. While PEDOT:PSS-coated wool is unlikely to achieve high electromagnetic interference (EMI) shielding ( $1$ – $100 \Omega/\text{sq}$ ) comparable to metallic coatings, it may still provide partial shielding for low-intensity applications [273]. These characteristics highlight the potential of wool-based conductive textiles for integration into wearable electronics, smart textiles, and functional garments, although improvements in coating stability and conductivity enhancement are necessary for broader applicability.

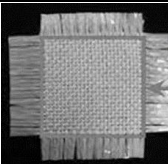
## 4. EXPERIMENTAL PART

### 4.1 Materials

#### 4.1.1 Textile materials

In this research, worsted wool fabric was used. The pure wool fabric was purchased from JSC “Drobė” (Kaunas, Lithuania). Structural parameters of wool fabric are presented in Table 11.

**Table 11.** Technical parameters of wool fabric.

Content of yarn, %	Mass per unit area, $\text{g/m}^2$	Type of yarn: linear density, tex		Weave
		Warp	Weft	Plane wave (1:1)
Wool, 100	$123 \pm 3$	$31.0 \times 2$ S twist	$31.0 \times 1$ Z twist	

#### 4.1.2 Conductive polymer and auxiliaries

Wool fabric has been coated with PEDOT:PSS commercial products Clevios F ET and Clevios S V3 (Heraeus Holding GmbH, Hanau, Germany, Table 12). These commercial PEDOT:PSS products were selected for their electroconductivity characteristics and suitable viscosity for different conductive textile processing such as dyeing, flat-bed screen printing and digital printing methods.

**Table 12.** Main parameters of Clevios F ET and Clevios S V3.

Characteristics	Clevios F ET	Clevios S V3
Chemical composition, %	Ethane-1,2-diol $\geq 5$ – $<10$ Poly(3,4-ethylenedioxythiophene) polystyrene sulfonate (PEDOT: PSS) $\geq 1$ – $<3$	2,2'-ossidiethanol $\geq 10$ – $<20$ Poly(3,4-ethylenedioxythiophene) polystyrene sulfonate (PEDOT: PSS) $\geq 1$ – $<3$
The weight ratio of PEDOT to PSS	1:2.5	1:2.5
Conductivity (dried layer)	200 S/cm	-
Resistivity (test print)	-	700 ohm/sq
Viscosity at (20 °C)	$0.2 \div 0.8$ dPa·s	$15 \div 60$ dPa·s

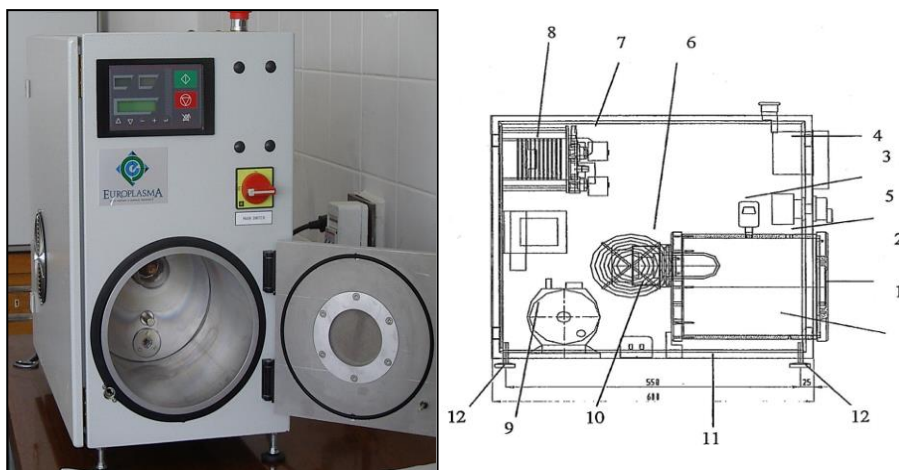
To increase rubbing and wash resistance without changing electrical conductivity [37] some of the samples were coated with PEDOT:PSS and melamine resins with low formaldehyde content (< 1,26%) commercially available product named Tubicoat fixing agent HT (CHT Germany GmbH, Tübingen) mixture.

## 4. 2 Methodology

The methodology for this study involves several key steps to investigate the electroconductivity, hydrophilicity and wearing resistance properties of low pressure plasma treated and PEDOT:PSS coated wool fabric.

### 4.2.1 Sample low pressure plasma treatment

In order to improve the hydrophilicity, adhesion and dyability of the wool fabric with PEDOT:PSS the surface of the textile material samples was activated by N<sub>2</sub> low pressure plasma before dyeing using the Junior plasma system 004/123 (Europlasma, Oudenaarde, Belgium, Figure 6 a). For this purpose, wool fabric samples of 13 cm x 20 cm were prepared, mounted on a vertical aluminum frame and placed in the process chamber 1 of the plasma unit (Ø=200 mm) upstream of the plasma generating source, magnetron 6 (Figure 6 b). Plasma treatment parameters are presented in Table 13.



**Figure 6.** Junior Plasma System 004/123 (a) and its schema (b), 1 - process chamber, 2 - door, 3 - vacuum gauge, 4 - process control unit, 5 - gas inlet, 6 - magnetron, 7 - gas distribution panel, 8 - electrical panel, 9 - pump, 10 - vacuum valve, 11 - insert, 12 - adjustable stand.

**Table 13.** Processes parameters of low pressure plasma treatment.

Processes	Parameters
Gases	N <sub>2</sub>
Gas flow	10 cm <sup>3</sup> /min
Discharge power	200 W
Pressure	0,4 mbar
Processing time	120 s

#### 4.2.2 Dyeing with Clevios F ET

It is known that PEDOT:PSS can be assigned to “conductive acid dyes” [11]. In this work the untreated and N<sub>2</sub> plasma-treated 7 cm × 7 cm samples of wool fabric were dyed on a laboratory dyeing device, Ahiba Nuance ECO-B (Datacolor, Cheung Sha Wan, Hong Kong, Figure 7ab), using an immersion coating method (dyeing in exhaust) at 90 °C for 30 min in a bath based on water dispersion Clevios F ET, according to the following recipe and process parameters (Table 14).



**Figure 7.** Wool fabric sample immersed into PEDOT:PSS water dispersion (a), views of cups in laboratory dyeing device, Ahiba Nuance ECO (b).



**Table 14.** Technological parameters of wool fabric dyeing with Clevios F ET.

Process	Auxiliaries	Parameters
Dyeing in exhaust	Clevios F ET, v/v %	50
	Deionized water, v/v %	50
	pH of solution	2.2
	Liquor ratio	1:20
	Temperature, °C	90
	Time, min	30
	Rotation speed of dyeing containers, rpm	20
	Temperature rise rate, °C/min	2

#### 4.2.3 Flatbed screen printing with Clevios S V3

The Clevios F ET dyed and undyed fabric samples were fully coated using manually flat-bed screen-printing method (Figure 8a) with another PEDOT:PSS product Clevios S V3 (Table 12). The Clevios F ET, due to its low viscosity, is used for dyeing, while the Clevios S V3, with its higher viscosity, is used for the manually flat bed screen printing method, viscosities are written in Table 12. To enhance the resistance of samples to washing and mechanical treatment, some of them were also coated with a mixture of Clevios S V3 and 3 wt % Tubicoat fixing agent HT mixture. For this purpose, 3 g of Tubicoat fixing agent HT was added to 97 g of Clevios S V3 and mixed using a mechanical stirrer at 500 rpm for 2 minutes at room temperature.

At the end, all fabric samples were dried in a laboratory drying – thermosetting machine TFOS IM 350 (Roaches International, Batley, UK) at 100 °C for 3-5 min (Figure 8b).



(a)



(b)

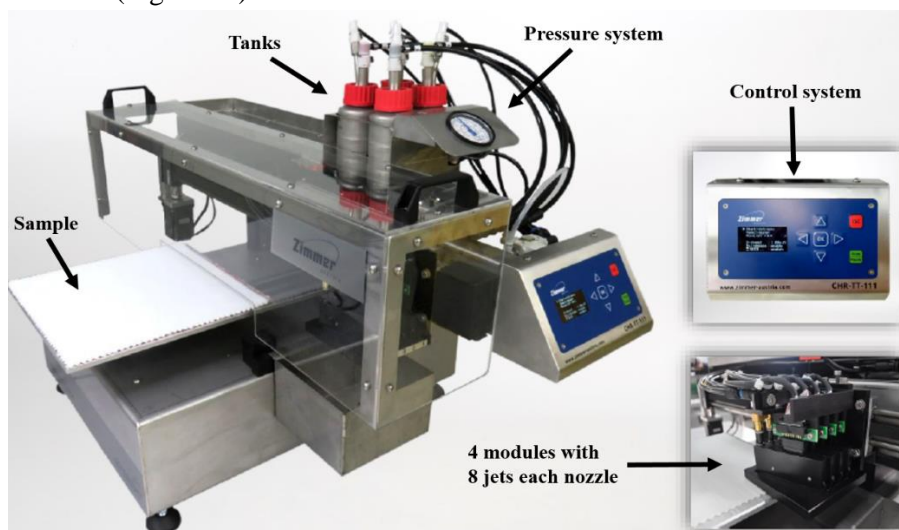
**Figure 8.** Flatbed screen printer (a), Laboratory drying-thermosetting machine - TFO S IM 350 (b).

#### 4.2.4 Digital printing with Clevios F ET and Clevios S V3

In this research, two PEDOT:PSS aqueous dispersions, Clevios F ET and Clevios S V3, were also used to fully coat the surface of wool fabric sample (15 cm x 15 cm) using a laboratory ChromoJET. TableTop (ZIMMER GmbH, Kufstein, Austria) digital printer (Figure 9). For this purpose 100 g of each of the four conductive polymer compositions presented below were prepared for digital printing of samples:

- (a) Clevios F ET;
- (b) Clevios S V3 mixed with water at a 7:3 ratio;
- (c) Clevios F ET followed by Clevios S V3 (7:3 H<sub>2</sub>O ratio);
- (d) Clevios F ET, followed by Clevios S V3 (7:3 H<sub>2</sub>O ratio) mixed with 3% Tubicoat fixing agent HT to improved washing and mechanical resistance.

The technological parameters of wool fabric printing using the ChromoJET TableTop printer are presented in Table 15. Printed samples were dried at 100 °C for 3–5 minutes using a laboratory drying–thermosetting machine (Figure 8b).



**Figure 9.** ChromoJET TableTop printer scheme.

**Table 15.** Technological parameters of wool fabric printing using the ChromoJET TableTop printer.

Processes	Parameters
Sample size	15 cm x 15 cm
Nozzle diameter	200 µm
Head speed	1 m/s

Pressure	2 bar
Viscosity	6 – 10 Pa·s
Resolution	63.5 dpi
Tank volume	300 ml
Clevios product	100 ml

### 4.3 Materials characterization

#### 4.3.1 Aqueous liquid repellence water/alcohol solution resistance test

The aqueous liquid repellency of the textile samples was evaluated according to ISO 23232:2009 “Textiles — Aqueous Liquid Repellency — Water/Alcohol Solution Resistance Test” [278]. This method involves applying a series of standardised water/alcohol solutions with varying surface tensions to the fabric surface to determine the highest-numbered solution that does not wet the fabric. The resulting grade reflects the material’s resistance to staining from aqueous liquids. A higher repellency grade indicates better hydrophobic performance, whereas lower grades signify increased wettability and hydrophilicity. The test was conducted both before and after plasma treatment to assess the effect of surface modification on liquid repellency.

#### 4.3.2 SEM analysis

The surface and cross section morphology of the dyed/coated wool fabric was investigated with scanning electron microscopy (SEM), Quanta 200 FEG (FEI, Eindhoven, The Netherlands), at 20 keV (low vacuum): electron beam heating voltage – 20.00 kV; beam spot – 5.0; magnification –500×, 5000×, 2000×, 6500× and 120,000×; work distance – 6.0 mm; low vacuum pressure – 80 Pa and large-field detector (LFD).

DTNW Scanning electron microscopy S-3400 N II SEM was used to analyses the surface and cross section morphology of samples coated with “Table Top” – digital printing method. SEM images were taken using an S-3400 N II SEM (Hitachi HighTech Europe GmbH, Mannheim, Germany) operating at an accelerating voltage of 10 kV. Prior to imaging, the surface of the sample was sputtered with gold for 4 min. in vacuum using a Quorum Emitech K500X sputter coater (Ashford, Kent, USA).

#### 4.3.3 Fourier transform infrared spectroscopy

Chemical bonding investigations of untreated and N<sub>2</sub> low plasma-treated wool samples dyed with PEDOT:PSS aqueous dispersion, Clevios F ET and coated with Clevios S V3, were performed using FTIR-ATR spectroscopy. The infrared (IR) spectra of tested samples were measured by means of FTIR Perkin Elmer Frontier (Waltham, Massachusetts, USA) spectrometer in ATR reflection mode (spectrum range: 600-4000 cm<sup>-1</sup>, resolution: 1 cm<sup>-1</sup>).

Of samples coated with “Table Top” – Printer method was used Fourier transform infrared spectroscopy (FT-IR) to analyze the functionalized wool surfaces before and after coating. The spectra were obtained using an IR Prestige-21 (Shimadzu Deutschland GmbH, Duisburg, Germany) at the attenuated total reflection (ATR) mode in the range of 550-4000 cm<sup>-1</sup> with an average of 40 scans and a resolution of 16 cm<sup>-1</sup>. Infrared spectroscopic analyses were carried out using an FT infrared spectrometer IR Prestige 21 from Shimadzu with an ATR from LOT-Quantum Design GmbH. FTIR-ATR spectroscopy was used to identify the chemical bonds present in the sample and to determine the chemical composition of the investigated sample.

#### 4.3.4 X-Ray photoelectron spectroscopy

XPS characterization of different wool samples was carried out using a Kratos AXIS Supra spectrometer (Manchester, UK) with monochromatic Al K $\alpha$  (1486.6 eV) X-ray radiation powered at 225 W. The base pressure in the analysis chamber was less than  $1 \times 10^{-8}$  mbar and a low electron flood gun was used as charge neutralizer. The survey spectra for each piece of fabric were recorded at a pass energy of 160 eV with a 1 eV energy step and high-resolution spectra (pass energy –10 eV, in 0.1 eV steps) over individual element peaks. The binding energy scale was calibrated by setting the adventitious carbon peak at 284.8 eV. XPS data was converted to VAMAS format and calculated with Advantage software (Thermo Scientific, East Grinstead, UK).

#### 4.3.5 Vis-NIR spectroscopy

The VIS-NIR absorption spectrum of PEDOT provides key insights into its electronic structure and charge transport properties. The broad absorption from the visible to the NIR region is indicative of the presence of polaron and bipolaron states, which are essential for its functionality in electronic and optoelectronic devices [274]. The absorption of coated samples with various

PEDOT:PSS compositions onto wool fabric by digital printing method was determined by UV-vis/NIR Perkin Elmer Lambda 950 spectrophotometer (Waltham, Massachusetts, USA) in the wavelength range of 600-1200 nm.

#### 4.3.6 Current sensing atomic force microscopy (CS-AFM) technique

Current sensing atomic force microscopy (CS-AFM) technique (Signatone, Gilroy, USA) for measuring the in-plane current. In spite of the wealth of scientist papers on the production and functionalization of CNFs and their electrical properties, there is a certain lack of understanding of the relationship between structure and electrical properties. Thus, current sensing atomic force microscopy (CS-AFM) as a new technique was proven to be effective for the characterization of electrical properties at the nanoscale. Generally, AFM senses the surface features by employing a microfabricated cantilever with a sharp tip. In the case of CS-AFM, a conductive cantilever is used and an electrode is positioned at a fixed point of the sample. The conductive probe is scanned over a surface and the current resulting from a voltage applied between the probe and the electrode is recorded. The possibility of decoupling the force feedback, which controls the tip height, from the current feedback allows the analysis of both surface topography and electrical conductivity simultaneously. Hence, relationships between the structural features and the electrical properties of the sample can be derived.

#### 4.3.7 Cyclic voltammetry (CV) electrochemical technique

For the electrochemical measurements, a TSC battery standard cell combination with a Microcell HC setup used for electrochemical measurements, is manufactured by rhd instruments GmbH & Co. KG, a company based in Darmstadt, Germany (Figure 10). As current collectors, two planar stainless steel disc electrodes ( $\varnothing$  8 mm) press-fitted into a PEEK sleeve were used. For calculating the cell constant, the area of the stainless-steel electrodes and the separator thickness were considered, resulting in a value of  $0.0043 \text{ cm}^{-1}$ . The contact pressure applied onto electrolyte-soaked separator (we used polypropylene as separator) stack inside of the TSC battery cell was adjusted to approximately 100 kPa using a gold-plated spring with a spring constant of  $2.3 \text{ N mm}^{-1}$  (was trying with our samples from 0 till  $4.6 \text{ N mm}^{-1}$ ). In our research at this contact pressure, no significant compression of the separator was found. In our research were used samples with loading the cell with one specimen of the electrolyte-filled PVA-KOH separator PP and

connecting it to the Microcell HC cell stand. We used Gamry interface 1010e is a value oriented, general purpose posttension for low current electrochemistry. Cyclic voltammograms were obtained at room temperature in the range -1 – 0 V at different scan rates (5, 10, 50 and 100 mV·s<sup>-1</sup>).

The specific capacitance was calculated from the CV curve using the following equations:

$$C = \frac{\int i v d v}{2 \mu m \Delta V} \quad (1)$$

C – specific capacitance (F/g)

i – Current (A)

v – Voltage (V)

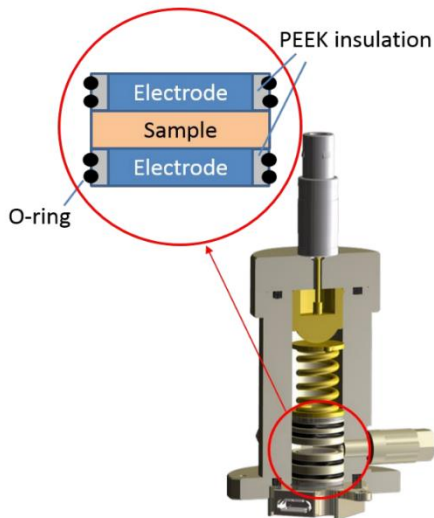
dv – differential voltage change

μ – scan rate (V/s)

m – mass of active materials (g)

ΔV – potential window of discharge.

This equation is used to calculate specific capacitance from cyclic voltammetry (CV) data. The integral  $\int i v d v$  represents the charge storage area under the CV curve, indicating the amount of charge stored within a given voltage range. Dividing by  $2 \mu m \Delta V$  gives the specific capacitance.



**Figure 10.** Schematic drawing of the measuring cell TSC battery standard. The separator foils filled with electrolyte were placed between the upper and lower electrode. TSC Battery - rhd instruments (rhd-instruments.de)

It was found how these methods applied it to textiles with conductive polymer. Both three electrode measurements can be performed by inserting a

micro reference electrode or a custom lithium reference from the side (Figure 10). We used polyvinyl alcohol (PVA) polymer powder dispersed in hot 80°C distilled water (3 wt %). The polymer-based porous alkaline gel electrolyte was prepared using the PVA-KOH system according to the ratio of 60:40 wt%; the appropriate proportion of the gel electrolyte was found to have a maximum ionic-conductivity. Briefly, the polyvinyl alcohol (PVA) polymer powder was dispersed in hot distilled water (3 wt %) in a glass beaker with slow continuous stirring (300 RPM) using a magnetic stirrer cum hot plate at 80°C. The potassium hydroxide (KOH) pellets (2g) were gradually added into the beaker containing the solution until the homogeneous colloidal gel is formed [279]. We put it in a battery on the separator, adjusting how to use it ourselves, because others soaked it overnight, and after overnight the wool fell apart.

#### 4.3.8 Colour fastness to washing and rubbing

Each untreated and N<sub>2</sub> low-pressure plasma-treated wool sample (each sample had 5 elementary samples) was washed and dried after coating with various Clevios products. The fabrics were washed in Scourotester Computex (Computex, Budapest, Hungary), according to the LST EN ISO 105-C06 [283] standard, method A1M: washing temperature 40 °C, duration 45 min, using 4 g/L of ECE reference detergent with phosphates without optical brightener. In order to demonstrate the resistance of the electrical and color properties of wool with a PEDOT PSS coating to repeated washing, at least 5 washing cycles were performed. Washed wool fabrics were line dried in ambient atmosphere.

A testing instrument Stainingtester FD-17/A (Komputekst, Budapest, Hungary) with rubbing finger and using a reciprocating straight rubbing action was used to determine the color fastness against dry rubbing. The specimen and rubbing cloth were subjected to conditioning in standard atmosphere of  $(20 \pm 2) ^\circ\text{C}$  and  $(65 \pm 4) \%$  for at least 4 h prior to testing [284]. Each specimen (each sample had 5 elementary samples) was secured to the testing device's base such that its long axis would align with the device's track. To minimize specimen movement, a space was established between the baseplate of the test fixture and the specimen and between the baseboard of the testing device and the specimen. When laid flat on the tip of the finger, the weaving of a conditioned rubbing cloth is parallel to the direction of finger rubbing. On the dry specimen, a track measuring  $10^4 \pm 3$  mm in length was rubbed 20 times in a straight line, 10 times forward and 10 times back, at a rate of one cycle per second, with a downward force of  $9 \pm 0.2$  N [285].

Following testing, the staining of the rubbing cloth was evaluated using a grey scale for assessing staining in proper lighting [286]. The color change of dyed and coated samples after washing (each sample had 5 elementary samples) was evaluated using the grey scale for assessing change in color [287]. Pairs of matte-finish gray color chips make up the basic scale, which has five stages. An enhanced scale also has four half-steps, making a total of 9 steps. The standard offers a precise colorimetric scale definition that can be used to compare samples that may have altered with newly prepared working referents [287]. Evaluations were performed in a Spectra LUX-II™ color matching cabinet. The Spectra LUX-II™ color matching cabinet is manufactured by X-Rite, Incorporated, a company headquartered in Grand Rapids, Michigan, USA. Each sample had 5 elementary samples, the results are reported with a  $\pm 0.5$  point accuracy, based on the average of the elementary samples.

Samples color parameters were determined: L\* - lightness, C\* - chroma, h – hue, a\* - redness-greenness and b\* - yellowness-blueness [288]. The average of 4 readings per specimen was recorded while measuring color parameters according the standard method LST EN ISO 105-J01 [289]. K/S value (Kubelka-Munk function) (Formula 2), the parameter that is typically used to describe the colour depth, was evaluated based on reflectance (R), absorption coefficient (K) and scattering coefficient (S) measurements. The equation is:

$$\frac{K}{S} = \frac{(1 - R)^2}{2R} \quad (2)$$

The color difference is composed of three components that comprise the differences between the reference and the specimen. These are as follows: a lightness, chroma and hue.

The color difference ( $\Delta E_{cmc}$  and  $\Delta E^*_{ab}$ ) of the wool samples with different compositions of Clevios F ET/Clevios S V3 before and after washing was calculated according to LST EN ISO 105-J03 [290] standard using software built into spectrophotometer, Datacolor Spectraflash SF450 (Datacolor AG, Rotkreuz ZG, Switzerland). Wavelength range of apparatus 360 –700 nm; light source D65; observation conditions 10°. Measurements were performed for 5 specimens, number of readings per sample – 4 and number of measured layers of fabric – 4. The measurement results are presented taking into account the combined standard measurement uncertainty U, evaluated in accordance with the standard operating procedure SVP-11 applied at the FTMC Laboratory for Testing and Certification of Textile



Materials and Products. The combined standard uncertainty was calculated based on identified uncertainty sources and quantified according to GUM principles. The expanded uncertainty  $U$  was obtained by applying a coverage factor  $k = 2$ , corresponding to a confidence level of approximately 95%. All calculations were performed using Microsoft Excel.

Prior to testing, specimens were stored under a standard atmosphere for conditioning temperature  $(20 \pm 2) ^\circ\text{C}$  and relative humidity  $(65 \pm 4) \%$  (according to LST EN ISO 139 [284]).

#### 4.3.9 Electrical conductivity measurements

##### 4.3.12.1 Test method for measurement of surface resistivity

The electrical conductivity for sample before and after plasma treatment dyed Clevios F ET was measured by determining the surface resistance with a Terra-Ohm-Meter 6206 (Eltex–Electrostatik GmbH, Weil am Rhein Germany) according to the LST EN 1149-1 [291] standard, applying a voltage of 10 V. The surface resistance  $R$  ( $\Omega$ ) is measured on the material's surface using the electrodes specified in the standard [291]. The specific surface resistivity  $\rho$  ( $\Omega$ ) is calculated by multiplying the measured surface resistance  $R$  by the coefficient  $k$ .

$$\rho = R \cdot k \quad (3)$$

where:

$\rho$  – calculated specific surface resistivity,  $\Omega$ ;

$R$  – measured surface resistance,  $\Omega$ ;

$k$  – geometrical electrode coefficient, equal to 19.8.

The combined standard uncertainty  $U(R)$  of the surface resistance measurement was evaluated in accordance with the procedures applied in the laboratory. The estimation was based on the Type A (statistical) and Type B (non-statistical) components of uncertainty, following the principles outlined in the Guide to the Expression of Uncertainty in Measurement (GUM).

The combined standard uncertainty  $U(R)$  was calculated using the following formula:

$$U(R) = \sqrt{u_A^2 + u_B^2} \quad (4)$$

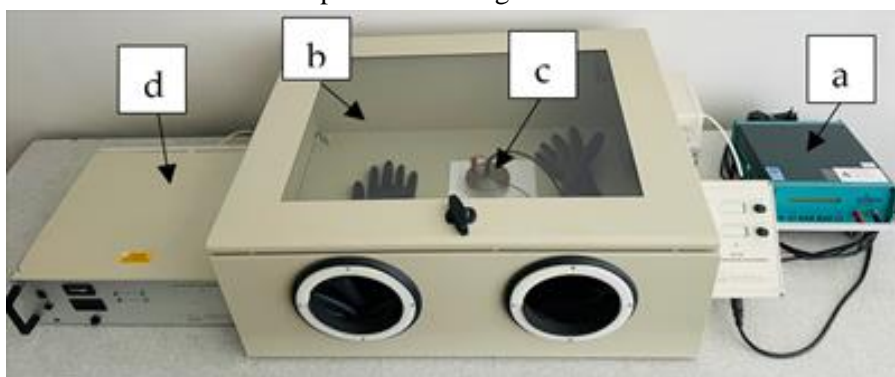
where:

$u_A$  is the standard uncertainty component evaluated from repeated measurements;

$u_B$  is the standard uncertainty component estimated from instrument specifications and calibration data.

All measurement results are presented with the associated uncertainty  $U(R)$ , reflecting the confidence level adopted by the laboratory.

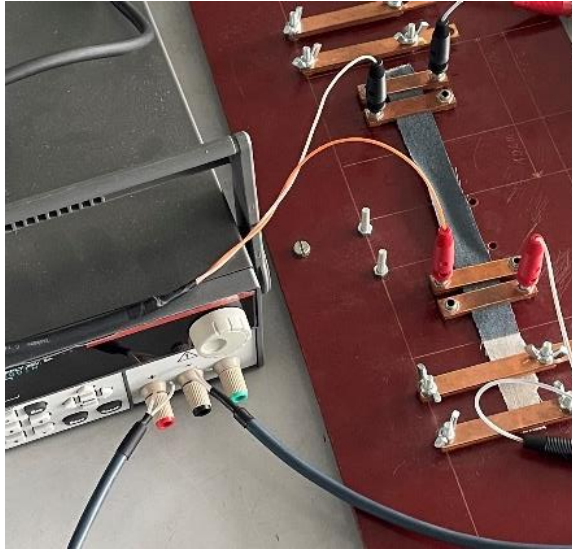
In the laboratory, a device used to determine the electrostatic properties of textile materials is the Teraohmmeter ELTEX 6206. According to the manufacturer, the ohmmeter has a measurement range of  $2 \times 10^3 \Omega$  to  $2 \times 10^{14} \Omega$ . The geometric mean is calculated from 5 measured samples using the Excel program. The diameter of the electrode used – 100 mm; specimens were pressed with a load of about 10 N. Measurements were carried out in dry conditions: air temperature  $(23 \pm 1) ^\circ\text{C}$  and relative humidity  $(25 \pm 5) \%$ . Conditioning prior to testing was performed for 24 h at the same dry conditions as the measurements. The assembly of measuring devices for resistance determination is presented in Figure 11.



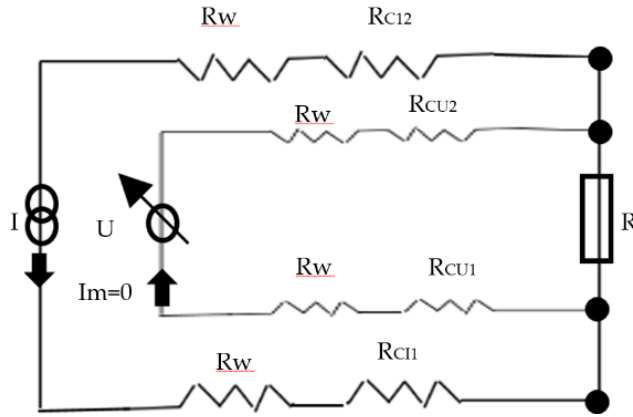
**Figure 11.** Device for surface resistance measurement: Tera-Ohm-Meter 6206 (a), JCI 191 climate control camera (b), test electrode (c) and JCI 192 dry air supply unit (d).

#### 4.3.10 Electrical resistance measurement

For textiles electrical resistance measurements was measurement was used “four electrode–four wire method”, which are the inverse of electrical conductivity measurements samples (Figure 12). Before testing, the specimens were left for at least 24 h in standard atmosphere conditions ( $20 ^\circ\text{C}$  and 65% RH) [284]. The voltage measurements were provided in the same conditions. The voltage was measured six times in 1 min, every 10 s, and the distance between the voltage electrodes is (d) 10 cm, and a sample width of 2 cm (Figure 12). Measurements were made according to the Four Point Kelvin method [292]. The electric current ( $I$ ) is  $0.01 \div 0.001 \text{ A}$ , the resulting voltage ( $U$ ) and the sample resistance ( $R$ ) is calculated according to Formula (4), and the linear resistance ( $R_L$ ) is calculated according to Formulas (3 and 5) (Figure 13).



**Figure 12.** Electrical resistance measurement. The electrodes were positioned and covered the entire width of the conductive track, as illustrated in the image.



**Figure 13.** Detailed scheme for the “four electrode–four wire method”; the four electrodes (contacts) are visualized by the four nodes indicated in the scheme.

It is the applied current in amperes;  $U$  is the measured voltage in volts, and  $I_m$  is the current in the voltage measurement circuit (equivalent to zero)  $R$  the resistance of sample (function of electrode spacing  $d$ ) =  $R_L d$ , in  $\Omega$  (5)

$R_{C11}$  and  $R_{C12}$  are the contact resistances in the current circuit in ohms;  $R_{CU1}$  and  $R_{CU2}$  are the contact resistance in the voltage circuit in  $\Omega$ ;  $R_w$  is the wire resistance in ohms.

$R_{Cl}$ ,  $R_{CV}$ , and  $R_W$  can be excluded due to the "four electrode–four wire measurement" so that the resistance of the specimen can be calculated by the simple formula

$$R = U/I \quad (6)$$

The linear resistance  $R_L$ , in  $\Omega/\text{cm}$ , is then calculated as

$$R_L = R/d \quad (7)$$

The distance  $d$  between the voltage electrodes is 10 cm.

Five elementary samples were measured, and their mean values were calculated. The data are presented with the standard error, calculated using Microsoft Excel software.

The standard error (SE) was obtained using the formula  $SE = SD / \sqrt{n}$  (8) where  $SD$  is the standard deviation of the measured values and  $n$  is the number of samples ( $n = 5$ ).

Electrical resistance measurements for Clevios F ET/Clevios S V3+3 % Tubicoated fixed agent HT coated samples coated with digital printing was measured by two-point probe method the resistance was measured six times in 1 min, every 10 s, and the distance between the voltage electrodes is ( $d$ ) 10 cm, and a sample width of 2 cm. The electric current ( $I$ ) is  $0.01 \div 0.001$  A, the resulting voltage ( $U$ ) and the sample resistance ( $R$ ) is calculated according to Formula (4), and the linear resistance ( $R_L$ ) is calculated according to Formulas 5-8.

Also sheet resistance of the  $10 \times 2$  cm samples printed with digital printing was measured by Four point method to check electrical conductivity in very small area. Was used Each Jandel Hand Applied Probe with one Cylindrical Four Point Probe Head (Bridge Technology, Garden Grove, California, USA). Probe make contact to the substrate, distance from probe 1 mm. Was measuring 5 samples, 3 times 5 different places in sample, measure size 5 mm  $\times$  10 mm. The device automatically calculates the sheet resistance in  $\Omega/\text{cm}^2$  based on the measured current (sheet resistance =  $4.5324 \times V/I$  (ohms/square)). Five elementary samples were measured, and their mean values were calculated. The data are presented with the standard error, calculated using Microsoft Excel software.

## 5.1 Results

### 5.1.1 Aqueous liquid repellency analysis

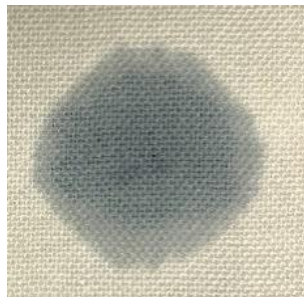
The increased hydrophilicity of low-pressure N<sub>2</sub> plasma treated wool fabric is shown in Table 16 as a change in fabric repellency grade number [278]. It was also found that the modified samples did not change their hydrophilicity when stored in a desiccator for 180 days. This sharp decrease in water absorption time after plasma treatment (Figure 14b) can be explained by the increase in surface hydrophilicity and absorbency due to the formation of microcracks and the removal of scales on wool fiber surface [293]. The untreated sample (Figure 14a) does not completely absorb the dye drops; it has been observed that dye drops are not absorbed, even after 30 min, thus they can be easily wiped off the surface of the fabric without getting wet.

**Table 16.** Fabric repellency grade.

Days	1	7	30	180
Non-treated fabric, repellency grade number	3	3	3	3
Treated fabric, repellency grade number	0	0	0	0



(a)



(b)

**Figure 14.** Photographs of “conductive acid dye” PEDOT:PSS and water (1:1) solution drop on (a) untreated and (b) plasma-treated wool.

### 5.1.2. Coding of samples according to modifying type

Various electrically conductive wool samples have been created with Clevios products using different processing and dyeing, printing and digital printing methods and their coding symbols are given in Tables 17, 18.

**Table 17.** Coding of samples processed using Clevios F ET by dyeing or/and Clevios S V3 by screen printing methods.

Code of Sample	F	PF	S	PS	FS
Modification type	Clevios F ET	Plasma/ Clevios F ET	Clevios S V3	Plasma/ Clevios S V3	Clevios F ET/ Clevios S V3
Code of Sample	PFS	SH	PSH	FSH	PFSH
Modification type	Plasma/ Clevios F ET/ Clevios S V3	Clevios S V3 + Tubicoat fixing agent HT	Plasma/ Clevios S V3 + Tubicoat fixing agent HT	Clevios F ET/ Clevios S V3 + Tubicoat fixing agent HT	Plasma/ Clevios FET/ Clevios S V3 + Tubicoat fixing agent HT

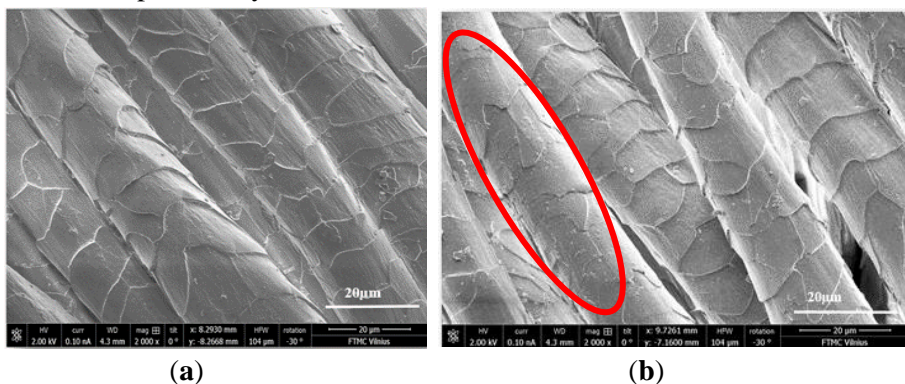
**Table 18.** Coding of samples processed using digital printing method with Clevios F ET and/or Clevios S V3 after plasma treatment.

Code of Sample	PF-p	PS-p	PFS-p	PFSH-p
Modification type	Plasma/ Clevios F ET	Plasma/ Clevios S V3	Plasma/ Clevios F ET/ Clevios S V3	Plasma/Clevios F ET/Clevios S V3 + Tubicoat fixing agent HT

### 5.1.3 SEM analysis

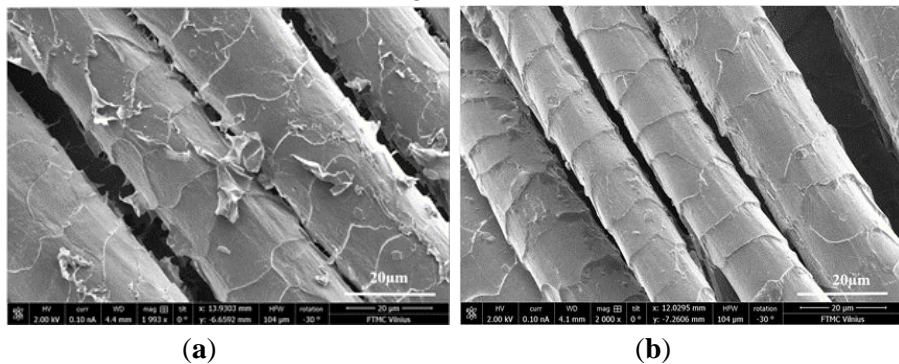
A scanning electron microscope (SEM) was used to investigate the morphology of the wool fiber surface. It can be seen from the SEM image (Figure 15a) that the surface of the untreated wool fiber was smooth, whereas the surface of the N<sub>2</sub> low-pressure plasma-treated wool fiber (Figure 15b) was etched, resulting in a rougher surface (shown in red circle). As excited and active plasma particles bombard the surface of the textile or polymer, they initiate a variety of reactions, such as chain scission, leading to surface etching, activation and surface cleaning [294,295]. We found that the 120 s plasma treatment resulted in more cracks and irregularities in the surface, and such an active surface provides better penetration of dyes and chemicals. The plasma treatment removes the epicuticle layer of the wool fiber, which has a

high density of cysteine bonds, is hydrophobic in nature and is a major barrier to the absorption of dyes and other chemicals [296,297].

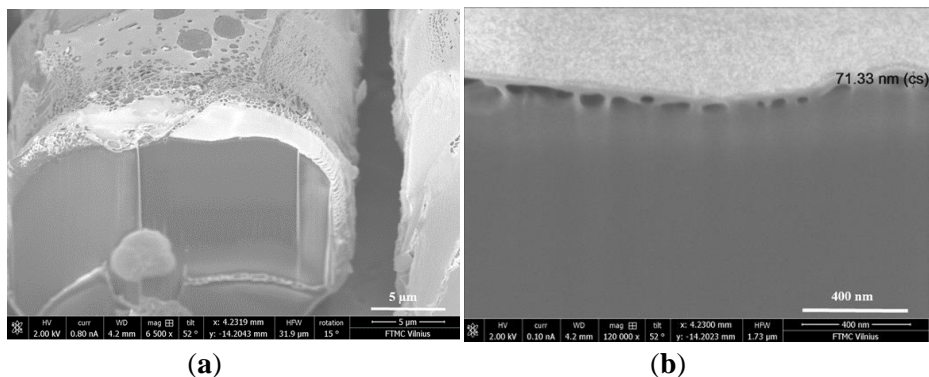


**Figure 15.** SEM images of untreated (a) and N<sub>2</sub> plasma-treated (b) wool fiber surfaces; magnification 2000 $\times$ .

SEM images show better exhaustion and bonding of PEDOT:PSS film to the fabric samples after plasma treatment. Analysis of the SEM view of the untreated coated substrate indicated that the thickness of the PEDOT:PSS coating is not uniform (Figure 16a). However, the plasma-treated wool fiber surface after dyeing with PEDOT:PSS formulation Clevios F ET is more homogeneous (PF, Figure 16b). Conductive polymer aggregates are observed on the dyed fiber surface and the penetration depth of the conductive polymer into the fiber is about 71.33 nm (Figure 17).



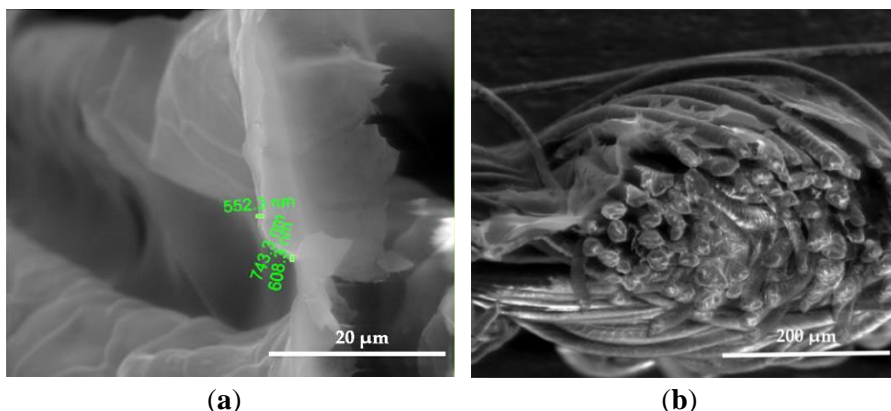
**Figure 16.** SEM images of wool fiber: Clevios F ET dyed sample F (a), N<sub>2</sub> plasma-treated and Clevios F ET dyed sample PF (b); magnification 2000 $\times$ .



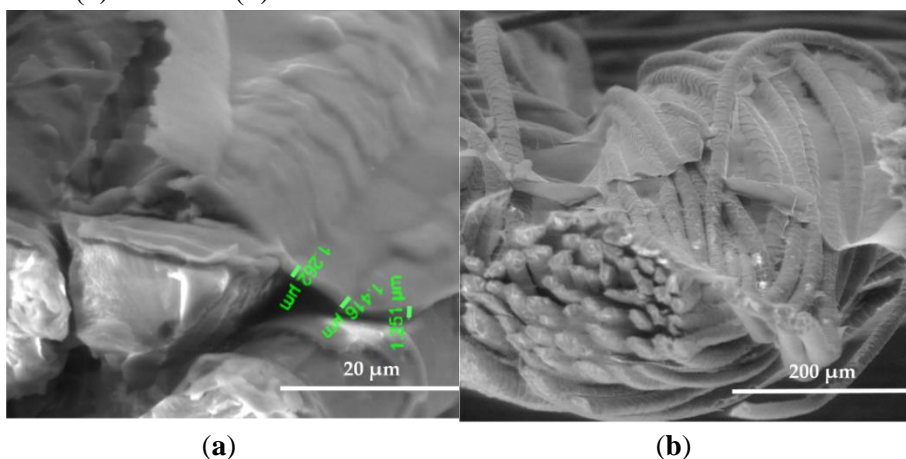
**Figure 17.** SEM images of N<sub>2</sub> plasma-modified and Clevios F ET dyed wool fiber (PF) cross section; magnification 6500× (a) and 120,000× (b).

SEM images show the differences between unmodified and modified plasma wool samples with different coating combinations, according to Table 17. When comparing the samples without (S) and after plasma modification (PS, PFS), the thickness of the sample (S) coating is thinner at  $0.552 \div 0.743 \mu\text{m}$ , uneven, and delaminated (Figure 18 a,b). However, after plasma modification of the sample (PS) we obtain a thicker coating  $1.251 \div 1.416 \mu\text{m}$ , the sample is ignited more evenly, and the spaces between the threads are filled with a coating (Figure 19 a,b) [297]. After plasma modification of samples (PFS) (Figure 20 a,b), the coating is thicker at  $1.193 \div 1.947 \mu\text{m}$  and more equal and well penetrated on the other side of the fabric in comparison to samples (PS) (Figure 19) [9, 102, 8] without initial dyeing, the coating is only formed and visible on the surface (Figure 18b). Comparing samples without (S, PS, PFS) and with Tubicoat fixing agent HT after plasma treatment (PFSH) the coating thickness is  $1.662 \div 2.187 \mu\text{m}$  (Figure 21a,b) and looks more homogeneous and uniform than without Tubicoat fixing agent HT (Figure 18–20). The thinner the layer, the higher its resistance. For biomedical and physiological sensors (EKG, EEG, EMG), the recommended thickness is 100 nm – 5 μm, as very thin layers ensure flexibility and good contact with the skin. They allow for the detection of very weak electrical signals without significant losses. For a 1000 Ω/sq resistance, the optimal thickness can be around 500 nm – 5 μm. The decrease in resistance of our samples can also be associated with the coating thickness, the deposition methods used, and the PEDOT:PSS compositions applied (Figure 17-26).





**Figure 18.** SEM images of the wool fiber cross-section sample (S) with Clevios S V3 coating applied by the screen printing method. Magnification 5000× (a) and 500× (b).



**Figure 19.** SEM images of the wool fiber cross-section sample (PS) N<sub>2</sub> plasma-treated and Clevios S V3 screen printing method coating; magnification 5000× (a) and 500× (b).

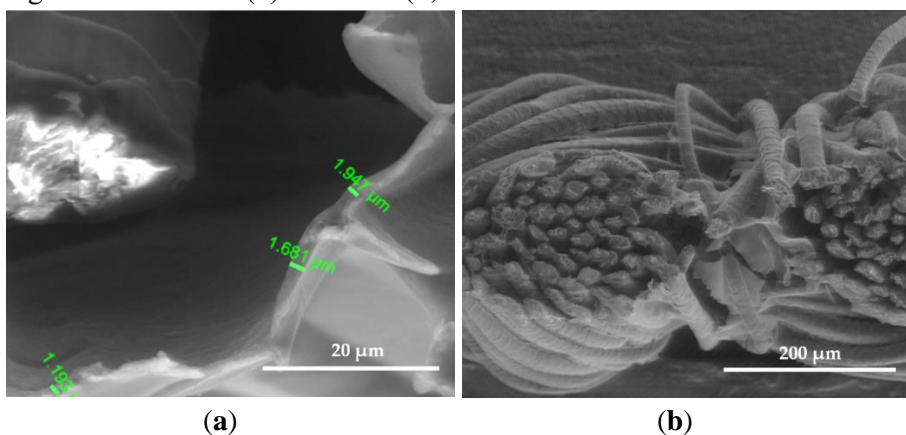
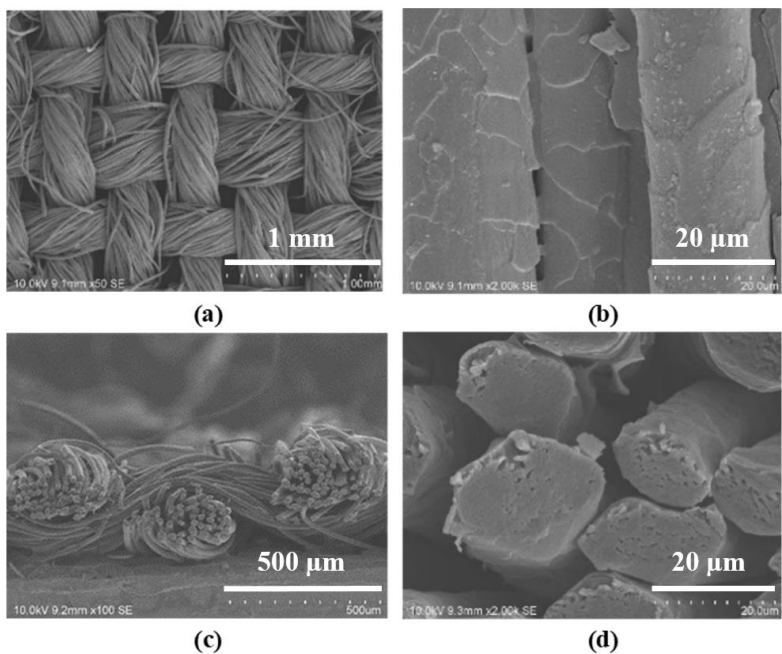
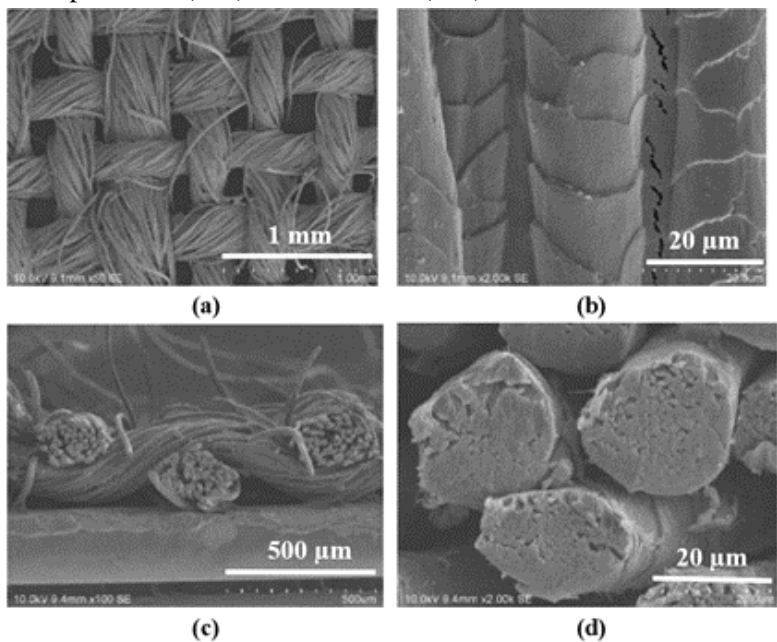


Figure 1 consists of two SEM images. Image (a) shows a surface with a 20 μm scale bar. Labels indicate surface roughness (Ra) and standard deviation (σ) values: 1.703 μm, 0.22 μm, 0.24 μm, 0.29 μm, and 0.31 μm. Image (b) shows a higher magnification view of the surface morphology with a 200 μm scale bar.

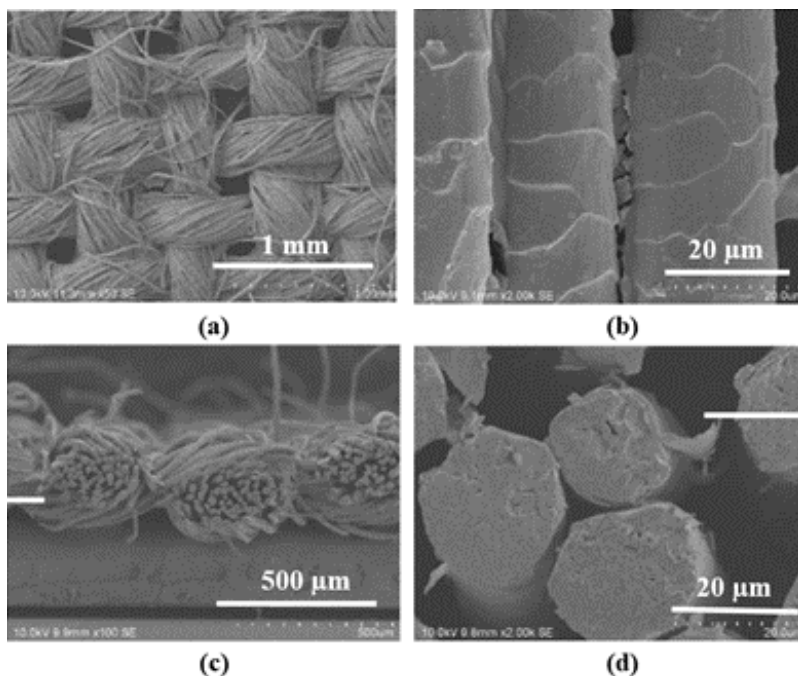
SEM images of wool samples, according to Table 18 coating by Clevios F ET or/and Clevios S V3 products using digital printing method after plasma treatment demonstrated better penetration of the coating. Using this printing method, the conductive coating not only covered the surface of the material, but also penetrated to the other side of the material. The digital printing method also does not change the structure of the wool fibre. Due to low viscosity Clevios F ET polymer penetrate through the fabric this can be seen in SEM of PF-p sample (Figure 22). SEM images of the wool PS-p sample showed that the lower viscosity of Clevios S V3 results in the coating filling the filament gaps more (Figure 23). In addition, compared PF-p, PS-p, PFS-p, PFSH-p sample with Tubicoat fixing agent HT coating looks more homogeneous and uniform (Figure 22-25).



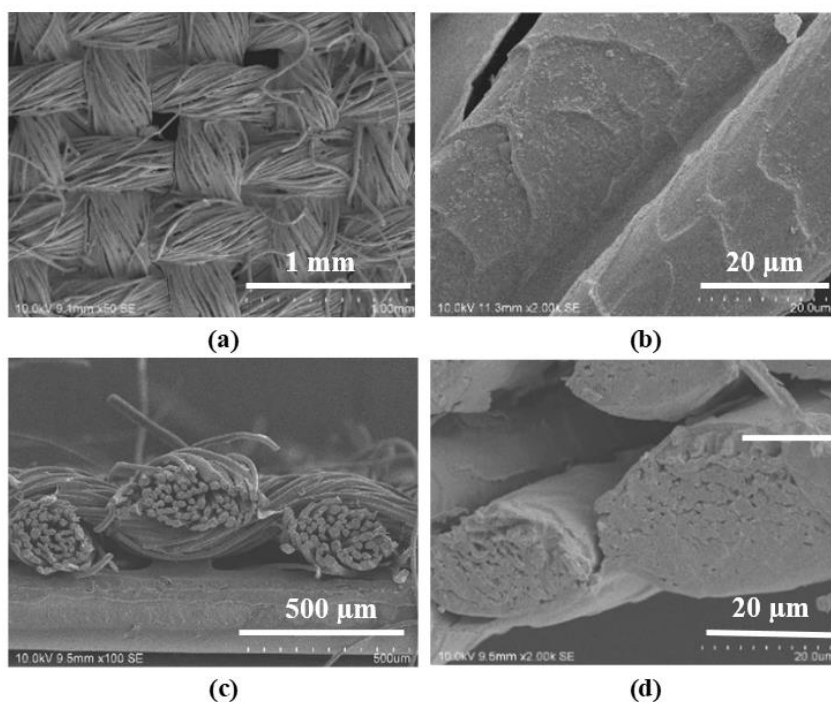
**Figure 22.** SEM images of wool fiber: by digital printing method coated sample PF-p surface (a, b), cross-section (c, d).



**Figure 23.** SEM images of wool fiber: by digital printing method coated sample PS-p surface (a, b), cross-section (c, d).



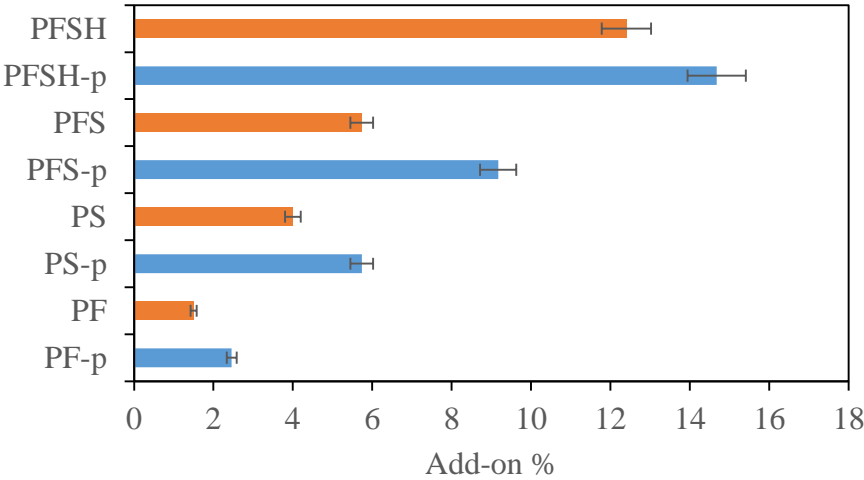
**Figure 24.** SEM images of wool fiber: by digital printing method coated sample PFS-p surface (a, b), cross-section (c, d).



**Figure 25.** SEM images of wool fiber: by digital printing method coated sample PFSH-p surface (a, b), cross-section (c, d).

5.1.4 Fabric analysis by weight

Using the digital printing method, the conductive coating not only covered the surface of the material, but also covered the filaments and penetrated to the other side of the material, which made it difficult to measure the thickness of the coating, and so we calculated a weighting analysis. Each experimental sample represents 5 elementary specimens. The average value of these specimens was calculated, and the results are presented in the graph as the mean  $\pm$  standard error (SE). Before Weighting analysis (Add-on Value), the specimens were left for at least 24 h in standard atmosphere conditions (20 °C and 65 % RH). Wool samples absorb the most conjugated polymer after plasma treatment, which may have an effect on electrical conductivity. The highest conjugated polymer mass - 15,6 % was found after treatment with plasma and digital printing with Clevios F ET/Clevios S V3 with Tubicoat fixing agent HT (PFSH-p) and the less with Clevios S V3 coating (Figure 26), because with product have high viscosity (Table 12) and can not penetrate into textile, we can see also from SEM photos that coating are more on surface (PS-p, Figure 23).

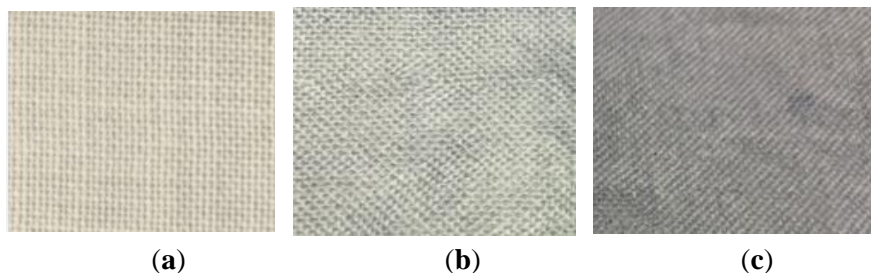


**Figure 26.** Coating Add-on percentage for different samples with standard error (SE).

5.1.5 Spectrophotometric measurements of color difference

Changes in color intensity were determined by performing color difference measurements with ColorTools™ QC software. This method can be used to determine the ratio of lightness differences. More intense color of

the material after treatment with plasma was observed (Figure 27). It is known that non-thermal plasma processing can be used to improve the dyeing ability of various textile materials [293]. The final shade of plasma-modified and Clevios F ET in the exhaust method at 90 °C dyed wool fabric sample appears darker than that of the correspondingly dyed untreated plasma material, indicating a plasma influence on the yield of used conductive polymer (Figure 27). Micropores in a hydrophobic epicuticular layer are treated with low-pressure plasma, which increases hydrophilicity and improves the adsorption capacity of the dyeing [168].







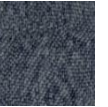

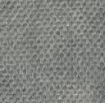



**Figure 27.** Wool fabric sample views: initial (a), unmodified and dyed at 90 °C with Clevios F ET (b) and N<sub>2</sub> low-pressure plasma-modified and dyed at 90 °C with Clevios F ET (c).

#### 5.1.6 Evaluation of conductive PEDOT:PSS coating durability after washing cycles









The photo images of plasma and PEDOT:PSS treated wool samples (F, PF, S, PS, FS, PFS, SH, FSH, PFSH) before and after five washing and drying cycles are present in Table 17. The color change analysis showed half-steps that the samples after plasma treatment are more darker [292] compared to samples coated without plasma treatment: F with PF, S with PS, and FSH with PFSH. This indicates that the plasma-treated samples became darker, possibly due to better absorption of PEDOT:PSS. After five washes, the plasma-treated samples (PF, PS, PFS, PSH) showed less color change compared to the untreated samples (F, S, FS, SH). Plasma treatment cleaned the surface of the wool fabric, and we assume that it increased the yield of absorbed PEDOT:PSS and resistance during washing as well [8, 102]. When we compared unwashed sample with sample after five washes cycles (F, PF, S, PS, PFS), according to gray scale a color change was found about one stages or more [298]. Furthermore, comparing PEDOT:PSS coated samples with (SH, FSH, PFSH) and without Tubicoat fixing agent HT (S, FS, PFS) before and after five washes, the color change was less than half-steps between washed and

unwashed samples according to grey scale. The received results showed that Tubicoat fixing agent HT increased the resistance to washing. The sample PFSH demonstrated the highest wash fastness and the lowest color changes after five washes (Table 19). By colour change analysis, we can determine how much PEDOT:PSS remains on the textile, which affects the electrical conductivity (Figure 29-32).

**Table 19.** Sample photo images before and after 5 washing 40 °C and drying cycles [262].

Code of Sample	F	PF	S	PS	FS
Before washing					
After 5 washing cycles					










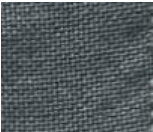





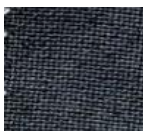
Code of Sample	PFS	SH	FSH	PFSH
Before washing				
After 5 washing cycles				

In Table 19, are demonstrated photo images depicting plasma-treated and PEDOT:PSS printed wool samples (PF-p, PS-p, PFS-p, PFSH-p) both before and after fifteen, twenty five, and thirty five washing and drying cycles. A color analysis indicates that after plasma treated and Clevios FET/CleviosSV3 (PFS-p and PFSH-p) samples a significant improvement of over half a step compared with sample with just one Clevios product Clevios FET (PF-p) or Clevios SV3 (PS-p). This suggests that PFS-p and PFSH-p leads to a darkening effect, possibly owing to enhanced PEDOT:PSS absorption. After thirty five washes all samples has changed by only half a step, but still retains



good properties, this also influenced the digital printing method, because the coating was better absorbed into the textile compared with another coating methods. Samples (PFSH-p) exhibit lesser color change compared to (PFS-p). This suggests that plasma treatment effectively cleanses the wool fabric surface, thereby potentially increasing the absorption yield of PEDOT:PSS and Tubicoat fixing agent HT enhancing resistance during washing [8, 102]. Among the samples, PFSH-p exhibits the highest wash fastness and the lowest color changes after thirty five washes (Table 20).

**Table 20.** Samples photo images before and after 15, 25, 35 washing 40 °C and drying cycles [280].

Code of Sample	PF-p	PS-p	PFS-p	PFSH-p
Before washing				
After 15 washing cycles				
After 25 washing cycles				
After 35 washing cycles				

Tubicoat fixing agent HT could function as a bridging agent between wool fibre functional groups and PEDOT, enhancing their compatibility and adhesion (Figure 28). The cationic part of Tubicoat fixing agent HT interacts with wool fibers through ionic and hydrogen bonds, particularly with the carboxyl groups in wool [135, 136]. Simultaneously, these same cationic groups in Tubicoat fixing agent HT could form ionic interactions with the anionic sulfonate groups in PSS, effectively establishing a bridge between the wool fibers and PEDOT [137, 138]. This setup facilitates electrostatic interactions, where positively charged regions in Tubicoat fixing agent HT are attracted to the negatively charged PSS, promoting adhesion between wool



and PEDOT by simultaneously binding to both the natural wool fiber and the synthetic PEDOT polymer structure [139, 140]. Consequently, this interaction enhances the durability and functionality of the coating on the fabric, resulting in a more stable composite material [141, 142].



**Figure 28.** Tubicoat fixing agent HT as a bridge between wool and PEDOT:PSS Tubicoat fixing agent.

The use of fixing agents, such as Tubicoat HT, significantly enhances coating stability, similar to findings where silicone-based fixatives improved PEDOT:PSS retention [272]. Additionally, previous studies have demonstrated that post-treatment with polar solvents like ethylene glycol (EG) or dimethyl sulfoxide (DMSO) enhances both conductivity and washing durability [276]. Furthermore, incorporating PEDOT:PSS with flexible polymer matrices, such as polyurethane, has been found to enhance mechanical flexibility and resistance to washing cycles [277]. Many of these studies were conducted on various textile substrates, including cotton, polyester, nylon, and synthetic blends, which often exhibit lower PEDOT:PSS adhesion and retention compared to wool.







The findings of this study align with existing research on enhancing the durability of PEDOT:PSS coatings on textiles. Plasma treatment has been shown to improve adhesion by increasing fiber surface roughness and wettability, leading to better wash resistance [275]. The results obtained in this study demonstrate superior wash durability compared to other research due to the combined use of plasma treatment and the Tubicoat fixing agent on wool fabrics. Wool natural surface characteristics, combined with plasma modification, allowed for better PEDOT:PSS absorption and retention. In contrast, studies on synthetic fabrics like polyester have reported lower wash durability due to weaker interactions between PEDOT:PSS and the hydrophobic surface. To further improve our results, additional optimization

of plasma treatment parameters, the incorporation of hybrid polymer matrices, and the exploration of alternative crosslinking agents could enhance long-term conductivity and mechanical stability.

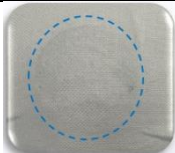



### 5.1.7 Color fastness to dry rubbing analysis

Improved resistance to dry rubbing was obtained by using the same combination of with or without plasma modification, dyeing, and dyeing/coating with PEDOT:PSS with or without Tubicoat fixing agent HT. After dyeing with Clevios F ET, the color of the sample (F) was so dull that it was difficult to evaluate the rubbing test result, but it became more visible after plasma treatment (PF) (Table 21). Better dry rubbing resistance of samples (SH, PSH, FSH, PFSH) was obtained when 3 wt. % of Tubicoat fixing agent HT was added to the Clevios S V3 (Table 22). The tests carried out showed that the best resistance of rubbing was obtained with the combined modification (PFSH): plasma treatment, PEDOT:PSS dyeing and coating, and Tubicoat fixing agent HT adding (Table 22).

**Table 21.** Wool samples with different PEDOT:PSS compositions after rubbing tests [270].

Code of sample	F	PF	S	PS	FS	PFS
Rubbing cloth						


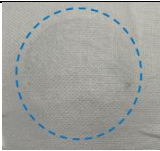
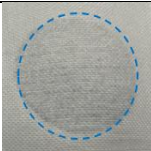
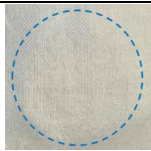
**Table 22.** Wool samples with different PEDOT:PSS composition and 3 wt. % of Tubicoat fixing agent HT after rubbing tests [270].

Code of Sample	SH	PSH	FSH	PFSH
Rubbing cloth				

Colour fastness was determined using dry rubbing test, the best resistance of rubbing was obtained with the combined modification (PFSH-p): plasma treatment, Clevios F ET/Clevios S V3 , and Tubicoat fixing agent HT adding by digital printing method. Wool samples with different modifications after

rubbing tests evaluated using a grey scale for staining in standard lighting (Table 23). The biggest colour fastness result was of PFSH-p sample.

**Table 23.** Wool samples with different PEDOT:PSS composition and Tubicoat fixing agent HT modifications by digital printing method after rubbing tests [270].

Code of Sample	PF-p	PS-p	PFS-p	PFSH-p
Rubbing cloth				

### 5.1.8 Comparison of color difference results

The measured and K/S values at the maximum wavelength of 520 nm are presented in Table 24. Although the literature sources say [282] that color depth K/S shows a higher dye ability of the material, the obtained results show that after plasma modification the value (K/S 23.45) was lower compared to the unmodified (K/S 28.56) and dyed wool fabrics. However, other values showed higher dye absorption of wool fabrics. Plasma-modified compared to unmodified and Clevios F ET dyed wool is darker in color ( $L^*$  54.47), bluer ( $h$  177.91), more saturated colors ( $C$  3.98) and has greener ( $a^*$  -3.98) and bluer ( $b^*$  0.15) components. Plasma treatment cleans the upper greasy layer of the wool fiber, increases the best dye ability and increases the resistance during washing [280]. After 5 washing cycles, unmodified and dyed Clevios F ET wool became lighter ( $L$  57.49), light blue ( $h$  107.15), yellowish ( $b^*$  6.16), less green ( $a^*$  -1.89), but with more saturated color ( $C$  3.98). The untreated wool fabrics may have felted and shrunk during washing, which may have increased the color deposition, thus being the reason for the higher saturated color result [283].

**Table 24.** Color parameters of the experimental samples before and after 5 wasking cycles.

Sample	$L^*$	$a^*$	$b^*$	$C^*$	$h$	K/S ( $\lambda_{max} =$ 520 nm)
F	56.60 $\pm 0.07$	-3.44 $\pm 0.07$	1.48 $\pm 0.07$	3.75 $\pm 0.07$	156.79 $\pm 0.07$	28.56 $\pm 0.07$
PF	54.47 $\pm 0.07$	-3.98 $\pm 0.07$	0.15 $\pm 0.07$	3.98 $\pm 0.07$	177.91 $\pm 0.07$	23.45 $\pm 0.07$

F sample						
after 5	57.49	-1.89	6.13	6.42	107.15	25.36
washing	± 0.07	± 0.07	± 0.07	± 0.07	± 0.07	± 0.07
cycles						
PF sample						
after 5	52.65	-2.97	1.66	3.4	150.85	21.31
washing	± 0.07	± 0.07	± 0.07	± 0.07	± 0.07	± 0.07
cycles						

Note: (±0.1) confidence intervals.

Table 25 displays the measured L\*, a\*, b\* coordinates and K/S values at the maximum wavelength of 700 nm. Color yield K/S shows a higher dyeing ability [165] to PEDOT: PSS of the tested wool fabric samples. This indicates that the PF sample becomes slightly darker (lower L\*) and slightly greener (less negative a\*) after 35 washes. PF sample the lightness value L\* initially decreases from 36.7 to 33.9 after 5 washes, indicating that the sample becomes darker. Over subsequent washes, the L\* value increases slightly to 36.4 after 25 washes, then slightly decreases to 35.4 after 35 washes, suggesting a minor fluctuation in lightness. The a\* value shifts from -3.6 to -2.9 after 5 washes, moving closer to neutral (less green). There is a slight increase in the green component after 25 washes, reaching -4.2, then returning to -3.0 after 35 washes. The b\* value moves from -6.3 to -5.9 after 5 washes, indicating a slight reduction in the blue component. After 15 washes, the blue component further decreases to -5.1. By 25 washes, it returns to -6.2, and finally, after 35 washes, it is -4.8, indicating a decrease in blue over time but with some fluctuation. The PFSH-p sample shows a slight darkening and a reduction in the blue component after multiple washes, with some fluctuations in green. The changes are relatively small, indicating that the sample maintains its color properties reasonably well over multiple washes. Furthermore, the Tubicoat fixing agent HT as cross-linker enhanced the sample's (PFSH-p) resistance to washing treatments. All samples exhibit changes in their Lab values over multiple washes, with PF generally maintaining higher lightness and showing slightly less variation in the green-red and blue-yellow axes compared to PFSH-p. The analysis shows that PF-p is more stable in terms of color consistency over washing cycles, while PFSH-p undergoes more noticeable changes, particularly in lightness and the blue component.

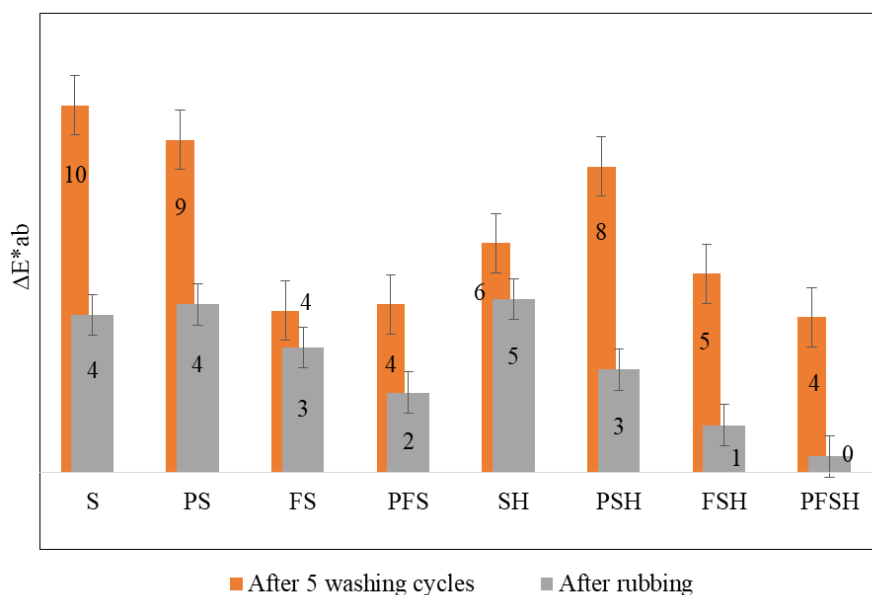
**Table 25.** Comparison of reference and PEDOT:PSS treated samples after 35 washing cycles according to the L\* a\* b\* color coordinates values.

Code of sample	Reference			After 5 Washes			After 15 Washes		
	L*	a*	b*	L*	a*	b*	L*	a*	b*
<b>PF-p</b>	47.5	-3.3	-4.2	46.5	-2.8	-4.2	47.0	-2.7	-3.9
<b>PS-p</b>	38.1	-3.8	-6.5	37.1	-3.0	-6.1	37.2	-3.0	-5.7
<b>PFS-p</b>	48.8	-3.7	-5.3	47.3	-3.5	-5.7	46.7	-3.4	-5.4
<b>PFSH-p</b>	36.7	-3.6	-6.3	33.9	-2.9	-5.9	34.0	-3.0	-5.1

Code of sample	After 25 Washes			After 35 Washes		
	L*	a*	b*	L*	a*	b*
<b>PF-p</b>	46.7	-3.5	-5.1	45.8	-2.7	-4.3
<b>PS-p</b>	38.7	-4.0	-6.1	37.0	-3.1	-5.6
<b>PFS-p</b>	48.3	-4.2	-5.8	46.9	-3.3	-5.4
<b>PFSH-p</b>	36.4	-4.2	-6.2	35.4	-3.0	-4.8

Note: ( $\pm 0.1$ ) confidence intervals.

Samples (S, PS, FS, PFS, SH, PSH, FSH, PFSH) of the wool fabric of different modifications references were compared with the same samples after washing and rubbing tests and performing color differences tests with a spectrophotometer. The PFSH sample has the least color difference ( $\Delta E^*_{ab}$ ) before and after washing and rubbing, resulting in the best resistance to washing and rubbing treatments. Samples (PS, PFS, PSH, PFSH) after plasma modification compared to unmodified plasma (S, FS, SH, FSH) showed lower color differences ( $\Delta E^*_{ab}$ ) and better resistance to mechanical treatment and washing (Figure 29). Providing the complex modification of sample (FS) dyeing with Clevios F ET and coating Clevios S V3, a smaller color difference compared to samples (S) printed only with Clevios S V3 was obtained (Figure 28).



**Figure 29.** Color difference ( $\Delta E^*ab$ ) test results after washing and rubbing testing with PEDOT: PSS-modified wool fabric samples by various methods. Values are presented with expanded uncertainty ( $\pm U$ ).

Table 24 displays the measured  $L^*$ ,  $a^*$ ,  $b^*$ ,  $C^*$ , and  $h$  coordinates and K/S values at the maximum wavelength of 1100 nm. The colour depth K/S shown dye absorption [133] of the PEDOT:PSS into the wool fabric samples (Table 26). The received results showed that after plasma treatment, the values K/S of samples (PS, PFS, PSH, PFSH) were lower compared to the unmodified K/S samples (S, FS, SH, FSH), as well as after washing and rubbing tests (Table 24). Plasma modified sample (PFSH) compared with the unmodified (FSH) was darker in color ( $L^* = 36$ ), had bluer ( $h = 240$ ), more saturated colors ( $C^* = 7$ ), and had greener ( $a^* = -4$ ) and bluer ( $b^* = -6$ ) shade (Table 24). After five washing cycles, sample PFSH became yellowish ( $b^* = 4$ ), reddish ( $a^* = 2$ ), had a saturated color ( $C^* = 5$ ), a darker ( $L^* = 34$ ) shade, and had higher dyeing ability ( $K/S = 36$ ) (Table 24). The K/S value determines the difference between the color strength of the sample PFSH reference ( $K/S = 35$ ) and of the same sample after the rubbing test ( $K/S = 37$ ). After the rubbing test, the sample PFSH color coordinates did not change much and were: darker ( $L^* = 38$ ), bluer ( $h = 239$ ), had the same saturated color ( $C^* = 7$ ), greener ( $a^* = -4$ ), and had a bluer ( $b^* = -6$ ) shade (Table 24). The received results showed that plasma treatment increased wool fiber's ability to react with PEDOT:PSS. Furthermore, the Tubicoat fixing agent HT enhanced the sample's (PFSH) resistance to washing and rubbing treatments [293].

**Table 26.** Following washing and rubbing testing, we compared the L\* a\* b\* C\* h color coordinates and the maximal K/S values of unwashed plasma and PEDOT: PSS treated samples.

Code of sample	Reference						After 5 Washes					
	L*	a*	b*	C*	h	K/S	L*	a*	b*	C*	h	K/S
<b>S</b>	43	-3	-7	7	246	50	46	-2	-5	5	243	0.065
<b>PS</b>	38	-2	-7	7	251	36	44	-2	-5	5	245	0.071
<b>FS</b>	40	-3	-6	7	242	44	35	-2	-3	3	232	0.038
<b>PFS</b>	37	-4	-6	7	240	33	36	-2	-5	5	242	0.035
<b>SH</b>	40	-2	-6	7	250	43	48	-2	-5	5	245	0.079
<b>PSH</b>	38	-2	-7	7	252	39	45	-2	-5	6	247	0.065
<b>PFSH</b>	36	-4	-6	7	240	35	34	2	4	5	240	0.036

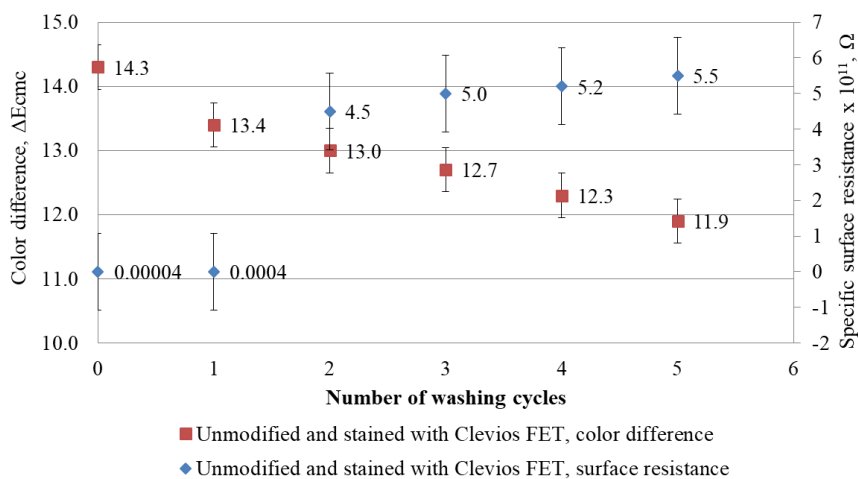
Code of sample	Reference						After Rubbing Test					
	L*	a*	b*	C*	h	K/S	L*	a*	b*	C*	h	K/S
<b>S</b>	43	-3	-7	7	246	50	45	-3	-5	5	244	65
<b>PS</b>	38	-2	-7	7	251	36	41	-2	-6	6	250	51
<b>FS</b>	40	-3	-6	7	242	44	41	-3	-5	6	242	55
<b>PFS</b>	37	-4	-6	7	240	33	38	-3	-5	6	239	40
<b>SH</b>	40	-2	-6	7	250	43	46	-3	-4	5	239	73
<b>PSH</b>	38	-2	-7	7	252	39	38	-2	-7	7	252	34
<b>PFSH</b>	36	-4	-6	7	240	35	38	-3	-6	7	239	37

Note: ( $\pm 0.1$ ) confidence intervals.

Compared to other studies on PEDOT:PSS coatings for textiles, our findings demonstrate superior dye retention and resistance to washing and rubbing. For instance, research by Y. Hou et al. (2020) [305] on polyester and cotton fabrics reported a significant reduction in K/S values after five washing cycles due to weaker adhesion between PEDOT:PSS and the textile surface. In contrast, the present study shows that wool, particularly when treated with plasma, exhibits stronger bonding with PEDOT:PSS, leading to higher color retention and mechanical stability. Additionally, a study by A. Haji et al. (2021) [306] found that plasma treatment of synthetic textiles enhanced PEDOT:PSS absorption, but the color stability was still lower than that observed in our wool-based samples. Furthermore, past research on PEDOT:PSS-coated nylon fabrics indicated substantial color fading due to weak polymer-fiber interactions [307]. In comparison, the results obtained in this study demonstrate that plasma-modified wool samples, especially when combined with Tubicoat fixing agent HT, maintain their color properties significantly better under both washing and rubbing conditions.

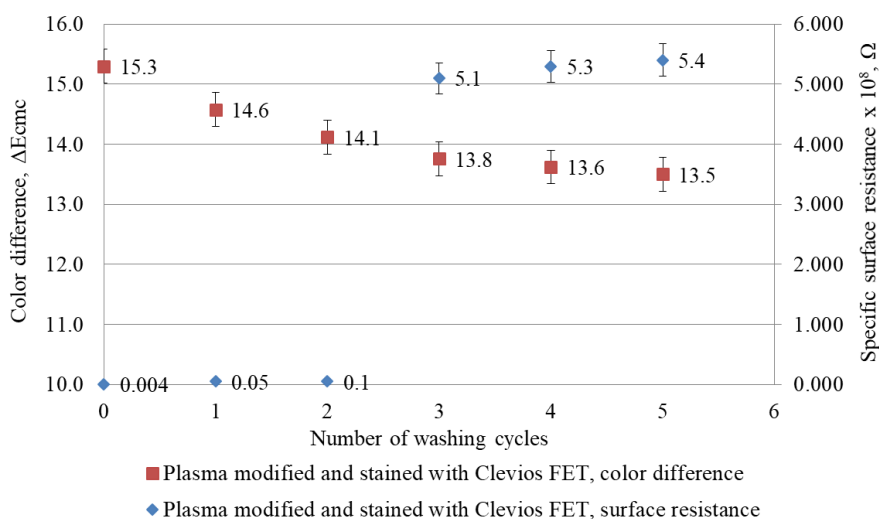
### 5.1.9 Specific surface resistance and linear resistance measurement

Measurements of the specific surface resistance of non-treated, Clevios F ET dyed, N<sub>2</sub> plasma-modified and Clevios F ET dyed wool fabric samples before and after repeated washing at 40 °C temperature were performed with a Terra-Ohm-Meter 6206 according to the LST EN 1149-1 [291] standard. The specific surface resistance of the non-treated initial sample was  $5.5 \times 10^{13} \Omega$  (this value is not presented in Figure 30). The plasma-modified and Clevios F ET dyed sample demonstrated lower specific surface resistance ( $4 \times 10^5 \Omega$ , Figure 31) compared with the unmodified Clevios F ET dyed sample ( $4 \times 10^6 \Omega$ , Figure 30). Furthermore, the decrease in color intensity and increase of resistivity was observed after washing. Improving of color fastness to washing and dyeing intensity was observed after the plasma treatment. Furthermore, this plasma-modified and Clevios F ET dyed sample demonstrated lower specific surface resistance ( $5.4 \times 10^8 \Omega$ , Figure 31) compared with the unmodified Clevios F ET dyed sample ( $5.5 \times 10^{11} \Omega$ ) after 5 washes (Figure 30). This is due to the better exhaustion and connectivity of PEDOT:PSS as “conductive acid dye” [11] to the wool fibers cationic amino sites after plasma treatment.



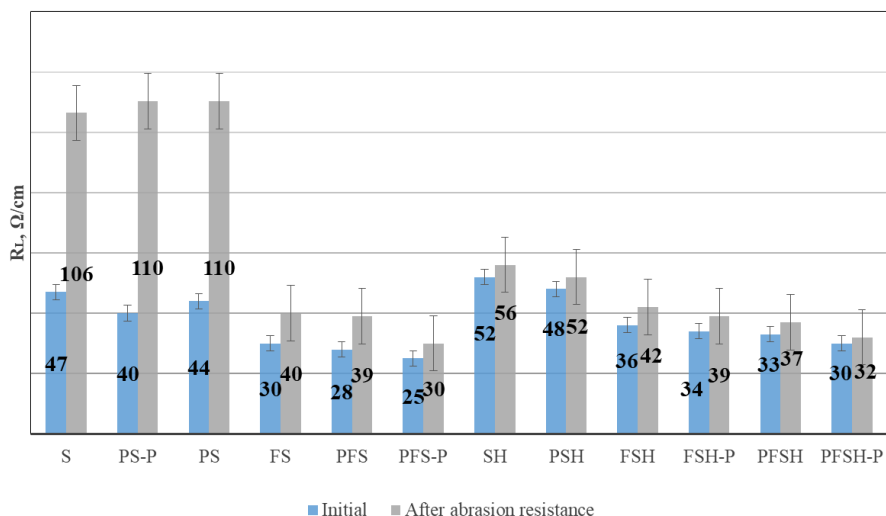
**Figure 30.** Change in color difference (values  $\pm$  U) after washing cycles and specific surface resistance (values  $\pm$  U) measurements of dyed with Clevios F ET wool fabric sample.



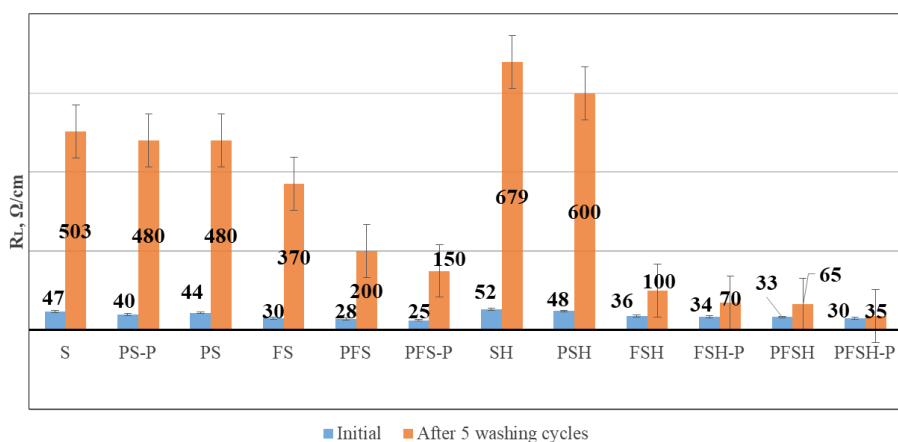


**Figure 31.** Change in color intensity (values  $\pm U$ ) after washing cycles and specific surface resistance measurements (values  $\pm U$ ) of  $N_2$  plasma-modified and Clevios FET dyed wool fabric sample.

Measurements of the linear resistance ( $R_L$ ) of wool fabrics of different compositions after the rubbing and washing tests (Figures 32-34) were carried out according to the Four-point Kelvin method [292], and the linear resistance ( $R_L$ ) was calculated according to Formula 5. The linear resistance ( $R_L$ ) of all samples with the same chemical modifications with PEDOT:PSS after plasma treatment (PS, PFS, PSH, PFSH, PFSH-p) were lower as without plasma treatment (S, FS, SH, FSH) (Figure 32, 33). This is due to the better affinity and binding of PEDOT:PSS as a “conductive acid dye” [11] to the cationic amine sites of the wool fiber after plasma treatment. Samples with Tubicoat fixing agent HT (SH, PSH, PFSH, PFSH-p) retained better electrical conductivity after washing and rubbing compared to those without Tubicoat fixing agent HT (S, PS, FS, PFS) (Figure 32, 33). It is assumed that Tubicoat fixing agent HT as a cross-linker [54] affected the formed fabric surface film resistance to rubbing; through this, the resistance ( $30 \Omega/\text{cm}$ ) did not increase (Figure 32). After rubbing and washing testing, the PFSH-p sample linear resistivity values were, respectively, ( $32 \Omega/\text{cm}$ ) and ( $35 \Omega/\text{cm}$ ), and had the lowest resistivity compared to the other samples (Figures 32 and 33).



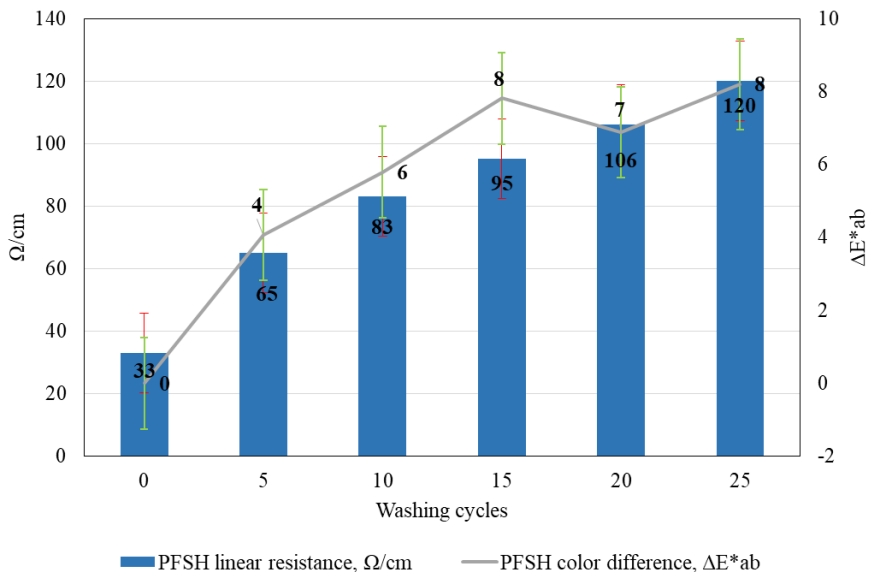
**Figure 32.** Measurements of linear resistance ( $R_L$ ) untreated and after plasma treatment with different modifications of wool fabrics after rubbing testing (values  $\pm$  SE).



**Figure 33.** Linear resistance ( $R_L$ ) measurements on untreated and plasma-treated wool fabrics coated with different modifications of Clevios F ET and Clevios S V3 after five washing cycles (values  $\pm$  SE).

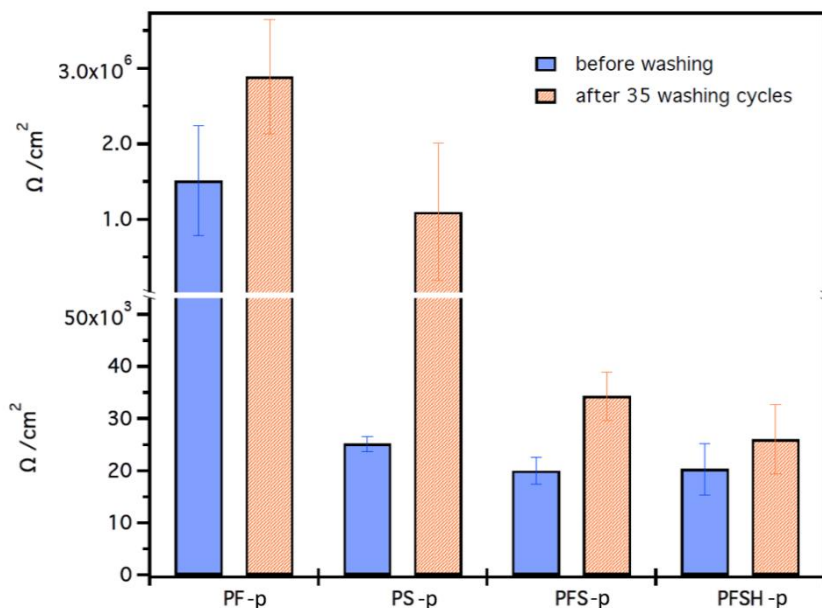
The sample PFSH with the best resistance after dyeing by Clevios F ET and coating by screen printing Clevios S V3 with Tubicoating fixing agent HT mixture to rubbing and washing was selected, and additionally, 25 washing cycles were carried out, measuring the linear resistance and color differences after every five washing cycles. The value of  $\Delta E^*_{ab}$  shows that the magnitude of the color differences after the washing cycles is not very wide; after 15 washing cycles, the value remains almost constant at  $\Delta E^*_{ab}$  of approximately

eight. Moreover, the  $R_L$  of sample PFSH before washing was 33  $\Omega/\text{cm}$  (Figure 34). The  $R_L$  steadily increased to 120  $\Omega/\text{cm}$  when the 25 washing cycles were carried out, but the material was still electrically conductive (Figure 34) and could be classified as a dissipative material and used for protective workwear [299].



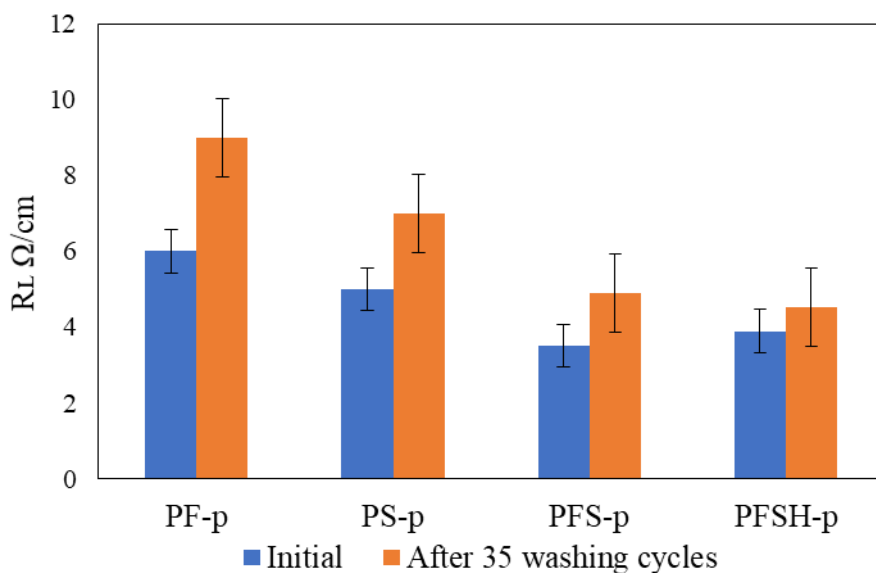
**Figure 34.** Linear resistance results (values  $\pm$  SE red) with color difference (values  $\pm$  U green) comparison after 25 washing cycles of sample PFSH.

Samples (PF-p, PS-p, PFS-p, PFSH-p) coated with digital printing was measured by Four point method to check electrical conductivity in very small area (measure size 5 mm  $\times$  10 mm, distance from probe 1 mm). The device automatically calculates the sheet resistance in  $\Omega/\text{cm}^2$  based on the measured current. The lowest average of sheet resistance and smallest standard deviation between the results before washing was obtained for samples PS-p ( $20 \times 10^3 \Omega/\text{cm}^2$ ) and PFS-p ( $25 \times 10^3 \Omega/\text{cm}^2$ ), is considered to have the most uniform coverage. However, after 35 washing cycles, the PS-p sample has the largest standard deviation, the sheet resistance after washing  $1 \times 10^6 \Omega/\text{cm}^2$  and the coating became uneven. The PFSH-p sample remained the most uniform after washing, and the sheet resistance only increased to  $26 \times 10^3 \Omega/\text{cm}^2$  comparing with before washing  $20 \times 10^3 \Omega/\text{cm}^2$  (Figure 35). The ability of this method to measure electrical conductivity over short distances makes it highly suitable for assessing the applicability of the developed coating in the production of fine conductive tracks for textile-based electronic applications.



**Figure 35.** Sheet resistance  $\Omega/\text{cm}^2$  by 4-point method for wool fabric with different conductive polymer coating before and after 35 washing cycles (values  $\pm$  SE).

Samples of  $10\text{ cm} \times 2\text{ cm}$  were measured using the two-point probe method and the linear resistance ( $R_L$ ) was calculated according to Formula 5. The linear resistance ( $R_L$ ) compared all samples with the chemical modifications with PEDOT:PSS after plasma treatment (PF-p, PS-p, PFS-p, PFSH-p) have low resistance using printing method [300]. The sample (PFS-p) with the lowest electrical resistance was after plasma treatment and modification with Clevios FET and Clevios SV 3 before washing. Samples with Tubicoat fixing agent HT (PFSH-p) retained better electrical conductivity. The sample (PFS-p) with the lowest electrical resistance was after plasma treatment and modification with Clevios FET and Clevios SV 3 before washing. After washing compared to those without Tubicoat fixing agent HT (PF-p, PS-p, PFS-p) (Figure 36). It is assumed that Tubicoat fixing agent HT as an additive that increases wash resistance [283,301] affected the formed fabric surface film resistance to washing (Figure 36).



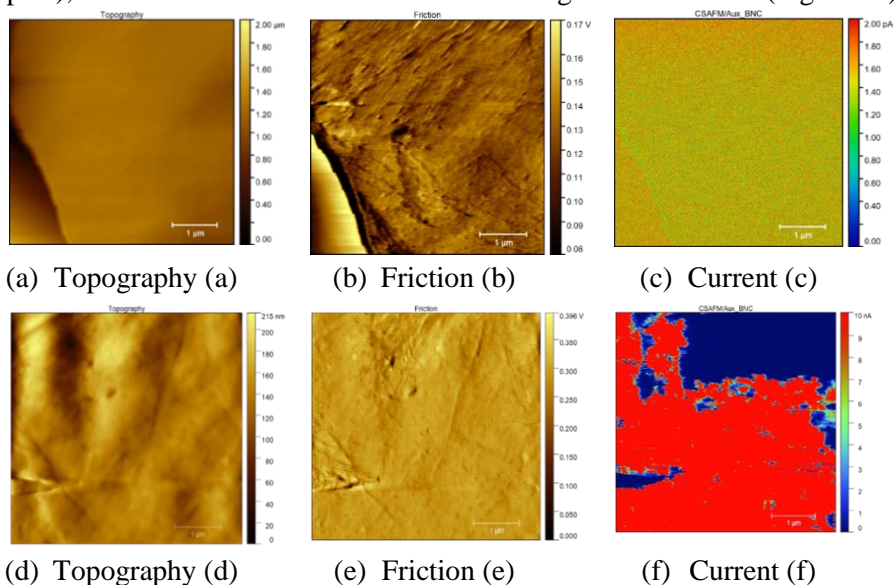
**Figure 36.** Measurements of The linear resistance ( $R_L$ ) of wool fabric coated with different modifying methods of Clevios F ET and Clevios S V3 after 35 washing cycles  $R_L$   $\Omega/\text{cm}$  by two point method (values  $\pm$  SE).

Compared to previous studies, this research demonstrates significant improvements in washing durability and electrical conductivity retention of PEDOT:PSS coated wool textiles. Ankhili et al. [302] achieved stable electrocardiographic signals after 50 washing cycles using screen-printed PEDOT:PSS on cotton, while Ryan et al. [103] reported 14 S/cm conductivity on silk yarns, which remained stable after washing. However, these studies focused on different textile substrates, whereas this study investigates wool, where plasma treatment and Tubicoat fixing agent significantly enhanced PEDOT:PSS adhesion, reducing color loss and improving wash resistance. Unlike Zahid et al. [303], who used spray coating with graphene-PEDOT:PSS, this study applied digital printing, which provided better polymer penetration, leading to improved stability after 35 washing cycles. Additionally, Ding et al. [304] reported PEDOT:PSS coatings on polyurethane nonwovens with surface resistance between 35–240  $\Omega/\text{cm}^2$ , stable up to 50% strain, but without detailed washing durability analysis. In contrast, this research shows that the PFSH-p sample exhibited the lowest color change and the best conductivity retention, with linear resistance increasing from  $20 \times 10^3 \Omega/\text{cm}^2$  to only  $26 \times 10^3 \Omega/\text{cm}^2$  after 35 washes (Figure 36). The results highlight that combining plasma treatment, Tubicoat crosslinking, and digital printing provides a superior method for improving the wash fastness of conductive wool textiles,

making them more suitable for wearable electronics and smart textile applications.

#### 5.1.10 Conductance atomic force microscopy (CS-AFM)

Conductance Atomic Force Microscopy (CS-AFM) images show the topography and electrical conductivity of wool samples. The initial tests on the wool sample were carried out at a current of 1-5 V, but the result of the CS-AFM at 2 pA shows that there is no electrical conductivity (Figure 37). For coated wool (PFSH-p, Figure 37) fabric, a current of 1 V shows an electrical conductivity of 10 nA, the highest that can be measured with the CS-AFM. From the images it can be seen that the coating is not very uniform (red spots), but this should be sufficient when looking at the total area (Figure 37).

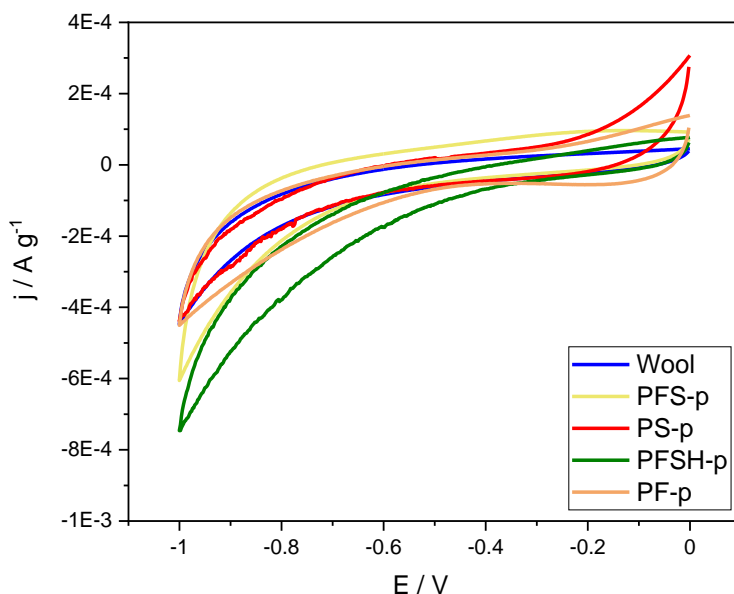


**Figure 37.** Topography and current distribution - electrical conductivity distribution of tissue samples of wool (a, b, c) and coated wool (PFSH-p) (d, e, f).

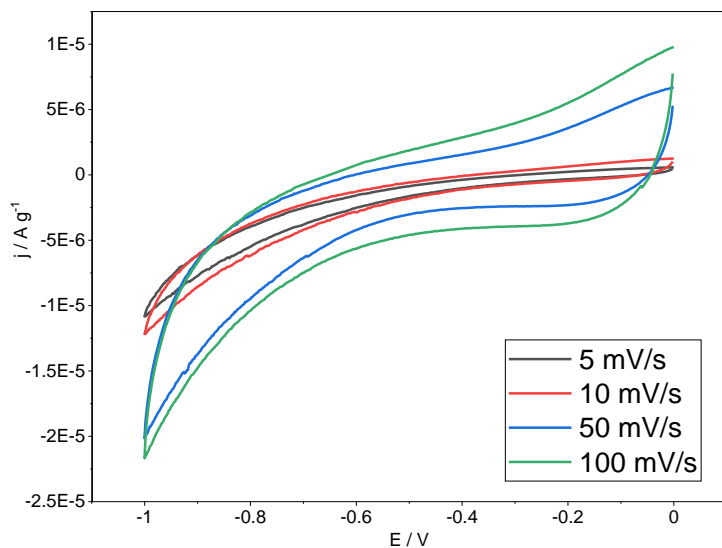
#### 5.1.11 Cyclic voltammetry measurements

Applying cyclic voltammetry (CV) measurement was observed that the samples with different conductive coatings was stable over 5 cycles. In CVs cycle graphs comparing different coating on textile samples shown that charge and discharge results was stable (Figure 38). Comparison of the different PEDOT:PSS polymer coating methods showed that the Clevios S V3 (PS-p) coating has better electrochemical properties in electrolyte (PVA-KOH),

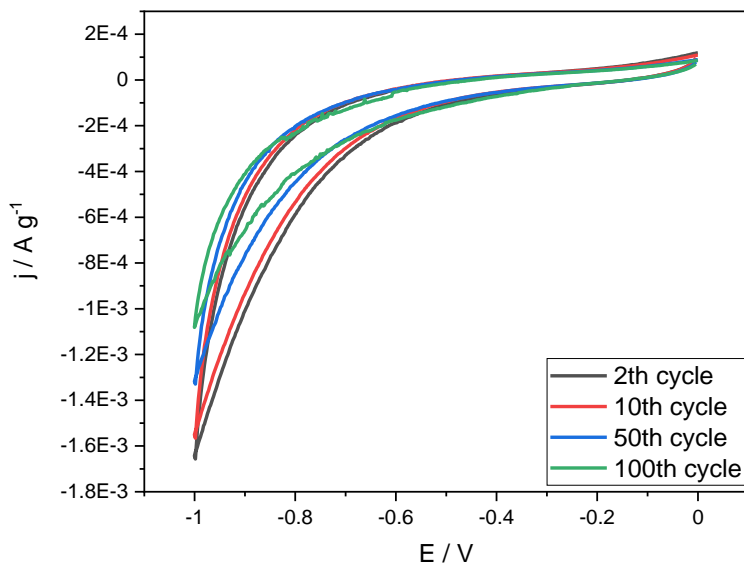
passes a higher current (mainly oxidation/reduction reactions). PFSH-p remained conductive and electrochemically stable after 100 charge-discharge cycles (Figure 40), which means it can be used in reusable devices (supercapacitors, sensors, E-textiles, etc). Different scan rate was chosen for wool samples PFSH-p (Figure 39). The presented graph shows the cyclic voltammetry (CV) response of the PFSH-p coated wool fabric at different scan rates (5, 10, 50, and 100 mV/s). The shape and area of the curves indicate typical pseudocapacitive behavior, suggesting that the material exhibits good electrochemical charge storage properties. As the scan rate increases, the current also increases, demonstrating efficient charge transfer and electrical conductivity. These results confirm that the PFSH-p coating enhances the wool fabric's potential for use in flexible energy storage devices.



**Figure 38.** Cyclic voltammogram of the wool fabric coated with PEDOT:PSS by different coating methods, measured at a potential window between -1 V and 0 V and a scan rate of 10 mV/s.



**Figure 39.** Cyclic voltammogram of PFSH-p wool fabric sample at the scan rate of 5, 10, 50 and 100 mV/s.



**Figure 40.** Cyclic voltammogram of PFSH-p wool fabric sample at the scan rate 10mV/s after 2, 10, 50 and 100 cycles. The measurement was performed at a potential window between -1 V and 0 V and a scan rate of 10 mV/s.

All coated samples have a higher specific capacity than the wool substrate. The capacitance of samples PF-p ( $7.83\text{E-}03$  F/g) and PFS-p ( $7.30\text{E-}03$  F/g) was approximately twice that of the initial sample (Table 28). Table 28 shows



that PF has the highest specific capacitance across all scan rates, indicating it may be the most efficient at storing charge. As the scan rate increases, the specific capacitance decreases for all coatings, which suggests that at faster scan rates, the materials become less capable of storing charge efficiently. Wool samples with PEDOT:PSS coating could be used as flexible supercapacitors by optimising the electrode composition and increasing their conductivity [279].

**Table 28.** Varying composition of conductive coating on wool fabric with specific capacitance at different scan rates.

Composition of investigated wool fabric samples	Specific capacitance, F/g			
	Scan rate			
	5 mV/s	10 mV/s	50 mV/s	100 mV/s
Wool	4.04E-03	3.43E-03	1.89E-03	1.54E-03
PF	7.83E-03	6.05E-03	4.12E-03	3.65E-03
PFS	7.30E-03	6.31E-03	3.16E-03	2.48E-03
PS	6.72E-03	4.52E-03	2.57E-03	2.18E-03
PFSH	5.56E-03	4.58E-03	3.24E-03	2.32E-03

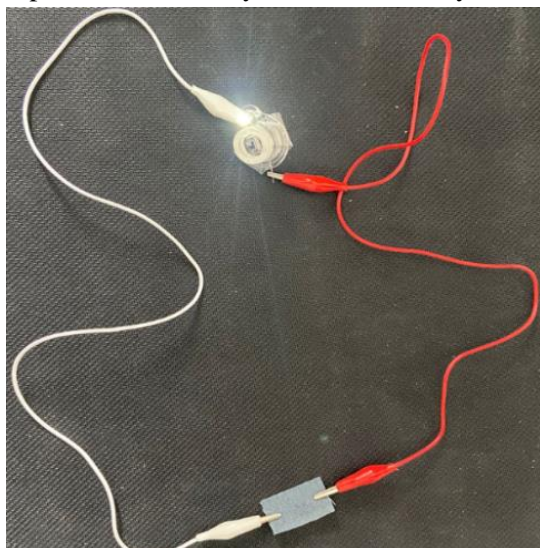
#### 5.1.12 PEDOT:PSS coated wool fabric electroconductivity demonstration

The experiment demonstrated the electrical conductivity properties of PEDOT:PSS-coated wool fabric. As shown in Figure 41, the fabric successfully conducts electricity from a direct current (DC) source, illuminating an LED in a series circuit. This confirms that the developed conductive wool fabric possesses sufficient conductivity for potential applications in e-textiles. Similar prototypes have previously been developed using carbon nanotubes [280] and silver nanoparticles [281]; however, these approaches often face challenges related to stability and environmental impact.

Recent studies have shown that PEDOT:PSS exhibits excellent electrical properties while maintaining textile flexibility and breathability, making it a promising alternative to traditional conductive textiles [282]. Zhang et al. (2023) demonstrated that PEDOT:PSS-coated materials can be effectively used in sensors and wearable electronic systems, though their water resistance remains a challenge[308]. This study builds upon these findings by applying PEDOT:PSS to wool fabric and proving not only its retained conductivity but also its mechanical flexibility, which is crucial for wearable electronics. Additionally, wool fabric naturally offers better environmental resistance

compared to synthetic substrates, providing an advantage in durability and sustainability [309].

This result is particularly significant because the PEDOT:PSS coating allows the textile to retain its softness and flexibility, unlike metallized or carbon-based conductive textiles, which are often more rigid and less resistant to mechanical deformations. Moreover, the flexibility of textile-based electrodes is a key factor in the development of supercapacitors for wearable electronics. The findings of this study suggest that PEDOT:PSS-coated wool fabrics could serve as a promising alternative to conventional conductive textiles, offering superior functionality and sustainability benefits [310].

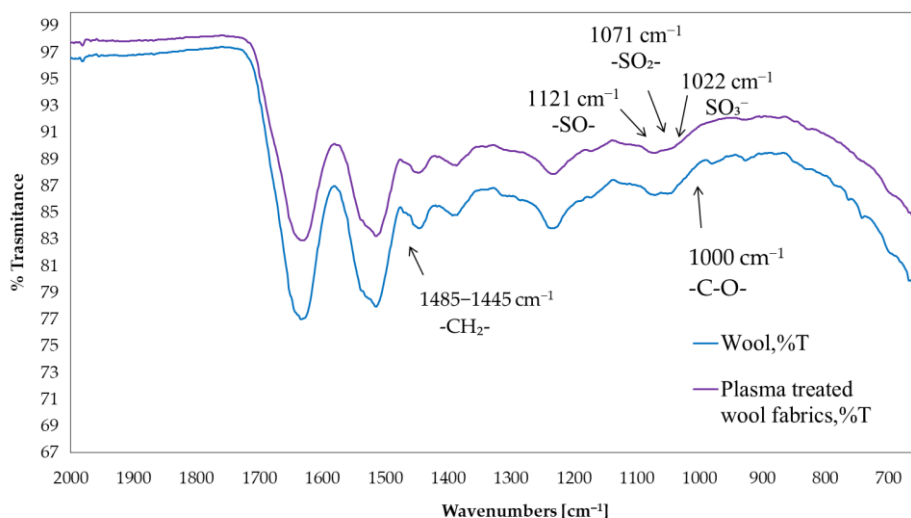


**Figure 41.** Demonstration of the conductive wool fabric with PEDOT:PSS circuit for lighting up an LED bulb.

#### 5.1.13 FTIR-ATR mode measurement

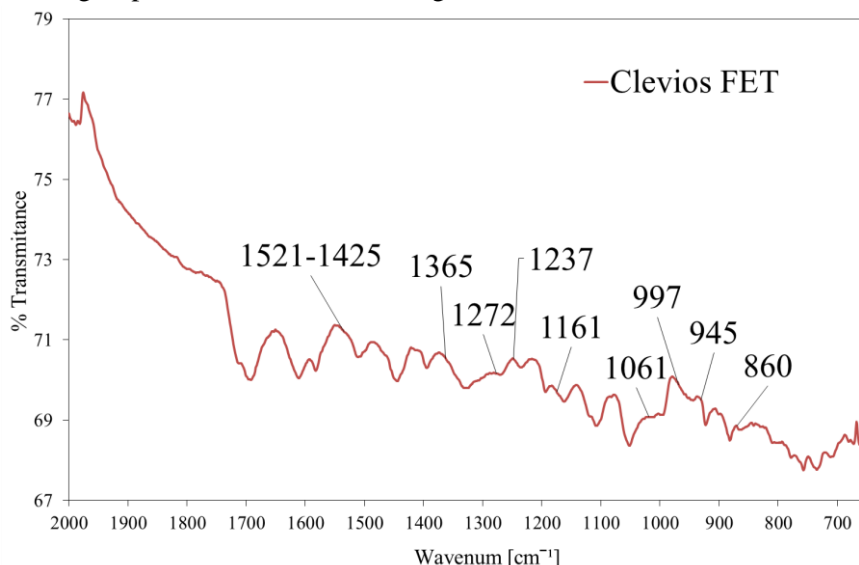
Attenuated total reflectance (ATR) infrared spectra of the untreated and plasma-treated wool samples are shown in Figure 42. As with J. Udakhe [296], it was found that two sharp peaks in the range of 2935–2915 and 2865–2845  $\text{cm}^{-1}$  are present in untreated fabric corresponding to methylene group's  $-\text{CH}_2-$  asymmetric/symmetric stretch and correspondingly in the range of 1485–1445  $\text{cm}^{-1}$  to the methylene (C–H) bend. Intensity of these peaks in the untreated sample is high, but after plasma modification the area of all these peaks was reduced [311]. Both spectra show that these bands can be assigned to the amide I and amide II oscillations, which are slightly shifted at 1600  $\text{cm}^{-1}$ . They show the combination of C=O and N–H modes of amides. There

is an H–O–H bending vibration at  $1640\text{ cm}^{-1}$ . There is an H–O–H bending mode at  $1640\text{ cm}^{-1}$ . M. Mori and N. Inagaki suggested that the intensity of the amide I peak should be increased after plasma treatment [296], but no significant change was detected in this study. After plasma treatment, Bunte salt ( $-\text{S}-\text{SO}_3-$ ) formation at  $1022\text{ cm}^{-1}$  is probably related to improved shrink-resistance properties of wool similarly detected by C. W. Kan [285]. Besides Bunte salt formation, cysteic acid was also formed as a result of the cleavage of disulphide linkage. In addition to Bunte salt and cysteic acid, other interesting cystine residues formed after plasma modification, namely, cystine monoxide ( $-\text{SO}-\text{S}-$ ) and cystine dioxide ( $-\text{SO}_2-\text{S}-$ ). This indicates the oxidation of  $-\text{S}-\text{S}-$  in the surface of wool after plasma treatment [312]. Cystine monoxide and cystine dioxide are interesting because they represent a more reactive form than the parent disulphide. The cysteic acid in the polypeptide chain, together with the Bunte salt, provide a polar surface for the wool fabric, which helps to improve the wool fabric's wettability [313]. Further, the cleavage of the disulphide bonds helps to remove the surface barrier of the wool fiber. The formation of cystine monoxide and cystine dioxide in wool generates a more reactive substrate, which provides a suitable site for introducing agents, such as dyes and softeners, carrying nucleophilic reactive groups [314]. Furthermore, it was found that plasma treatment modified pores on the fiber surface, creating a pathway for the penetration of caustic species into the fiber during the alkali solubility test [315].



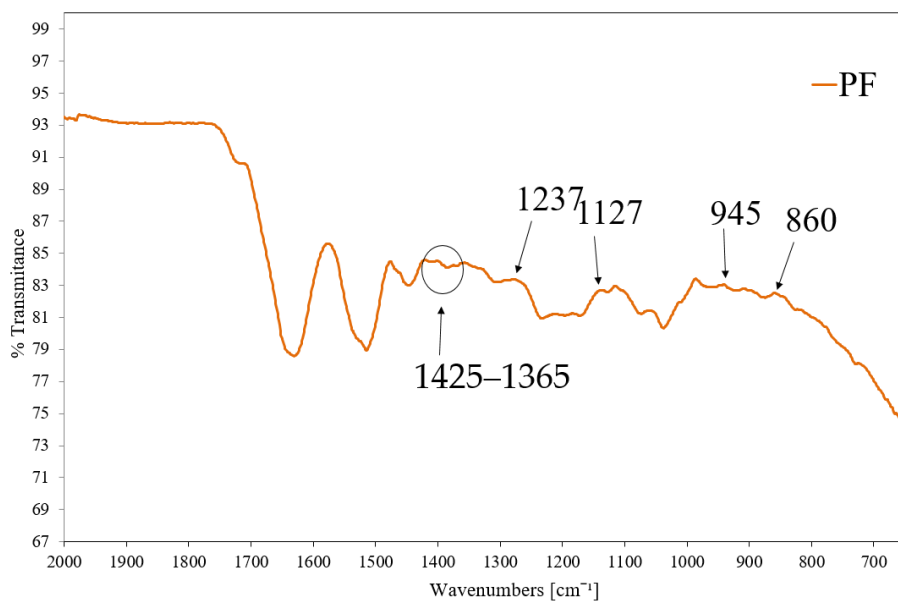
**Figure 42.** FTIR-ATR spectra illustrating untreated and plasma-treated wool fabric.

FTIR-ATR spectra of chemical structure of the Clevios F ET is presented in Figure 43. Similar to Hui Chung Chang and other scientists [316], the major absorption peaks were found at 1161–1170  $\text{cm}^{-1}$  symmetric and asymmetric stretch sulfonic acid ( $\text{SO}_3^-$ ) group of PSS, 1061–945  $\text{cm}^{-1}$  (C–O–C stretching), 945–860  $\text{cm}^{-1}$  (C–S) stretching and 1272  $\text{cm}^{-1}$  (C=C and C–C stretching of the quinoidal structure of PEDOT). The PEDOT:PSS film showed significant peaks at around 1425  $\text{cm}^{-1}$  and 1521  $\text{cm}^{-1}$  due to thiophene C=C symmetric and asymmetric stretching vibrations, respectively, while the peak at 1365  $\text{cm}^{-1}$  was attributed to C–C stretching vibrations of thiophene rings. In addition, the peaks at 1237  $\text{cm}^{-1}$  and 997  $\text{cm}^{-1}$  have been attributed to  $\text{CH}_2$  group rotation and C–O–C ring deformation [317,318].



**Figure 43.** FTIR-ATR spectra illustrating the chemical composition of the Clevios F ET.

FTIR-ATR spectra of wool fabric after  $\text{N}_2$  plasma and PEDOT PSS treatments is presented in Figure 44. All the mentioned peaks from the PEDOT:PSS dyed wool fiber were almost similar to the pristine film of PEDOT:PSS aqueous dispersion, Clevios F ET, (Figure 43). The successful interpolation of the PEDOT:PSS as conductive acid dye [11] on the wool fabric surface was evidenced by the presence of the peaks at 1425  $\text{cm}^{-1}$  and 1365  $\text{cm}^{-1}$ , which correspond to the C = C and C–C stretching vibrations originating from the thiophene ring and increased absorption of PSS at 1127  $\text{cm}^{-1}$  (sulfonic acid group). Mingwei Tian et al. found similar PEDOT:PSS peaks at 1517  $\text{cm}^{-1}$  and 1300  $\text{cm}^{-1}$  on cotton fabric surfaces [315].

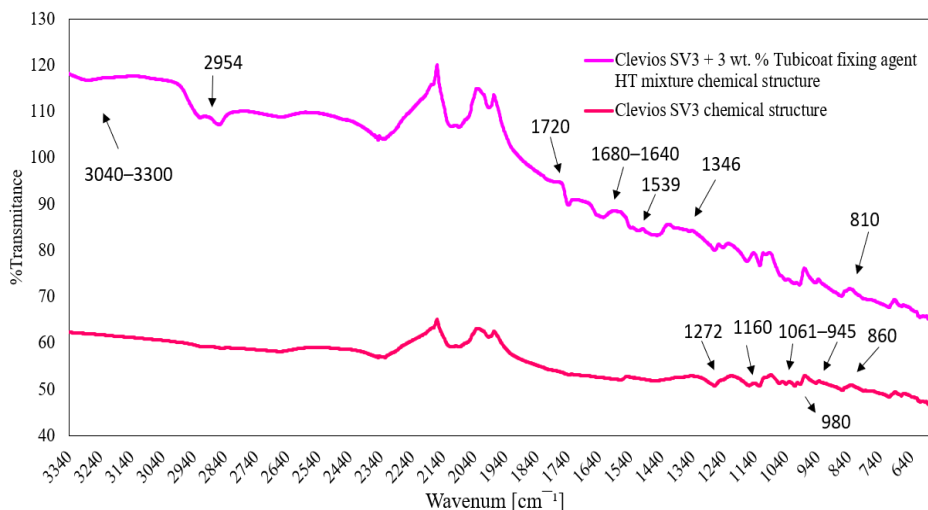


**Figure 44.** FTIR-ATR spectra of wool fabric after plasma treatment and dyeing in exhaust with PEDOT:PSS commercially available water dispersion Clevios F ET.

FTIR-ATR spectra of the chemical structure of the pristine Clevios S V3 and composition of Clevios S V3 + 3 wt. % Tubicoat fixing agent HT spectra are presented in Figure 44. The principal absorption peaks of the PEDOT:PSS water dispersion in the form of Clevios S V3 were discovered at  $1160\text{ cm}^{-1}$ , corresponding to the symmetric and asymmetric stretch vibrations of the PSS sulfonic acid group [296,301,319]. The C–S bond stretching vibrations in the thiophene ring are responsible for the absorption peaks at approx. 860 and  $980\text{ cm}^{-1}$  [320,321], as well as the C–O–C stretching at  $1061$  and  $945\text{ cm}^{-1}$  and the C=C and C–C stretching in the quinoidal structure of PEDOT at  $1272\text{ cm}^{-1}$  [322,323] (Figure 45).

IR spectra of sample Clevios S V3 + 3 wt. % Tubicoat fixing agent HT can be found in melamine resin from the band between  $3040$  and  $3300\text{ cm}^{-1}$ , with poor signal intensity, suggesting the potential O–H bond stretching vibration and N–H stretching vibration in primary aryl amines (Figure 44). These bands demonstrated that the cross-linking of formaldehyde and melamine was successful. The stretching vibration of C–H corresponds to the band of  $2954\text{ cm}^{-1}$ . Additionally, the methane vibration is represented by the new peak at roughly  $1346\text{ cm}^{-1}$  [323]. The wavenumbers of amino-substituted triazines, which would exhibit a distinct absorption band in the range  $1680$ – $1640\text{ cm}^{-1}$ , can be because of the reduced number of unreacted amino groups

in the resin structure. The absorption band at  $810\text{ cm}^{-1}$  corresponds to the out-of-plane bending vibrations of C–H bonds. Another clue that a tiny amount of aldehyde is still not engaged in the cross-linking process of melamine resin is the faint signal detected at  $1720\text{ cm}^{-1}$  (a band characteristic for the C=O group) (Figure 45).



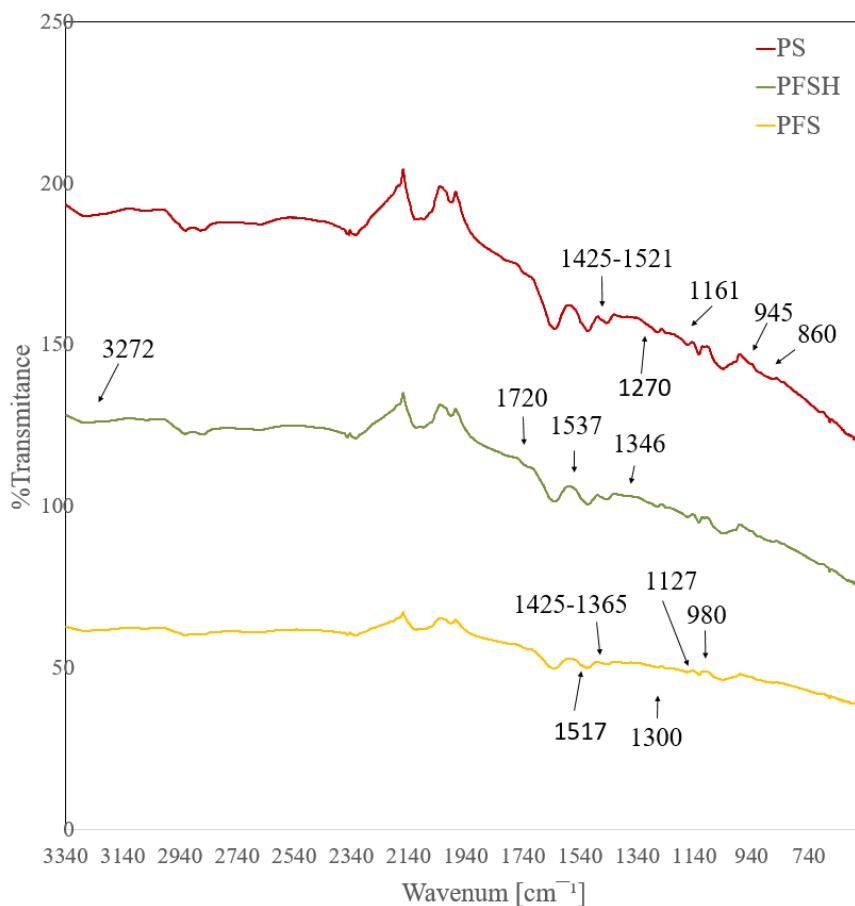
**Figure 45.** ATR infrared spectra of the Clevios S V3 with Tubicoat fixing agent HT and Clevios S V3 chemical structure.

FTIR-ATR infrared spectra of plasma treated samples: dyed with Clevios F ET and coated with Clevios S V3 (PFS) and Clevios F ET/Clevios S V3 + 3 wt. % Tubicoat fixing agent HT (PFSH) are shown in Figure 46. The peaks from the wool fiber covered with PEDOT:PSS were nearly identical to the pure film of PEDOT:PSS dispersion. The principal peaks of the sample (PS) absorption were located at  $1161\text{ cm}^{-1}$  (sulfonic acid group of PSS),  $945\text{ cm}^{-1}$  and  $860\text{ cm}^{-1}$  (C–S stretching), and  $1270\text{ cm}^{-1}$  (C=C and C–C stretching of the quinoidal structure of PEDOT) [316,323] (Figure 46). Specific wavelengths of specific PEDOT: PSS absorption peaks were found in PFS sample spectra,—peaks at  $1127\text{ cm}^{-1}$  (sulfonic acid group) and  $1425\text{ cm}^{-1}$  (corresponding to the C=C and C–C stretching vibrations coming from the thiophene ring) were also found, showing that the PEDOT: PSS was successfully interpolated on the surface of the wool fabric (Figure 46) [321,324]. Similar PEDOT:PSS peaks were found by Mingwei Tian et al. on cotton fabric surfaces at  $1517\text{ cm}^{-1}$  and  $1300\text{ cm}^{-1}$  [301]. Similar spectra to Figure 45 are found on sample PFSH near  $3272\text{ cm}^{-1}$  and  $1537\text{ cm}^{-1}$ ,  $1346\text{ cm}^{-1}$  wavelength range. These results, when combined with the signal at  $1720\text{ cm}^{-1}$ , which represents the stretching vibrations of the C=O, may indicate that

there are still a few unreacted O–H molecules in the polymer and a small amount of aldehyde that is not yet involved in the cross-linking of melamine resin [325,326] (Figure 46).

The FTIR-ATR spectra further confirm the successful integration of PEDOT:PSS onto the wool fabric, highlighting distinct molecular interactions influenced by plasma treatment and the addition of the fixing agent. Notably, the shift in sulfonic acid and thiophene-related peaks between PS, PFS, and PFSH suggests variations in molecular organization and possible alterations in conductivity properties. The presence of a strong absorption band at  $1720\text{ cm}^{-1}$  in PFSH indicates residual carbonyl functionalities, which could affect the durability and long-term stability of the conductive coating. Additionally, the observed peak at  $3272\text{ cm}^{-1}$  in PFSH, absent in other samples, may imply hydrogen bonding interactions or moisture retention within the polymer matrix (Figure 46).

From a practical perspective, these spectral differences raise important considerations regarding the functional properties of the coated textiles. The changes in chemical structure could directly impact electrical conductivity, mechanical flexibility, and chemical stability. For instance, the incorporation of a fixing agent may enhance adhesion and washing durability but could also introduce structural modifications that alter charge transport efficiency. Similarly, residual unreacted groups in PFSH might influence the material's aging behavior, potentially affecting its performance in wearable electronics or sensing applications. Analysis, such as conductivity measurements and mechanical durability tests, determined these molecular modifications lead to significant improvements in textile-based electronic applications.

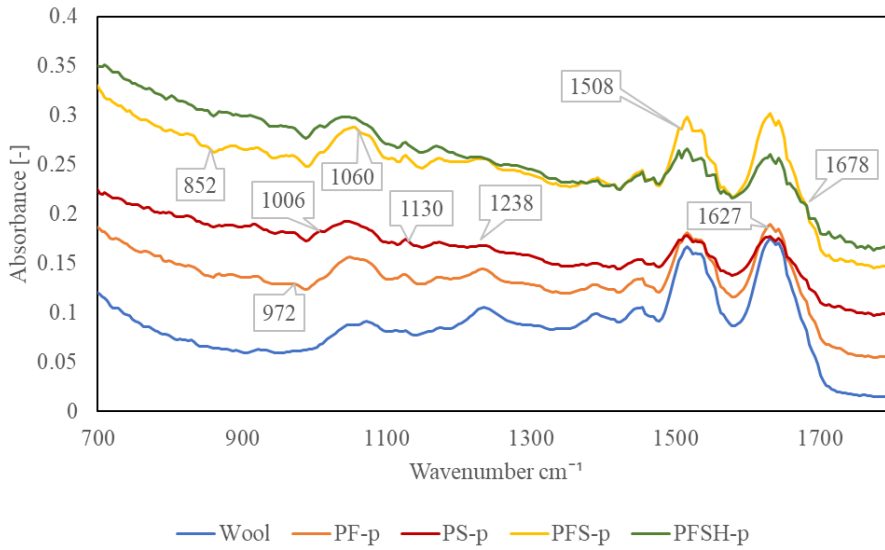


**Figure 46.** ATR infrared spectra of the wool samples PS, PFS, and PFSH.

FTIR-ATR spectra of the chemical structure of the wool composition with Clevios F ET and Clevios S V3 + 3 wt. % Tubicoat fixing agent HT (PFSH-p) spectra after digital printing method are presented in Figure 47. The principal absorption peaks of the PEDOT:PSS usually absorbs at  $1130\text{ cm}^{-1}$  of the PSS sulfonic acid group, and around  $1060\text{ cm}^{-1}$  of benzene sulfonate. The C–S bond stretching vibrations in the thiophene ring are responsible for the absorption peaks at approx.  $852$  and  $972\text{ cm}^{-1}$ , as well as the C–O–C stretching at  $1060\text{ cm}^{-1}$  and the C=C stretching in the quinoidal structure of PEDOT at  $1508\text{ cm}^{-1}$ . In addition, the peaks at  $1238\text{ cm}^{-1}$  and  $1006\text{ cm}^{-1}$  have been attributed to  $\text{CH}_2$  group rotation and C–O–C ring deformation [317,318]. The wavenumbers of amino-substituted triazines, which would exhibit a distinct absorption band in the range around  $1678\text{--}1640\text{ cm}^{-1}$ , can be because of the reduced number of unreacted amino groups in the resin structure.



From a practical perspective, these spectral variations provide valuable insights into the material's functional performance. The preservation of key PEDOT:PSS peaks suggests that the conductive polymer remains structurally intact after the printing process, which is crucial for maintaining electrical conductivity. Additionally, the presence of amino-substituted triazines in the  $1678\text{ cm}^{-1}$  range might contribute to enhanced adhesion and mechanical resilience, potentially improving the fabric's washing durability and wear resistance. The modifications observed in  $\text{CH}_2$  and  $\text{C-O-C}$  structures could also influence flexibility and mechanical properties, ensuring the fabric remains suitable for wearable electronic applications.



**Figure 47.** FTIR-ATR characterization of wool fabrics coated with Clevios products

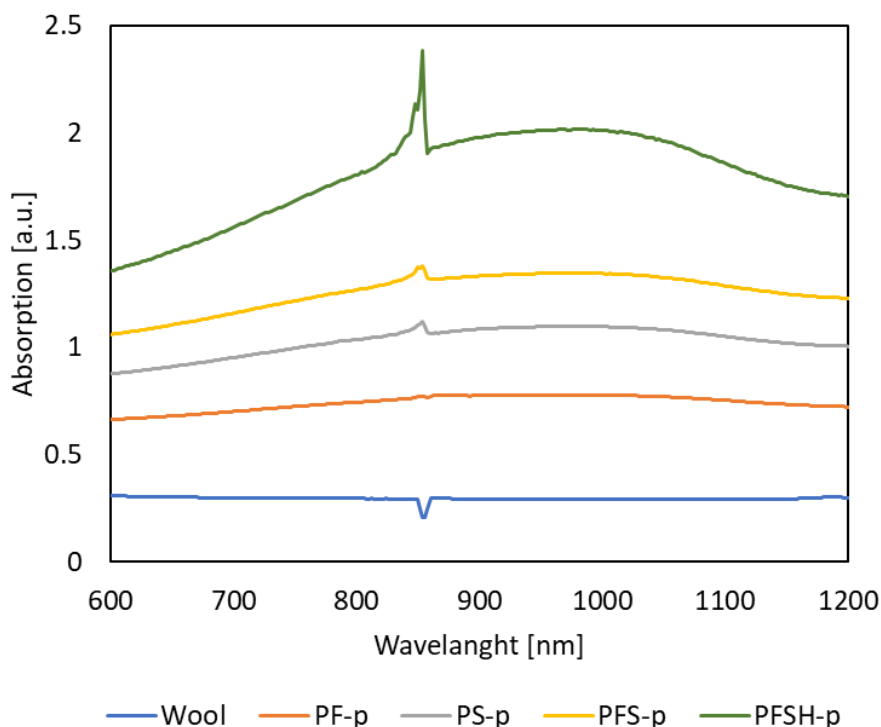
#### 5.1.14 VIS-NIR absorption spectra

Different PEDOT:PSS compositions on wool textile was investigated by the VIS/NIR absorption in the range of 600-1200 nm. Typically polaron bands of PEDOT observed in the visible region, around 600-900 nm. These bands are associated with singly charged states (polarons) in the polymer chain. Bipolaron bands we can find in the NIR region, often around 900-1200 nm (Figure 48). Bipolarons are doubly charged states that result in deeper energy states compared to polarons. Using the digital printing method, wool fabric obtained the highest absorption using Clevios FET and Clevios SV3 (PFSH-p, Figure 48). In PFSH-p PEDOT coated samples peaks can be found

at around 990 nm, which can be assigned to polaronic and bipolaron bands, characteristic of oxidized PEDOT with a large conjugation length [327]. Increased doping or oxidation of PEDOT leads to a higher density of charge carriers (polarons and bipolarons), which shifts the absorption peaks and increased the overall absorption in the NIR region. Highly doped PEDOT shows strong absorption in the NIR region, indicative of a high density of bipolarons. Additionally, the strong absorption in the PFSH-p sample suggests higher polymer crystallinity, which could improve charge transport properties. [328].

The PFSH-p sample exhibits the highest absorption due to the combined effects of digital printing, the Clevios FET and Clevios SV3 coatings, and the addition of Tubicoat fixing agent, which is a melamine-formaldehyde-based crosslinker. The presence of this crosslinker likely enhances the stability and fixation of PEDOT:PSS on the wool fabric, leading to stronger adhesion and a more uniform conductive coating. Additionally, melamine-formaldehyde resins are known for their ability to form covalent crosslinks, which may contribute to a denser PEDOT:PSS network, improving mechanical robustness and wash durability [329]. The increased crosslinking density could also influence polymer oxidation and doping levels, leading to a higher concentration of charge carriers (polarons and bipolarons) and, consequently, greater absorption in the NIR region (900–1200 nm) [330]. The characteristic absorption peak around 990 nm confirms the presence of highly oxidized PEDOT with an extended conjugation length, which is typically associated with enhanced electrical conductivity [331]. Furthermore, the improved molecular organization resulting from crosslinking could increase PEDOT crystallinity, thereby further enhancing charge carrier mobility and optical absorption [332]. These factors collectively indicate that the synergistic effect of crosslinking, improved adhesion, and optimized molecular ordering leads to higher absorption and conductivity, making this system highly suitable for conductive textile applications.

These findings reinforce the relationship between doping levels, oxidation states, and material functionality, suggesting that increased absorption in the NIR region correlates with enhanced electrical properties, which could be beneficial for applications in conductive textiles and smart fabrics.



**Figure 48.** Wool with different coating absorption in the VIS-NIR-range.

#### 5.1.15 XPS surface analysis

Table 29 presents the elemental analysis and atomic ratio of wool fibers before and after nitrogen plasma treatment. The data indicate significant changes in surface composition, particularly in carbon (C), nitrogen (N), oxygen (O), and sulfur (S) content, which provide insights into the chemical modifications induced by plasma activation. After 120 seconds of nitrogen plasma treatment, the relative atomic concentration of carbon decreased by 3.22%, suggesting the removal of organic surface contaminants and partial degradation of the outer lipid layer of the wool fiber [298]. In contrast, the oxygen concentration increased by 0.56%, likely due to oxidation reactions facilitated by reactive plasma species, leading to the incorporation of functional oxygen-containing groups (-OH, -C=O, -COOH) [333]. The most notable change is the increase in nitrogen content from 8.46% to 15.62%, which indicates the successful incorporation of nitrogen functional groups (-NH-, -NH<sub>2</sub>, -C≡N) onto the fiber surface, as observed in previous plasma treatment studies [334]. Additionally, a slight increase in sulfur content

suggests some degradation of disulfide bonds (-S-S-) within the keratin structure, which could influence the fiber's structural integrity and reactivity [335].

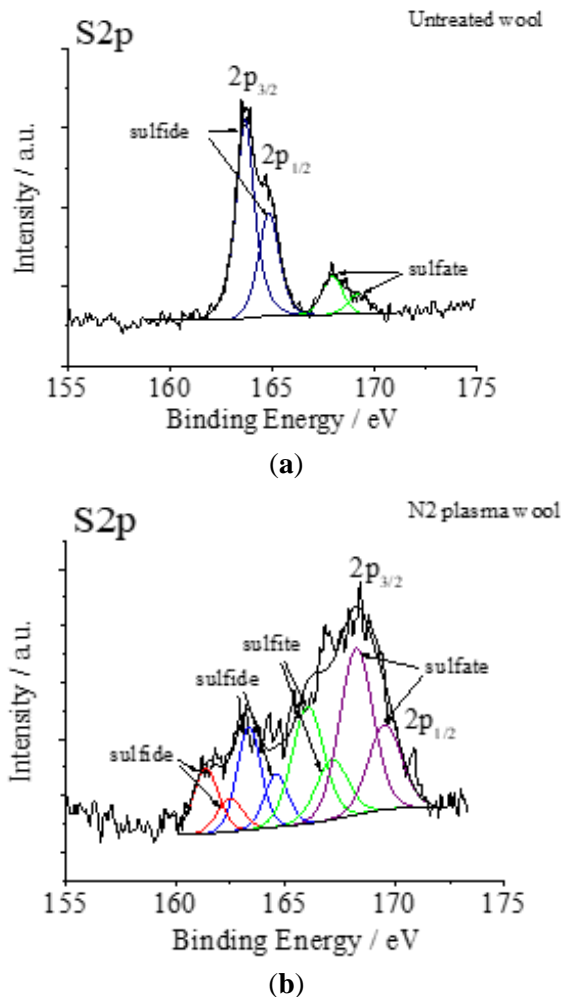
These chemical modifications have a direct impact on the wool fiber's surface properties, particularly in relation to electrical conductivity and coating adhesion. The increase in nitrogen content enhances surface polarity, leading to improved wettability and hydrophilicity, which are crucial for stronger interactions with conductive polymer coatings such as PEDOT:PSS [333]. This improved adhesion can lead to more uniform coating deposition, reducing the risk of delamination and enhancing long-term durability. Furthermore, the increase in oxygen-containing functional groups contributes to higher surface energy, promoting stronger hydrogen bonding and electrostatic interactions with PEDOT:PSS, which can enhance charge transport across the coated fabric [298]. Conversely, the decrease in carbon content and partial degradation of the cuticle layer may increase surface roughness, further improving mechanical interlocking between the polymer coating and the fiber [334,336]. These factors combined suggest that nitrogen plasma treatment optimizes the wool fiber for conductive textile applications by improving coating adhesion, charge carrier mobility, and overall electrical conductivity, making it a valuable pre-treatment for functional and smart textile development.

**Table 29.** Element analysis (wt. %) and atomic ratio of wool treated with nitrogen plasma gas.

Sample	Elemental Concentration (wt. %)					Atomic Ratio		
	Si2p	C1s	Ca2p	N1s	O1s	S2p	C/N	O/C
Untreated	1.00	72.16	0.79	8.46	15.08	2.51	8.53	0.20
After plasma treatment	1.69	50.3	1.22	15.62	28.13	3.04	3.22	0.56

XPS spectra of untreated and N<sub>2</sub> gas plasma-treated wool fabrics are shown in Figure 49. For untreated wool fiber (Figure 49a), the S2p region consists of two broad peaks at 163.6 eV and 167.9 eV, corresponding to disulfide (-S-S-) groups in cystine residues and oxidized sulfur species (e.g., sulfonates or sulfones), respectively. After plasma treatment (Figure 49b), the intensity of the oxidized sulfur peak (~168.2 eV) increases relative to the lower binding energy peak (163.3 eV), indicating sulfur oxidation at the fiber surface [298]. This shift suggests that disulfide bonds are converted into cysteic acid (-SO<sub>3</sub>H) or sulfate groups (-SO<sub>4</sub><sup>2-</sup>), contributing to increased surface hydrophilicity and coating adhesion [333]. The broad peak at ~168 eV further

indicates possible intermediate oxidation states, consistent with a stepwise oxidation mechanism of cystine residues [334]. These changes in sulfur chemistry may significantly enhance polymer coating adhesion and wettability, making plasma treated wool a promising substrate for conductive coatings such as PEDOT:PSS.



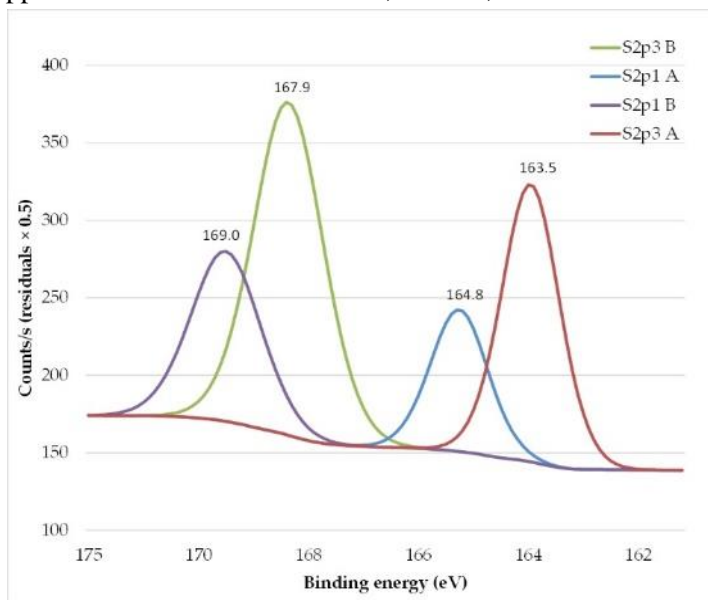
**Figure 49.** XPS spectra S2p peaks of wool fabric: untreated (a) and after N<sub>2</sub> plasma treatment (b).

The chemical structure of PEDOT:PSS was analyzed using X-ray Photoelectron Spectroscopy (XPS), and the obtained spectra are shown in Figure 50. The S2p spectrum (Figure 50a) exhibits two distinct doublets (S2p<sub>3/2</sub> A and S2p<sub>3/2</sub> B), corresponding to the two different sulfur chemical states in PEDOT:PSS. The thiophene-derived sulfur from PEDOT appears at 163.5 eV and 164.8 eV, whereas the oxidized sulfur species from PSS, such

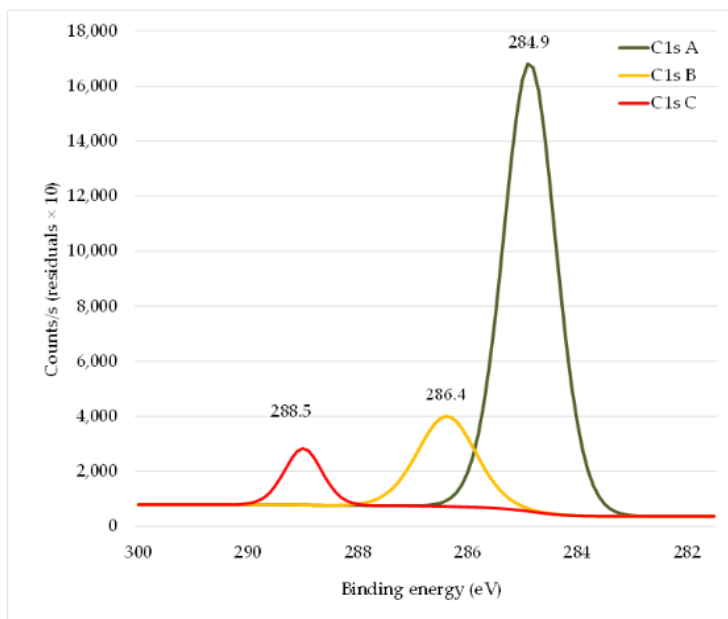
as sulfone ( $-\text{SO}_2-$ ) and sulfonate ( $-\text{SO}_3^-$ ) groups, are found at 167.9 eV and 169.0 eV, respectively [335]. This distribution confirms the presence of both conjugated thiophene structures from PEDOT and oxidized sulfonate functionalities from PSS, which are crucial for the electronic and ionic conductivity of PEDOT:PSS-based materials.

The C1s core-level spectrum (Figure 50b) was deconvoluted into three primary peaks. The strongest peak at 284.9 eV corresponds to conjugated and saturated carbon atoms in both PEDOT and PSS chains, forming the backbone of the polymer structure. The shoulder peak at 286.4 eV is attributed to the C–O–C ether bonds in PEDOT, which play a key role in the polymer’s electronic delocalization [304]. Additionally, the lower intensity peak at 288.5 eV is associated with C=O bonds, likely due to some oxidized PEDOT resonant structures or potential crosslinking interactions [337]. Notably, the carbon atoms directly bonded to the sulfonate ( $-\text{SO}_3^-$ ) groups in PSS exhibit only a slight shift towards higher binding energy, meaning their contribution remains within the 284.9 eV peak [338].

These findings confirm the expected chemical composition and electronic structure of PEDOT:PSS, supporting its role as a conductive polymer with ionic and electronic transport properties. The XPS data further indicate that the polymer maintains a stable oxidation state, which is crucial for its application in flexible electronics, sensors, and conductive textiles.



(a)

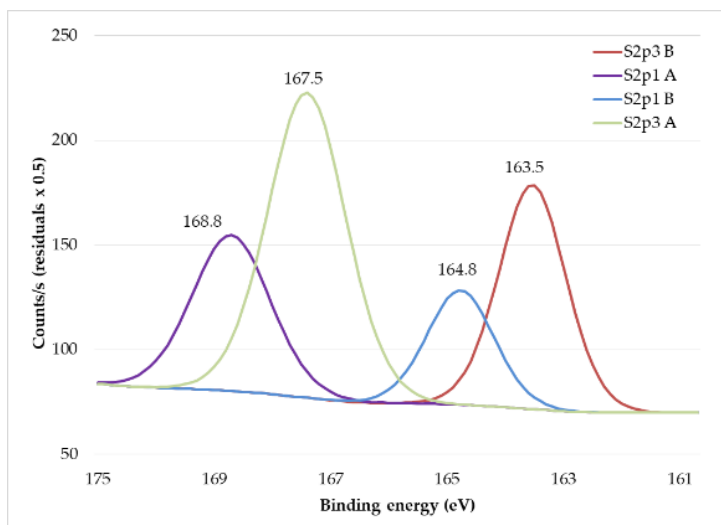


(b)

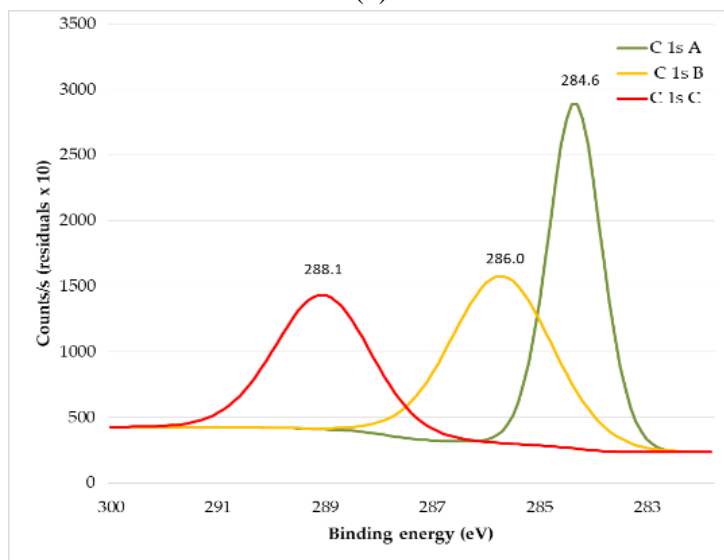
**Figure 50.** XPS spectra of the chemical composition of the PEDOT:PSS: S2p spectra (a) and C (1s) spectra (b).

The XPS spectra of N<sub>2</sub> plasma-treated wool fabric coated with PEDOT:PSS water dispersion (Clevios F ET-dyed), presented in Figure 51, confirm the successful deposition of the conductive polymer. The S2p spectrum (Figure 51a) reveals the presence of PEDOT and PSS, with the thiophene doublet at 163.5 eV and 164.8 eV showing an asymmetric tail extending towards higher binding energies, attributed to positive charge delocalization in the oxidized PEDOT chain. The sulfonate ( $-\text{SO}_3^-$ ) peak at 167.5 eV confirms the presence of PSS. An increase in the relative intensity of PEDOT-related peaks suggests partial removal of PSS during the coating process, leaving behind a higher PEDOT concentration on the wool surface. The C1s spectrum (Figure 51b) further supports this observation, with the appearance of a small peak at 288.1 eV, assigned to C=O bonds in PEDOT resonance structures, whose intensity increases with higher PEDOT content. Additionally, the sulfonate peaks shift towards lower binding energies, indicating a decrease in sulfonic acid ( $-\text{SO}_3\text{H}$ ) content relative to sulfonate counterions, likely due to interactions between PEDOT:PSS and the wool fiber surface. Comparing these spectra with the pristine PEDOT:PSS formulation (Clevios F ET) confirms that the same PEDOT and PSS

signatures are present, verifying that the fabric was successfully coated with PEDOT:PSS and acquired electrically conductive properties [339].



(a)



(b)

**Figure 51.** XPS spectra of wool fabric: N<sub>2</sub> plasma-treated and PEDOT:PSS water dispersion Clevious F ET dyed: S2p spectra (a) and C (1s) spectra (b).



## CONCLUSION

1. Scanning electron microscopy images confirmed that nitrogen plasma surface modification improved the uniformity and penetration of the PEDOT:PSS coating into the wool fibers, while the binder enhanced the coating's adhesion and integrity. FTIR-ATR and XPS spectroscopic analysis verified the formation of the PEDOT:PSS coating, revealed the presence of oxidized sulfur compounds, and indicated increased surface hydrophilicity after plasma treatment, which facilitated better fixation of the coating.

2. The formation of PEDOT:PSS coatings on wool fabric was carried out using three methods: dyeing, screen printing and digital printing. During these methods, coating parameters were optimized to suit the wool substrate and the acidic PEDOT:PSS dye. The most wear resistant coating with the best electrical conductivity was achieved using the sustainable digital printing method.

3. Among the wool samples coated with different PEDOT:PSS composites and methods, the sample PFSH-p, which was treated with nitrogen plasma and coated using digital printing with a mixture of Clevios F ET, Clevios S V3, and the Tubicoat fixing agent HT, showed the lowest linear electrical resistance after friction and 35 washing cycles ( $35\ \Omega/\text{cm}$ ), retained an intense color, and preserved the wool fiber structure. Additionally, this sample exhibited higher NIR absorption, indicating a greater amount of bipolarons and better electrical conductivity.

4. For the first time, the effect of the PEDOT:PSS coating on the electrical conductivity of wool fabric was investigated using current-sensing atomic force microscopy (CS-AFM). The measured current of the PFSH-p sample reached 10 nA, while uncoated wool showed a significantly lower current (2 pA). Although the coating was not fully uniform at the microscale, the macroscopic conductivity was sufficient.

5. The sample treated with nitrogen plasma and coated via digital printing with a mixture of Clevios F ET, Clevios S V3, and Tubicoat fixing agent HT (PFSH-p) remained conductive and electrochemically stable after 100 charge–discharge cycles, suggesting its potential for use in reusable devices. The PEDOT:PSS composition of the coated samples exhibited a higher specific capacitance compared to the wool substrate, indicating potential for application in rechargeable devices.

6. A sustainable PEDOT:PSS textile coating technology was developed: surface modification with nitrogen plasma and digital printing with a mixture of Clevios F ET, Clevios S V3, and Tubicoat fixing agent HT. The resulting coating is electrically conductive and wear-resistant, maintains textile

properties, and can be applied in wearable electronic devices (e.g., antistatic garments, smart textiles, sensors, etc.).

## REFERENCES

1. Van Langenhove, L., Puers, R., & Matthys, D. (2005). Intelligent textiles for protection. *Textiles for protection*, 176-195.
2. Cherenack, K., & Van Pieterse, L. (2012). Smart textiles: Challenges and opportunities. *Journal of Applied Physics*, 112(9).
3. Van Langenhove, L. (2013). Smart textiles for protection: an overview. *Smart textiles for protection*, 3-33.
4. Koncar, V. (2016). Introduction to smart textiles and their applications. In *Smart textiles and their applications* (pp. 1-8). Woodhead Publishing.
5. Kongahage, D., & Foroughi, J. (2019). Actuator materials: review on recent advances and future outlook for smart textiles. *Fibers*, 7(3), 21.
6. Köhler, A. R. (2013). Challenges for eco-design of emerging technologies: The case of electronic textiles. *Materials & Design*, 51, 51-60.
7. Rotzler, S., von Krshiwoblozki, M., Kallmayer, C., & Schneider-Ramelow, M. (2025). Washability of E-Textiles: Washing Behavior of Textile Integrated Circuits Depending on Textile Substrate, Circuit Material and Integration Method. *Advanced Functional Materials*, 35(11), 2417344.
8. Tseghai, G. B., Mengistie, D. A., Malengier, B., Fante, K. A., & Van Langenhove, L. (2020). PEDOT: PSS-based conductive textiles and their applications. *Sensors*, 20(7), 1881.
9. Rubeziene, V., Baltusnikaite-Guzaitiene, J., Abraitiene, A., Sankauskaite, A., Ragulis, P., Santos, G., & Pimenta, J. (2021). Development and investigation of PEDOT: PSS composition coated fabrics intended for microwave shielding and absorption. *Polymers*, 13(8), 1191.
10. Guo, Y., Otley, M. T., Li, M., Zhang, X., Sinha, S. K., Treich, G. M., & Sotzing, G. A. (2016). PEDOT: PSS “wires” printed on textile for wearable electronics. *ACS Applied Materials & Interfaces*, 8(40), 26998-27005.
11. Lund, A., van der Velden, N. M., Persson, N. K., Hamed, M. M., & Müller, C. (2018). Electrically conducting fibres for e-textiles: An open playground for conjugated polymers and carbon nanomaterials. *Materials Science and Engineering: R: Reports*, 126, 1-29.
12. Kaynak, A. (2016). Conductive polymer coatings. In *Active coatings for smart textiles* (pp. 113-136). Woodhead Publishing.
13. Ding, Y., Invernale, M. A., & Sotzing, G. A. (2010). Conductivity trends of PEDOT-PSS impregnated fabric and the effect of conductivity on electrochromic textile. *ACS applied materials & interfaces*, 2(6), 1588-1593.
14. Otley, M. T., Alamer, F. A., Guo, Y., Santana, J., Eren, E., Li, M., ... & Sotzing, G. A. (2017). Phase segregation of PEDOT: PSS on textile to

produce materials of  $> 10 \text{ A mm}^{-2}$  current carrying capacity. *Macromolecular Materials and Engineering*, 302(3), 1600348.

15. Åkerfeldt, M., Strååt, M., & Walkenström, P. (2013). Electrically conductive textile coating with a PEDOT-PSS dispersion and a polyurethane binder. *Textile Research Journal*, 83(6), 618-627.

16. Gordon, W. O., Peterson, G. W., & Durke, E. M. (2015). Reduced chemical warfare agent sorption in polyurethane-painted surfaces via plasma-enhanced chemical vapor deposition of perfluoroalkanes. *ACS Applied Materials & Interfaces*, 7(12), 6402-6405.

17. Hegemann, D., Brunner, H., & Oehr, C. (2003). Plasma treatment of polymers for surface and adhesion improvement. *Nuclear instruments and methods in physics research section B: Beam interactions with materials and atoms*, 208, 281-286.

18. Jelil, R. A. (2015). A review of low-temperature plasma treatment of textile materials. *Journal of materials science*, 50(18), 5913-5943.

19. Zhou, Y., Sun, Z., Jiang, L., Chen, S., Ma, J., & Zhou, F. (2020). Flexible and conductive meta-aramid fiber paper with high thermal and chemical stability for electromagnetic interference shielding. *Applied Surface Science*, 533, 147431.

20. Su, M., Gu, A., Liang, G., & Yuan, L. (2011). The effect of oxygen-plasma treatment on Kevlar fibers and the properties of Kevlar fibers/bismaleimide composites. *Applied Surface Science*, 257(8), 3158-3167.

21. Krifa, M. (2021). Electrically conductive textile materials—Application in flexible sensors and antennas. *Textiles*, 1(2), 239-257.

22. Abd El-Hady, R. A. M., Nassar, K., & Abo-Basha, S. (2024). Antistatic textiles: current status and future outlook. *Journal of Art, Design and Music*, 3(2), 7.

23. ESDA, E. (2009). Association Advisory for Electrostatic Discharge Terminology. *ESD Association*. Available online: [www.esda.org/assets/Documents/c23d92d4ab/Fundamentals-of-ESD-Part-1-An-Introduction-to-ESD.pdf](http://www.esda.org/assets/Documents/c23d92d4ab/Fundamentals-of-ESD-Part-1-An-Introduction-to-ESD.pdf) (accessed on 25 April 2023).

24. Kirstein, T. (2013). The future of smart-textiles development: new enabling technologies, commercialization and market trends. In *Multidisciplinary know-how for smart-textiles developers* (pp. 1-25). Woodhead Publishing.

25. Zhang, X. (2011). Antistatic and conductive textiles. In *Functional textiles for improved performance, protection and health* (pp. 27-44). Woodhead Publishing.

26. Liu, L., Xu, W., Ding, Y., Agarwal, S., Greiner, A., & Duan, G. (2020). A review of smart electrospun fibers toward textiles. *Composites Communications*, 22, 100506.
27. Barakzehi, M., Montazer, M., Sharif, F., Norby, T., & Chatzitakis, A. (2019). A textile-based wearable supercapacitor using reduced graphene oxide/polypyrrole composite. *Electrochimica Acta*, 305, 187-196.
28. Yun, Y. J., Hong, W. G., Kim, W. J., Jun, Y., & Kim, B. H. (2013). A novel method for applying reduced graphene oxide directly to electronic textiles from yarns to fabrics. *Advanced Materials (Deerfield Beach, Fla.)*, 25(40), 5701-5705.
29. Shawl, R. K., Long, B. R., Werner, D. H., & Gavrin, A. (2007). The characterization of conductive textile materials intended for radio frequency applications. *IEEE Antennas and Propagation Magazine*, 49(3), 28-40.
30. Rahman, M. A., Kumar, P., Park, D. S., & Shim, Y. B. (2008). Electrochemical sensors based on organic conjugated polymers. *Sensors*, 8(1), 118-141.
31. Palaniappan, S., & John, A. (2008). Polyaniline materials by emulsion polymerization pathway. *Progress in polymer science*, 33(7), 732-758.
32. Shawl, R. K., Long, B. R., Werner, D. H., & Gavrin, A. (2007). The characterization of conductive textile materials intended for radio frequency applications. *IEEE Antennas and Propagation Magazine*, 49(3), 28-40.
33. Bayram, Y., Zhou, Y., Shim, B. S., Xu, S., Zhu, J., Kotov, N. A., & Volakis, J. L. (2010). E-textile conductors and polymer composites for conformal lightweight antennas. *IEEE Transactions on Antennas and Propagation*, 58(8), 2732-2736.
34. Hu, L., Pasta, M., La Mantia, F., Cui, L., Jeong, S., Deshazer, H. D., ... & Cui, Y. (2010). Stretchable, porous, and conductive energy textiles. *Nano letters*, 10(2), 708-714.
35. Lu, C., Meng, J., Zhang, J., Chen, X., Du, M., Chen, Y., ... & Zhang, K. (2019). Three-dimensional hierarchically porous graphene fiber-shaped supercapacitors with high specific capacitance and rate capability. *ACS Applied Materials & Interfaces*, 11(28), 25205-25217.
36. Xu, Q., Lu, C., Sun, S., & Zhang, K. (2019). Electrochemical properties of PEDOT: PSS/V2O5 hybrid fiber based supercapacitors. *Journal of Physics and Chemistry of Solids*, 129, 234-241.
37. Lee, Y. H., Kim, J. S., Noh, J., Lee, I., Kim, H. J., Choi, S., ... & Choi, J. W. (2013). Wearable textile battery rechargeable by solar energy. *Nano letters*, 13(11), 5753-5761.

38. Huang, Q., Wang, D., & Zheng, Z. (2016). Textile-based electrochemical energy storage devices. *Advanced Energy Materials*, 6(22), 1600783.
39. Mičušík, M., Nedelčev, T., Omastová, M., Krupa, I., Olejníková, K., Fedorko, P., & Chehimi, M. M. (2007). Conductive polymer-coated textiles: The role of fabric treatment by pyrrole-functionalized triethoxysilane. *Synthetic metals*, 157(22-23), 914-923.
40. Zysset, C., Cherenack, K., Kinkeldei, T., & Tröster, G. (2010, October). Weaving integrated circuits into textiles. In *International symposium on wearable computers (ISWC) 2010* (pp. 1-8). IEEE.
41. Joshi, B. (2021). *Formation of Woven Structures with Embedded Flexible Supercapacitor Yarns and Their Applications*. North Carolina State University.
42. Armano, A., & Agnello, S. (2019). Two-dimensional carbon: a review of synthesis methods, and electronic, optical, and vibrational properties of single-layer graphene. *C*, 5(4), 67.
43. Witkowska, B., & Frydrych, I. (2005). Protective clothing—test methods and criteria of tear resistance assessment. *International Journal of Clothing Science and Technology*, 17(3/4), 242-252.
44. Zhong, Y. L., Tian, Z., Simon, G. P., & Li, D. (2015). Scalable production of graphene via wet chemistry: progress and challenges. *Materials Today*, 18(2), 73-78.
45. Tang, X., Tian, M., Qu, L., Zhu, S., Guo, X., Han, G., ... & Xu, X. (2015). Functionalization of cotton fabric with graphene oxide nanosheet and polyaniline for conductive and UV blocking properties. *Synthetic Metals*, 202, 82-88.
46. Liu, L., Yu, Y., Yan, C., Li, K., & Zheng, Z. (2015). Wearable energy-dense and power-dense supercapacitor yarns enabled by scalable graphene-metallic textile composite electrodes. *Nature communications*, 6(1), 7260.
47. Liu, J., Qiao, Y., Guo, C. X., Lim, S., Song, H., & Li, C. M. (2012). Graphene/carbon cloth anode for high-performance mediatorless microbial fuel cells. *Bioresource technology*, 114, 275-280.
48. Liu, W. W., Yan, X. B., Lang, J. W., Peng, C., & Xue, Q. J. (2012). Flexible and conductive nanocomposite electrode based on graphene sheets and cotton cloth for supercapacitor. *Journal of Materials Chemistry*, 22(33), 17245-17253.
49. Neves, A. I. S., Bointon, T. H., Melo, L. V., Russo, S., De Schrijver, I., Craciun, M. F., & Alves, H. (2015). Transparent conductive graphene textile fibers. *Scientific reports*, 5(1), 9866.

50. Woltornist, S. J., Alamer, F. A., McDannald, A., Jain, M., Sotzing, G. A., & Adamson, D. H. (2015). Preparation of conductive graphene/graphite infused fabrics using an interface trapping method. *Carbon*, 81, 38-42.
51. Karim, N., Afroj, S., Leech, D., & Abdelkader, A. M. (2021). Flexible and Wearable Graphene-Based E-Textiles. *Oxide Electronics*, 21-49.
52. Rayhan, M. G. S., Khan, M., Shaily, M. T., Rahman, H., Rahman, M. R., Akon, M. T., ... & Sayem, A. S. M. (2023). Conductive textiles for signal sensing and technical applications. *Signals*, 4(1), 1-39.
53. Kumar, S., Kumari, N., & Seo, Y. (2024). MXenes: Versatile 2D materials with tailored surface chemistry and diverse applications. *Journal of Energy Chemistry*, 90, 253-293.
54. Chen, X., Zhao, Y., Li, L., Wang, Y., Wang, J., Xiong, J., ... & Yu, J. (2021). MXene/polymer nanocomposites: preparation, properties, and applications. *Polymer Reviews*, 61(1), 80-115.
55. Sen, A. K. (2007). *Coated textiles: principles and applications*. Crc Press.
56. Yang, K., Torah, R., Wei, Y., Beeby, S., & Tudor, J. (2013). Waterproof and durable screen printed silver conductive tracks on textiles. *Textile Research Journal*, 83(19), 2023-2031.
57. Osório, I., Igreja, R., Franco, R., & Cortez, J. (2012). Incorporation of silver nanoparticles on textile materials by an aqueous procedure. *Materials Letters*, 75, 200-203.
58. Depla, D., Segers, S., Leroy, W., Van Hove, T., & Van Parys, M. (2011). Smart textiles: an explorative study of the use of magnetron sputter deposition. *Textile Research Journal*, 81(17), 1808-1817.
59. Zhang, H., Shen, L., & Chang, J. (2011). Comparative study of electroless Ni-P, Cu, Ag, and Cu-Ag plating on polyamide fabrics. *Journal of Industrial Textiles*, 41(1), 25-40.
60. VandeVoort, A. R., & Arai, Y. (2012). Environmental chemistry of silver in soils: Current and historic perspective. *Advances in agronomy*, 114, 59-90.
61. Rezić, I. (2012). Engineered nanoparticles in textiles and textile wastewaters. In *Comprehensive Analytical Chemistry* (Vol. 59, pp. 235-264). Elsevier.
62. Cochrane, C., & Cayla, A. (2013). Polymer-based resistive sensors for smart textiles. In *Multidisciplinary know-how for smart-textiles developers* (pp. 129-153). Woodhead Publishing.
63. Shirakawa, H. (2001). The discovery of polyacetylene film—the dawning of an era of conducting polymers. *Current Applied Physics*, 1(4-5), 281-286.

64. Tseghai, G. B., Mengistie, D. A., Malengier, B., Fante, K. A., & Van Langenhove, L. (2020). PEDOT: PSS-based conductive textiles and their applications. *Sensors*, 20(7), 1881.
65. Le, T. H., Kim, Y., & Yoon, H. (2017). Electrical and electrochemical properties of conducting polymers. *Polymers*, 9(4), 150.
66. Ding, Y., Invernale, M. A., & Sotzing, G. A. (2010). Conductivity trends of PEDOT-PSS impregnated fabric and the effect of conductivity on electrochromic textile. *ACS applied materials & interfaces*, 2(6), 1588-1593.
67. Nardes, A. M., Kemerink, M., Janssen, R. A., Bastiaansen, J. A., Kiggen, N. M., Langeveld, B. M., ... & De Kok, M. M. (2007). Microscopic understanding of the anisotropic conductivity of PEDOT: PSS thin films. *Advanced Materials*, 19(9), 1196-1200.
68. Nardes, A. M., Kemerink, M., De Kok, M. M., Vinken, E., Maturova, K., & Janssen, R. A. J. (2008). Conductivity, work function, and environmental stability of PEDOT: PSS thin films treated with sorbitol. *Organic electronics*, 9(5), 727-734.
69. Kawamura, R., & Michinobu, T. (2023). PEDOT: PSS versus polyaniline: a comparative study of conducting polymers for organic electrochemical transistors. *Polymers*, 15(24), 4657.
70. Zare, E. N., Agarwal, T., Zarepour, A., Pinelli, F., Zarrabi, A., Rossi, F., ... & Makvandi, P. (2021). Electroconductive multi-functional polypyrrole composites for biomedical applications. *Applied Materials Today*, 24, 101117.
71. Tyler, D., Wood, J., Sabir, T., McDonnell, C., Sayem, A. S. M., & Whittaker, N. (2019). Wearable electronic textiles. *Textile Progress*, 51(4), 299-384.
72. Mattila, H. (Ed.). (2006). *Intelligent textiles and clothing*. Woodhead Publishing.
73. Tao, X. (Ed.). (2005). *Wearable electronics and photonics*. Elsevier.
74. Malinauskas, A. (2001). Chemical deposition of conducting polymers. *polymer*, 42(9), 3957-3972.
75. Åkerfeldt, M., Strååt, M., & Walkenström, P. (2013). Electrically conductive textile coating with a PEDOT-PSS dispersion and a polyurethane binder. *Textile Research Journal*, 83(6), 618-627.
76. Wang, J. P., Xue, P., & Tao, X. M. (2011). Strain sensing behavior of electrically conductive fibers under large deformation. *Materials Science and Engineering: A*, 528(6), 2863-2869.
77. Pratt, C. (1996, February 22). *Conducting Polymers*. Retrieved from <https://www.studymode.com/essays/Conducting-Polymers-778834.html>.
78. Maity, S., & Chatterjee, A. (2015). Conductive polymer based electro-conductive textiles for novel applications. *Technical Textiles, I*, E16-E18.



79. Lange, U., Roznyatovskaya, N. V., & Mirsky, V. M. (2008). Conducting polymers in chemical sensors and arrays. *Analytica chimica acta*, 614(1), 1-26.
80. Matilla, H. (2006). *Intelligent textiles and clothing*. Woodhead Publishing Ltd., 217–236.
81. Kuhn, H. H., Child, A. D., & Kimbrell, W. C. (1995). Toward real applications of conductive polymers. *Synthetic Metals*, 71(1-3), 2139-2142.
82. Knittel, D., & Schollmeyer, E. (2009). Electrically high-conductive textiles. *Synthetic Metals*, 159(14), 1433-1437.
83. Patil, A. J., & Deogaonkar, S. C. (2012). Conductivity and atmospheric aging studies of polypyrrole-coated cotton fabrics. *Journal of applied polymer science*, 125(2), 844-851.
84. Eeonyx Corporation. *EeonTex conductive fabrics*. Retrieved from <http://www.eeonyx.com/eeontex.php>
85. Sigma-Aldrich. (2022, October 21). *PEDOT:PSS conductive polymers*. Retrieved from <http://www.sigmaaldrich.com/catalog/product/aldrich/483095>
86. Heraeus Epurio. (2022, October 21). *Clevios conductive polymers*. Retrieved from <https://www.heraeus-epurio.com/en/applications/clevios/clevios-overview/>
87. Onggar, T., Kruppke, I., & Cherif, C. (2020). Techniques and processes for the realization of electrically conducting textile materials from intrinsically conducting polymers and their application potential. *Polymers*, 12(12), 2867.
88. Namsheer, K., & Rout, C. S. (2021). Conducting polymers: a comprehensive review on recent advances in synthesis, properties and applications. *RSC advances*, 11(10), 5659-5697.
89. Stoppa, M., & Chiolerio, A. (2014). Wearable electronics and smart textiles: A critical review. *sensors*, 14(7), 11957-11992.
90. Wen, N., Fan, Z., Yang, S., Zhao, Y., Cong, T., Xu, S., ... & Pan, L. (2020). Highly conductive, ultra-flexible and continuously processable PEDOT: PSS fibers with high thermoelectric properties for wearable energy harvesting. *Nano Energy*, 78, 105361.
91. Ojstršek, A., Jug, L., & Plohl, O. (2022). A review of electro conductive textiles utilizing the dip-coating technique: their functionality, durability and sustainability. *Polymers*, 14(21), 4713.
92. Groenendaal, L., Jonas, F., Freitag, D., Pielartzik, H., & Reynolds, J. R. (2000). Poly (3, 4-ethylenedioxythiophene) and its derivatives: past, present, and future. *Advanced materials*, 12(7), 481-494.

93. Wypych, G., & Knovel, L. (2000). *Handbook of Fillers*. Norwich, NY: ChemTec.
94. Osório, I., Igreja, R., Franco, R., & Cortez, J. (2012). Incorporation of silver nanoparticles on textile materials by an aqueous procedure. *Materials Letters*, 75, 200-203.
95. Simpson, J., Kirchmeyer, S., & Reuter, K. (2005). Advances and applications of inherently conductive polymer technologies based on poly(3,4-ethylenedioxythiophene). In 2005 AIMCAL Fall Technical Conference and 19th International Vacuum Web Coating Conference. Myrtle Beach, South Carolina.
96. Reuter, K., Kirchmeyer, S., & Elschner, A. (2009). PEDOT—properties and technical relevance. *Handbook of Thiophene-Based Materials: Applications in Organic Electronics and Photonics*, 549-576.
97. Van Reenen, S., Scheepers, M., van De Ruit, K., Bollen, D. G. F. M., & Kemerink, M. (2014). Explaining the effects of processing on the electrical properties of PEDOT: PSS. *Organic electronics*, 15(12), 3710-3714.
98. Ahsen Khan, M. (2012). Dyeing of Wool and Silk Fibres with a Conductive Polyelectrolyte and Comparing Their Conductance.
99. Hebert, D. D., Naley, M. A., Cunningham, C. C., Sharp, D. J., Murphy, E. E., Stanton, V., & Irvin, J. A. (2021). Enabling conducting polymer applications: methods for achieving high molecular weight in chemical oxidative polymerization in alkyl-and ether-substituted thiophenes. *Materials*, 14(20), 6146.
100. Alhashmi Alamer, F., Althagafy, K., Alsalmi, O., Aldeih, A., Alotaiby, H., Althebaiti, M., ... & Alnefaie, M. A. (2022). Review on PEDOT: PSS-based conductive fabric. *ACS omega*, 7(40), 35371-35386.
101. Shahid, M. A., Rahman, M. M., Hossain, M. T., Hossain, I., Sheikh, M. S., Rahman, M. S., ... & Hoque, M. I. U. (2025). Advances in Conductive Polymer-Based Flexible Electronics for Multifunctional Applications. *Journal of Composites Science*, 9(1), 42.
102. Elschner, A., Loevenich, W., Eiling, A., & Bayley, J. (2012). ITO Alternative: solution deposited Clevis TM PEDOT: PSS for transparent conductive applications. *Heraeus Trade Artic*.
103. Ryan, J. D., Mengistie, D. A., Gabrielsson, R., Lund, A., & Müller, C. (2017). Machine-washable PEDOT: PSS dyed silk yarns for electronic textiles. *ACS Applied Materials & Interfaces*, 9(10), 9045-9050.
104. Ankhili, A., Tao, X., Cochrane, C., Koncar, V., Coulon, D., & Tarlet, J. M. (2019). Ambulatory evaluation of ECG signals obtained using washable textile-based electrodes made with chemically modified PEDOT: PSS. *Sensors*, 19(2), 416.

105. Tao, X., Huang, T. H., Shen, C. L., Ko, Y. C., Jou, G. T., & Koncar, V. (2018). Bluetooth Low Energy-Based Washable Wearable Activity Motion and Electrocardiogram Textronic Monitoring and Communicating System. *Advanced Materials Technologies*, 3(10), 1700309.
106. Tao, X., Koncar, V., Huang, T. H., Shen, C. L., Ko, Y. C., & Jou, G. T. (2017). How to make reliable, washable, and wearable textronic devices. *Sensors*, 17(4), 673.
107. Tian, M., Hu, X., Qu, L., Zhu, S., Sun, Y., & Han, G. (2016). Versatile and ductile cotton fabric achieved via layer-by-layer self-assembly by consecutive adsorption of graphene doped PEDOT: PSS and chitosan. *Carbon*, 96, 1166-1174.
108. Shim, E. (2019). Coating and laminating processes and techniques for textiles. In *Smart textile coatings and laminates* (pp. 11-45). Woodhead Publishing.
109. Hunger, K. (Ed.). (2007). *Industrial dyes: chemistry, properties, applications*. John Wiley & Sons.
110. Musa, H., Abdulmumini, A., Folashade, M. O., Usman, B., & Abba, H. (2013). Studies on the dyeing of wool and nylon fabrics with some acid dyes. *IOSR J. Appl. Chem*, 5(1), 11-17.
111. Clark, M. (Ed.). (2011). *Handbook of textile and industrial dyeing: principles, processes and types of dyes*. Elsevier.
112. Mantione, D., Del Agua, I., Schaafsma, W., ElMahmoudy, M., Uguz, I., Sanchez-Sanchez, A., ... & Mecerreyes, D. (2017). Low-temperature cross-linking of PEDOT: PSS films using divinylsulfone. *ACS applied materials & interfaces*, 9(21), 18254-18262.
113. Colucci, R., Quadros, M. H., Feres, F. H., Maia, F. B., de Vicente, F. S., Faria, G. C., ... & Gozzi, G. (2018). Cross-linked PEDOT: PSS as an alternative for low-cost solution-processed electronic devices. *Synthetic Metals*, 241, 47-53.
114. He, G., Ning, F., Liu, X., Meng, Y., Lei, Z., Ma, X., ... & Qu, L. (2024). High-performance and long-term stability of MXene/PEDOT: PSS-decorated cotton yarn for wearable electronics applications. *Advanced Fiber Materials*, 6(2), 367-386.
115. del Agua, I., Mantione, D., Ismailov, U., Sanchez-Sanchez, A., Aramburu, N., Malliaras, G. G., ... & Ismailova, E. (2018). DVS-Crosslinked PEDOT: PSS Free-Standing and Textile Electrodes toward Wearable Health Monitoring. *Advanced Materials Technologies*, 3(10), 1700322.
116. Simonič, M., & Fras Zemljč, L. (2020). Functionalized wool as an efficient and sustainable adsorbent for removal of Zn (II) from an aqueous solution. *Materials*, 13(14), 3208.

117. Sessolo, M., Khodagholy, D., Rivnay, J., Maddalena, F., Gleyzes, M., Steidl, E., ... & Malliaras, G. G. (2013). Easy-to-fabricate conducting polymer microelectrode arrays. *Advanced Materials (Deerfield Beach, Fla.)*, 25(15), 2135-2139.
118. Mantione, D., Del Agua, I., Schaafsma, W., ElMahmoudy, M., Uguz, I., Sanchez-Sanchez, A., ... & Mecerreyes, D. (2017). Low-temperature cross-linking of PEDOT: PSS films using divinylsulfone. *ACS applied materials & interfaces*, 9(21), 18254-18262.
119. Jennings, M., Kendrick, I., Green, C., & Lustig, S. (2018). PEDOT: PSS-DVS Crosslinking Reaction Monitored via ATR-FTIR for Air Cathode Application in Microbial Fuel Cells. *Boston, MA: RISE: Research, Innovation, and Scholarship Expo, Northeast University. Available online at: [http://hdl.handle.net/2047 D, 20287676](http://hdl.handle.net/2047D.20287676).*
120. Mantione, D., Del Agua, I., Schaafsma, W., ElMahmoudy, M., Uguz, I., Sanchez-Sanchez, A., ... & Mecerreyes, D. (2017). Low-temperature cross-linking of PEDOT: PSS films using divinylsulfone. *ACS applied materials & interfaces*, 9(21), 18254-18262.
121. Kim, M. L., Otal, E. H., Sinatra, N. R., Dobson, K., & Kimura, M. (2023). Washable PEDOT: PSS Coated Polyester with Submicron Sized Fibers for Wearable Technologies. *ACS omega*, 8(4), 3971-3980.
122. Tadesse, M. G., Loghin, C., Chen, Y., Wang, L., Catalin, D., & Nierstrasz, V. (2017). Effect of liquid immersion of PEDOT: PSS-coated polyester fabric on surface resistance and wettability. *Smart Materials and Structures*, 26(6), 065016.
123. Park, M. U., Lee, S. M., & Chung, D. W. (2019). Model system of cross-linked PEDOT: PSS adaptable to an application for an electrode with enhanced water stability. *Synthetic Metals*, 258, 116195.
124. Kergoat, L., Piro, B., Simon, D. T., Pham, M. C., Noël, V., & Berggren, M. (2014). Detection of glutamate and acetylcholine with organic electrochemical transistors based on conducting polymer/platinum nanoparticle composites. *Advanced Materials*, 26(32), 5658-5664.
125. Berezhetska, O., Liberelle, B., De Crescenzo, G., & Cicoira, F. (2015). A simple approach for protein covalent grafting on conducting polymer films. *Journal of Materials Chemistry B*, 3(25), 5087-5094.
126. Håkansson, A., Han, S., Wang, S., Lu, J., Braun, S., Fahlman, M., ... & Fabiano, S. (2017). Effect of (3-glycidyloxypropyl) trimethoxysilane (GOPS) on the electrical properties of PEDOT: PSS films. *Journal of Polymer Science Part B: Polymer Physics*, 55(10), 814-820.
127. Huang, T. M., Batra, S., Hu, J., Miyoshi, T., & Cakmak, M. (2013). Chemical cross-linking of conducting poly (3, 4-ethylenedioxythiophene):

poly (styrenesulfonate)(PEDOT: PSS) using poly (ethylene oxide)(PEO). *Polymer*, 54(23), 6455-6462.

128. Hang, Z. S., Jang, F. S., Ju, F. Y., Ying, S. J., & Xu, F. M. (2010). Advances in preparation and application of melamine foam [J]. *Thermosetting Resin*, 25(4), 44-52.

129. Wang, D., Zhang, X., Luo, S., & Li, S. (2013). Preparation and property analysis of melamine formaldehyde foam. *Advances in Materials Physics and Chemistry*, 2(4), 63-67.

130. Varnaitė-Žuravliova, S., Sankauskaitė, A., Stygienė, L., Krauledas, S., Bekampienė, P., & Milčienė, I. (2016). The investigation of barrier and comfort properties of multifunctional coated conductive knitted fabrics. *Journal of Industrial Textiles*, 45(4), 585-610.

131. Dehabadi, V. A., Buschmann, H. J., & Gutmann, J. S. (2013). Durable press finishing of cotton fabrics: An overview. *Textile Research Journal*, 83(18), 1974-1995.

132. Wang, J., Fang, K., Liu, X., Zhang, S., Qiao, X., & Liu, D. (2023). A review on the status of formaldehyde-free anti-wrinkle cross-linking agents for cotton fabrics: Mechanisms and applications. *Industrial Crops and Products*, 200, 116831.

133. Pupeikė, J., Sankauskaitė, A., Varnaitė-Žuravliova, S., Rubežienė, V., & Abraitienė, A. (2023). Investigation of Electrical and Wearing Properties of Wool Fabric Coated with PEDOT: PSS. *Polymers*, 15(11), 2539.

134. Skrifvars, M., Rehnby, W., & Gustafsson, M. (2008). Coating of textile fabrics with conductive polymers for smart textile applications. In *Ambience 08, Borås, Sweden, June 2-3, 2008*.

135. Kiran, E., & Duran, K. (2021). Surface modification of wool fibers for enhanced dyeing performance: A review. *Journal of Textile Engineering & Fashion Technology*, 7(1), 1-7.

136. Baykal, B., & Kan, C. (2016). Functionalization of wool textiles: A review of treatment methods and applications. *Textile Progress*, 48(2), 61-89.

137. Montazer, M., & Khoddami, A. (2019). Electrically conductive textiles and wearable devices. *Journal of Textile Science & Fashion Technology*, 3(3), 1-12.

138. Montazer, M., & Harifi, T. (2018). *Nanofinishing of textile materials*. Woodhead Publishing.

139. Ding, Y., Jiang, J., Wu, Y., Zhang, Y., Zhou, J., Zhang, Y., ... & Zheng, Z. (2024). Porous conductive textiles for wearable electronics. *Chemical reviews*, 124(4), 1535-1648.

140. Niu, Z., & Yuan, W. (2021). Smart nanocomposite nonwoven wearable fabrics embedding phase change materials for highly efficient energy

conversion–storage and use as a stretchable conductor. *ACS Applied Materials & Interfaces*, 13(3), 4508–4518.

141. Miah, M. R., Yang, M., Hossain, M. M., Khandaker, S., & Awual, M. R. (2022). Textile-based flexible and printable sensors for next generation uses and their contemporary challenges: A critical review. *Sensors and Actuators A: Physical*, 344, 113696.

142. Jost, K., Durkin, D. P., Haverhals, L. M., Brown, E. K., Langenstein, M., De Long, H. C., ... & Dion, G. (2015). Natural fiber welded electrode yarns for knittable textile supercapacitors. *Advanced Energy Materials*, 5(4), 1401286.

143. Lux, F. (1993). Models proposed to explain the electrical conductivity of mixtures made of conductive and insulating materials. *Journal of materials science*, 28, 285–301.

144. Müller, C., Hamed, M., Karlsson, R., Jansson, R., Marcilla, R., Hedhammar, M., & Inganäs, O. (2011). Woven electrochemical transistors on silk fibers. *Advanced Materials*, 23(7), 898–901.

145. Hwang, B., Lund, A., Tian, Y., Darabi, S., & Muller, C. (2020). Machine-washable conductive silk yarns with a composite coating of Ag nanowires and PEDOT:PSS. *ACS Applied Materials & Interfaces*, 12(24), 27537–27544.

146. Müller, C., Jansson, R., Elfving, A., Askarieh, G., Karlsson, R., Hamed, M., Rising, A., Johansson, J., & Inganäs, O. (2011). Functionalisation of recombinant spider silk with conjugated polyelectrolytes. *Journal of Materials Chemistry*, 21(8), 2909–2915.

147. Khan, A. (2012). Dyeing of wool and silk fibres with a conductive polyelectrolyte and comparing their conductance. Independent thesis (Master's). University of Borås, Swedish School of Textiles.

148. Moraes, M. R., Alves, A. C., Toptan, F., Martins, M. S., Vieira, E. M. F., Paleo, A. J., Souto, A. P., Santos, W. L. F., Esteves, M. F., & Zille, A. (2017). Glycerol/PEDOT:PSS coated woven fabric as a flexible heating element on textiles. *Journal of Materials Chemistry C*, 5(15), 3807–3822.

149. Hebeish, A. A., El-Gamal, M. A., Said, T. S., & El-Hady, R. A. A. (2010). Major factors affecting the performance of ESD-protective fabrics. *Journal of the Textile Institute*, 101(5), 389–398.

150. Åkerfeldt, M., Lund, A., & Walkenström, P. (2015). Textile sensing glove with piezoelectric PVDF fibers and printed electrodes of PEDOT:PSS. *Textile Research Journal*, 85(17), 1789–1799.

151. Tsukada, S., Nakashima, H., & Torimitsu, K. (2012). Conductive polymer combined silk fiber bundle for bioelectrical signal recording. *PLoS One*, 7(3), e33689.

152. Petrovic, S., Jovanovic, M., & Blagojevic, S. (2024). Advanced methods for PEDOT:PSS application on textiles. *Industria Textila*, 75(1), 21-28.
153. Wu, T., Shi, X. L., Liu, W. D., Li, M., Yue, F., Huang, P., ... & Chen, Z. G. (2024). High Thermoelectric Performance and Flexibility in Rationally Treated PEDOT: PSS Fiber Bundles. *Advanced Fiber Materials*, 6(2), 607-618.
154. Chen, W., Xu, Y., & Lee, J. (2023). Flexible wet-spun PEDOT:PSS microfibers integrating thermal-sensing and Joule heating functions for smart textiles. *Polymers*, 15(16), 3432.
155. Ahmad Shahrim, N. A., Ahmad, Z., Solah, W. N. A. N. W., Azman, A. W., Sarifuddin, N., & Buys, Y. F. (2023, May). Electrical Resistance of Fabric Immersed with PEDOT: PSS Doped Ag NPs and DMSO Solution. In *Proceeding of 5th International Conference on Advances in Manufacturing and Materials Engineering: ICAMME 2022, 9–10 August, Kuala Lumpur, Malaysia* (pp. 381-388). Singapore: Springer Nature Singapore.
156. Tadesse, M. G., Mengistie, D. A., Chen, Y., Wang, L., Loghin, C., & Nierstrasz, V. (2019). Electrically conductive highly elastic polyamide/lycra fabric treated with PEDOT: PSS and polyurethane. *Journal of Materials Science*, 54(13), 9591-9602.
157. Sarabia-Riquelme, R., Andrews, R., Anthony, J. E., & Weisenberger, M. C. (2020). Highly conductive wet-spun PEDOT: PSS fibers for applications in electronic textiles. *Journal of Materials Chemistry C*, 8(33), 11618-11630.
158. Åkerfeldt, M. (2015). Electrically conductive textile coatings with PEDOT: PSS (Doctoral dissertation). Högskolan i Borås.
159. Bihar, E., Roberts, T., Zhang, Y., Ismailova, E., Herve, T., Malliaras, G. G., ... & Saadaoui, M. (2018). Fully printed all-polymer tattoo/textile electronics for electromyography. *Flexible and Printed Electronics*, 3(3), 034004.
160. Rathore, P., & Schiffman, J. D. (2023). Effect of pH value on the electrical properties of PEDOT:PSS-based fiber mats. *ACS Engineering Au*, 3(6), 527–536.
161. Kazani, I., Hertleer, C., De Mey, G., Schwarz, A., Guxho, G., & Van Langenhove, L. (2012). Electrical conductive textiles obtained by screen printing. *Fibres & Textiles in Eastern Europe*, 20(1), 57–63.
162. Tehrani, M., et al. (2019). Eco-friendly printing technologies in the textile industry. *Journal of Cleaner Production*, 233, 748–757.
163. Sinha, S. K., Noh, Y., Reljin, N., Treich, G. M., Hajeb-Mohammadalipour, S., Guo, Y., ... & Sotzing, G. A. (2017). Screen-printed

PEDOT: PSS electrodes on commercial finished textiles for electrocardiography. *ACS applied materials & interfaces*, 9(43), 37524-37528.

164. Zhao, X., Ding, J., Bai, W., Wang, Y., Yan, Y., Cheng, Y., & Zhang, J. (2018). PEDOT: PSS/AuNPs/CA modified screen-printed carbon based disposable electrochemical sensor for sensitive and selective determination of carmine. *Journal of Electroanalytical Chemistry*, 824, 14-21.

165. Zhao, X., Ding, J., Bai, W., Wang, Y., Yan, Y., Cheng, Y., & Zhang, J. (2018). PEDOT: PSS/AuNPs/CA modified screen-printed carbon based disposable electrochemical sensor for sensitive and selective determination of carmine. *Journal of Electroanalytical Chemistry*, 824, 14-21.

166. Gorczyca, T., & Cieślak, M. (2019). "Antistatic properties of textiles: Mechanisms, applications, and advances." *Textile Research Journal*, 89(2), 147-165. Smith, R. (2018). "Static Electricity and its Control in Textiles." *Journal of Textile Science and Technology*, 6(3), 211-225.

167. Oh, K. W., & Park, S. J. (2020). "Conductive textiles for antistatic applications: Fabrication and properties." *Journal of Materials Science*, 55(5), 2324-2335.

168. Teli, M. D., Pandit, P., Samanta, K. K., Basak, S., & Gayatri, T. N. (2021). Salt-free and low-temperature colouration of silk using He–N<sub>2</sub> non-thermal plasma irradiation. *Journal of Cleaner Production*, 296, 126576.

169. International Electrotechnical Commission (IEC). (2018). *IEC 61340: Standard for electrostatics – Protection of electronic devices from electrostatic phenomena*. Geneva, Switzerland: IEC.

170. International Organization for Standardization (ISO). (2016). *ISO 6356: Determination of electrical resistivity of textiles*. Geneva, Switzerland: ISO.

171. European Committee for Standardization (CEN). (2008). *EN 1149: Protective clothing – Electrostatic properties*. Brussels, Belgium: CEN.

172. European Committee for Standardization (CEN). (2006). *EN 1149-1: Method for determining surface resistivity of protective clothing*. Brussels, Belgium: CEN.

173. European Committee for Standardization (CEN). (2006). *EN 1149-2: Method for measuring the electrical resistance of dissipative textiles*. Brussels, Belgium: CEN.

174. European Committee for Standardization (CEN). (2006). *EN 1149-3: Method for measuring charge decay and electrostatic discharge of protective clothing*. Brussels, Belgium: CEN.



175. Zhang, C., Cui, Y., Lin, S., & Guo, J. (2022). Preparation and applications of hydrophilic quaternary ammonium salt type polymeric antistatic agents. *e-Polymers*, 22(1), 370-378.
176. Patel, J. P., Schneider, Y., Sankarasubramanian, M., & Jayaram, V. (2022). Fundamentals of polymer additives.
177. Roh, J. S., Chi, Y. S., Kang, T. J., & Nam, S. W. (2008). Electromagnetic shielding effectiveness of multifunctional metal composite fabrics. *Textile Research Journal*, 78(10), 825–835.
178. Rubežienė, V., Varnaitė-Žuravlio, S., Sankauskaitė, A., Pupeikė, J., Ragulis, P., & Abraitienė, A. (2023). The impact of structural variations and coating techniques on the microwave properties of woven fabrics coated with PEDOT:PSS composition. *Polymers*, 15(21), 4224.
179. Berezenko, S., Berezenko, N., Vasylenko, V., Merezhko, N., Koshevko, J., Horiashchenko, S., ... & Gakhovych, S. (2020). Study of effectiveness of UV electromagnetic waves shielding by textile materials. *Computer*, 1(100), 5–500.
180. Almirall, O., Fernández-García, R., & Gil, I. (2022). Wearable metamaterial for electromagnetic radiation shielding. *The Journal of The Textile Institute*, 113(8), 1586–1594.
181. King, J. A., Pisani, W. A., Klimek-McDonald, D. R., Perger, W. F., Odegard, G. M., & Turpeinen, D. G. (2016). Shielding effectiveness of carbon-filled polypropylene composites. *Journal of Composite Materials*, 50(16), 2177–2189.
182. Rubežienė, V., & Varnaitė-Žuravlio, S. (2020). EMI shielding textile materials. In *Materials for Potential EMI Shielding Applications* (pp. 357-378). Elsevier.
183. King, J. A., Pisani, W. A., Klimek-McDonald, D. R., Perger, W. F., Odegard, G. M., & Turpeinen, D. G. (2016). Shielding effectiveness of carbon-filled polypropylene composites. *Journal of Composite Materials*, 50(16), 2177–2189.
184. Bushko, W. C., Stokes, V. K., & Wilson, J. (1999). EMI shielding effectiveness of fiber-filled plastics—material testing issues. *ANTEC. New York (USA)*, 1499-502.
185. Ott, H. W. (2011). *Electromagnetic compatibility engineering*. John Wiley & Sons.
186. Rubežienė, V., Baltušnikaitė, J., Varnaitė-Žuravlio, S., Sankauskaitė, A., Abraitienė, A., & Matuzas, J. (2015). Development and investigation of electromagnetic shielding fabrics with different electrically conductive additives. *Journal of Electrostatics*, 75, 90–98.

187. Teber, A., Unver, I., Kavas, H., Aktas, B., & Bansal, R. (2016). Knitted radar absorbing materials (RAM) based on nickel–cobalt magnetic materials. *Journal of Magnetism and Magnetic Materials*, 406, 228–232.
188. Scott, R. A. (Ed.). (2005). Textiles for Protection. Cambridge, UK: Woodhead Publishing.
189. Mattila, H. R. (Ed.). (2006). Intelligent Textiles and Clothing. Cambridge, UK: Woodhead Publishing.
190. European Committee for Standardization (CEN). (2008). EN 1149-5: Protective clothing – Electrostatic properties – Part 5: Material, performance and design requirements. Brussels, Belgium: CEN.
191. Varnaitė, S., & Katunskis, J. (2009). Influence of washing on electric charge decay of fabrics with conductive yarns. *Fibres and Textiles in Eastern Europe*, 17(5), 69–75.
192. Roh, J. S., et al. (2008). Electromagnetic shielding effectiveness of multifunctional metal composite fabrics. *Textile Research Journal*, 78(9), 825–835.
193. Lai, K., Sun, R. J., Chen, M. Y., et al. (2007). Electromagnetic shielding effectiveness of fabrics with metalized polyester filaments. *Textile Research Journal*, 77(4), 242–246.
194. Onar, N., Aksit, A. C., Ebeoglulil, M. F., et al. (2009). Structural, electrical, and electromagnetical properties of cotton fabrics coated with polyaniline and polypyrrole. *Journal of Applied Polymer Science*, 114(6), 2003–2010.
195. Avloni, J., Ouyang, M., Florio, L., et al. (2007). Shielding effectiveness evaluation of metalized and polypyrrole-coated fabrics. *Journal of Thermoplastic Composite Materials*, 20(3), 241–254.
196. Akerfeldt, M., Straat, M., & Walkenstrom, P. (2012). Electrically conductive textile coating with a PEDOT-PSS dispersion and a polyurethane binder. *Textile Research Journal*, 83(6), 618–627.
197. Xue, P., Tao, X. M., Kwok, K. W. Y., et al. (2004). Electromechanical behaviour of fibres coated with an electrically conductive polymer. *Textile Research Journal*, 74(10), 929–936.
198. Kaynak, A. (2009). Characterization of conducting polymer coated fabrics at microwave frequencies. *International Journal of Clothing Science and Technology*, 21(2–3), 117–126.
199. Yan, H., Jo, T., & Okuzaki, H. (2009). Highly conductive and transparent poly(3,4-ethylenedioxythiophene)/poly(4-styrenesulfonate) (PEDOT/PSS) thin films. *Polymer Journal*, 41(12), 1028–1029.

200. Avloni, J., Florio, L., Henn, A. R., Lau, R., Ouyang, M., & Sparavigna, A. (2006). Electromagnetic shielding with polypyrrole-coated fabrics. *arXiv preprint cond-mat/0608664*.
201. Kaynak, A., & Hakansson, E. (2009). Characterization of conducting polymer coated fabrics at microwave frequencies. *International Journal of Clothing Science and Technology*, 21, 117–126.
202. Wang, Y., & Jing, X. (2005). Intrinsically conducting polymers for electromagnetic interference shielding. *Polymers for Advanced Technologies*, 16(5), 344–351.
203. Baltušnikaitė, J., Padleckienė, I., Rubežienė, V., & Varnaitė, S. (2012). Reduction of electromagnetic interference using textiles with conductive additives. In *Radiation interaction with material and its use in technologies: 4th international conference* (pp. 14-17).
204. Håkansson, E., Amiet, A., & Kaynak, A. (2007). Dielectric characterization of conducting textiles using free-space transmission measurements: Accuracy and methods for improvement. *Synthetic Metals*, 157(24), 1054–1063.
205. Onar, N., Akşit, A. C., Ebeoglugil, M. F., Birlik, I., Celik, E., & Ozdemir, I. (2009). Structural, electrical, and electromagnetic properties of cotton fabrics coated with polyaniline and polypyrrole. *Journal of Applied Polymer Science*, 114(4), 2003–2010.
206. Rubežienė, V., Abraitienė, A., Baltušnikaitė-Guzaitienė, J., Varnaitė-Žuravlio, S., Sankauskaitė, A., Kancleris, Ž., ... & Šlekas, G. (2018). The influence of distribution and deposit of conductive coating on shielding effectiveness of textiles. *The Journal of the Textile Institute*, 109(3), 358–367.
207. King, J. A., Pisani, W. A., Klimek-McDonald, D. R., Perger, W. F., Odegard, G. M., & Turpeinen, D. G. (2015). Shielding effectiveness of carbon-filled polypropylene composites. *Journal of Composite Materials*, 50(16), 2177–2189.
208. Kim, S. H., Jang, S. H., Byun, S. W., Lee, J. Y., Joo, J. S., Jeong, S. H., & Park, M. J. (2003). Electrical properties and EMI shielding characteristics of polypyrrole-nylon 6 composite fabrics. *Journal of Applied Polymer Science*, 87(13), 1969–1974.
209. Avloni, J., Ouyang, M., Florio, L., Henn, A. R., & Sparavigna, A. (2007). Shielding effectiveness evaluation of metallized and polypyrrole-coated fabrics. *Journal of Thermoplastic Composite Materials*, 20(3), 241–254.
210. Onar, N., Akşit, A. C., Ebeoglugil, M. F., Birlik, I., Celik, E., & Ozdemir, I. (2009). Structural, electrical, and electromagnetic properties of

cotton fabrics coated with polyaniline and polypyrrole. *Journal of Applied Polymer Science*, 114(6), 2003–2010.

211. Joseph, N., Varghese, J., & Sebastian, M. T. (2017). In situ polymerized polyaniline nanofiber-based functional cotton and nylon fabrics as millimeter-wave absorbers. *Polymer Journal*, 49(5), 391–399.

212. Engin, F. Z., & Usta, İ. (2015). Development and characterisation of polyaniline/polyamide (PANI/PA) fabrics for electromagnetic shielding. *Journal of The Textile Institute*, 106(8), 872–879.

213. Lee, C. Y., Lee, D. E., Jeong, C. K., Hong, Y. K., Shim, J. H., Joo, J., ... & Byun, S. W. (2002). Electromagnetic interference shielding by using conductive polypyrrole and metal compound coated on fabrics. *Polymer Advanced Technology*, 13(8), 577–583.

214. Wang, Y., & Jing, X. (2005). Intrinsically conducting polymers for electromagnetic interference shielding. *Polymers for Advanced Technologies*, 16(5), 344–351.

215. Akerfeldt, M., Straat, M., & Walkenstrom, P. (2012). Electrically conductive textile coating with a PEDOT-PSS dispersion and a polyurethane binder. *Textile Research Journal*, 83(6), 618–627.

216. Weiser, M., Pohlers, S., & Neudec, A., et al. (2010). Application of intrinsic conductive polymers (ICP) on textile materials. *Melliand International*, 16(4), 226–228.

217. Roh, J. S., et al. (2008). Electromagnetic shielding effectiveness of multifunctional metal composite fabrics. *Textile Research Journal*, 78(9), 825–835.

218. Koprowska, J., Pietranik, M., & Stawski, W. (2004). New type of textiles with shielding properties. *Fibres and Textiles in Eastern Europe*, 12(3), 39–42.

219. Brzezinski, S., Rybicki, T., Malinowska, G., et al. (2009). Effectiveness of shielding electromagnetic radiation, and assumptions for designing the multi-layer structures of textile shielding materials. *Fibres and Textiles in Eastern Europe*, 17(1), 60–65.

220. Wieckowski, T. W., & Janukiewicz, J. M. (2006). Methods for evaluating the shielding effectiveness of textiles. *Fibres and Textiles in Eastern Europe*, 14(5), 18–22.

221. ASTM D4935-10. (2010). Standard test method for measuring the electromagnetic shielding effectiveness of planar materials.

222. Michalak, M., Brazis, R., Kazakevicius, V., et al. (2006). Nonwovens with implanted split rings for barriers against electromagnetic radiation. *Fibres and Textiles in Eastern Europe*, 14(5), 64–68.

223. Wilson, P. F. (1988). Techniques for measuring the electromagnetic shielding effectiveness of materials: Part I: Far-field source simulation. *IEEE Transactions on Electromagnetic Compatibility*, 30(3), 239–250.
224. Wilson, P. F., Ma, M. T., & Adams, J. W. (1988). Techniques for measuring the electromagnetic shielding effectiveness of materials. I. Far-field source simulation. *IEEE Transactions on Electromagnetic Compatibility*, 30(3), 239–250.
225. El Gharbi, M., Fernández-García, R., Ahyoud, S., & Gil, I. (2020). A review of flexible wearable antenna sensors: Design, fabrication methods, and applications. *Materials*, 13(17), 3781.
226. Huang, J., Virji, S., Weiller, B. H., & Kaner, R. B. (2003). Polyaniline nanofibers: Facile synthesis and chemical sensors. *Journal of the American Chemical Society*, 125(2), 314–315.
227. U.S. Patent No. 0093238. Issued by U.S. Patent and Trademark Office.
228. Patent No. EP 3 854 933 B1. EMR shielding fabrics. Issued by European Patent Office.
229. Chung, D. D. L. (2001). Electromagnetic interference shielding effectiveness of carbon materials. *Carbon*, 39(2), 279–285.
230. Saini, P., Arora, M., & Dhawan, S. K. (2013). Polymer-based nanocomposites for electromagnetic interference (EMI) shielding. *Polymer Reviews*, 53(4), 567–622.
231. Das, N. C., Khastgir, D., Chaki, T. K., & Chakraborty, A. (2000). Electromagnetic interference shielding effectiveness of carbon black and carbon fibre filled EVA and NR based composites. *Composites Part A: Applied Science and Manufacturing*, 31(10), 1069–1081.
232. Redlich, G., Obersztyn, E., Olejnik, M., Fortuniak, K., Bartczak, A., Szugajew, L., & Jarzowski, J. (2014). New textiles designed for anti-radar camouflage. *Fibres and Textiles in Eastern Europe*, 1(103), 34–43.
233. Loomis, D., Huang, W., & Chen, G. (2014). The International Agency for Research on Cancer (IARC) evaluation of the carcinogenicity of outdoor air pollution: Focus on China. *Chinese Journal of Cancer*, 33(4), 189.
234. Tunáková, V., Militký, J., & Mishra, R. (2015). Comparison of methods for evaluating the electromagnetic shielding of textiles. *Indian Journal of Fibre & Textile Research*, 40(3), 361–365.
235. IEEE 299. (1991). Standard technique for gauging shielding enclosure performance.
236. MIL-STD-285. (1956). A military standard used to assess electromagnetic shielding's attenuation.

237. ASTM D4935. (2010). Standard test procedure for gauging planar materials' ability to shield electromagnetic radiation.
238. Grancarić, A. M., Jerković, I., Koncar, V., Cochrane, C., Kelly, F. M., Soulat, D., et al. (2018). Conductive polymers for smart textile applications. *Journal of Industrial Textiles*, 48(6), 612–642.
239. Haque, S. M., Ardila-Rey, J. A., Umar, Y., Mas'ud, A. A., Muhammad-Sukki, F., Jume, B. H., ... & Bani, N. A. (2021). Application and suitability of polymeric materials as insulators in electrical equipment. *Energies*, 14(10), 2758.
240. ISO/TR 23383. (2020). Textiles and textile products—Smart (intelligent) textiles: Definitions, categorisation, applications, and standardization needs.
241. Orgilés-Calpena, E., Arán-Aís, F., Torró-Palau, A. M., Orgilés-Barceló, C., & Martín-Martínez, J. M. (2009). Effect of annealing on the properties of waterborne polyurethane adhesive containing urethane-based thickener. *International Journal of Adhesion and Adhesives*, 29(8), 774–780.
242. Pretl, S., Hamáček, A., Řeboun, J., Čengery, J., Džugan, T., & Kroupa, M. (2010, September). Electrical characterization of PEDOT: PSS. In *3rd Electronics System Integration Technology Conference ESTC* (pp. 1-4). IEEE.
243. Farboodmanesh, S., Chen, J., Mead, J. L., et al. (2005). Effect of coating thickness and penetration on shear behavior of coated fabrics. *Journal of Elastomers and Plastics*, 37(3), 197–227.
244. Wang, L., Wang, X., & Lin, T. (2010). Conductive coatings for textiles. In *Smart textile coatings and laminates* (pp. 155-188). Woodhead Publishing.
245. Hatch, K. L. Textile Science, 1993 West Publishing Co., 1.
246. Maity, S., Singha, K., & Pandit, P. (2021). Advanced applications of green materials in wearable e-textiles. In *Applications of Advanced Green Materials* (pp. 239-263). Woodhead Publishing.
247. Islam, M. R., Afroj, S., Novoselov, K. S., & Karim, N. (2022). Smart electronic textile-based wearable supercapacitors. *Advanced Science*, 9(31), 2203856.
248. Azani, M. R., & Hassanpour, A. (2024). Electronic textiles (E-Textiles): Types, fabrication methods, and recent strategies to overcome durability challenges (washability & flexibility). *Journal of Materials Science: Materials in Electronics*, 35(29), 1897.
249. Ayyagari, M. R., Rane, L., Kadam, P. S., Subasree, N., Pant, K., & Yurievich, S. Y. (2023, April). Smart e-textiles for personalized healthcare

diagnosis and management. In *AIP Conference Proceedings* (Vol. 2603, No. 1). AIP Publishing.

250. Kang, M., & Kim, T. W. (2021). Recent advances in fiber-shaped electronic devices for wearable applications. *Applied Sciences*, 11(13), 6131.

251. Ruckdashel, R. R., Khadse, N., & Park, J. H. (2022). Smart e-textiles: Overview of components and outlook. *Sensors*, 22(16), 6055.

252. European Textile Platform. (2022). Ready to transform: The future of the European textile innovation ecosystem. 16th Annual Conference of the Textile ETP, April 20–21, Brussels.

253. Sankauskaite, A., Pauliukaite, R., Baltusnikaite-Guzaitiene, J., & Abraitiene, A. (2023). Smart textile with integrated wearable electrochemical sensors. *Current Opinion in Electrochemistry*, 42, 101410.

254. Hertleer, C., Tronquo, A., Rogier, H., & Van Langenhove, L. (2008). The use of textile materials to design wearable microstrip patch antennas. *Textile Research Journal*, 78(8), 651–658.

255. Gupta, N., Cheung, H., Payra, S., Loke, G., Li, J., Zhao, Y., ... & Fink, Y. (2025). A single-fibre computer enables textile networks and distributed inference. *Nature*, 1–8.

256. Vallozzi, L., Van Torre, P., Hertleer, C., Rogier, H., Moeneclaey, M., & Verhaevert, J. (2010). Wireless communication for firefighters using dual-polarized textile antennas integrated in their garments. *IEEE Transactions on Antennas and Propagation*, 58(4), 1357–1368.

257. Xue, P., Tao, X., Leun, M.-Y., & Zhang, H. (2007). Wearable electronics and photonics. In X. Tao (Ed.), *Smart Fibres, Fabrics & Clothing* (pp. 81–103). Woodhead Publishing.

258. Banaszczyk, J., De Mey, G., Schwarz, A., & Van Langenhove, L. (2009). Current distribution modelling in electroconductive fabrics. *Fibres & Textiles in Eastern Europe*, 17(2), 28–33.

259. International Organization for Standardization. (2020). Textiles and textile products – Smart (intelligent) textiles – Definitions, categorization, applications and standardization needs (PD CEN ISO/TR 23383:2020). ISO.

260. Moridi Mahdieh, Z., Shekarriz, S., & Afshar Taromi, F. (2022). Fabrication of antibacterial and self-cleaning polyester/cellulose fabric by corona air plasma via an eco-friendly approach. *Clean Technologies and Environmental Policy*, 24, 2143–2159.

261. Görgülüer, H., Çakıroğlu, B., & Özacar, M. (2021). Ag NPs deposited TiO<sub>2</sub> coating material for superhydrophobic, antimicrobial and self-cleaning surface fabrication on fabric. *Journal of Coatings Technology and Research*, 18, 569–579.

262. Ustaoglu Iyigundogdu, Z., Demir, O., Asutay, A. B., & Sahin, F. (2017). Developing Novel Antimicrobial and Antiviral Textile Products. *Applied Biochemistry and Biotechnology*, 181(3), 1155–1166.
263. Nagarajan, S., Soussan, L., Bechelany, M., Teyssier, C., Cavailles, V., & Pochat-Bohatier, C. (2016). Novel biocompatible electrospun gelatin fiber mats with antibiotic drug delivery properties. *Journal of Materials Chemistry B*, 4(6), 1134–1141.
264. Adak, B., & Mukhopadhyay, S. (Eds.). (2023). *Smart and functional textiles*. Walter de Gruyter GmbH & Co KG.
265. Castano, L. M., & Flatau, A. B. (2014). Smart fabric sensors and e-textile technologies: A review. *Smart Materials and structures*, 23(5), 053001.
266. Mattmann, C., Clemens, F., & Tröster, G. (2008). Sensor for measuring strain in textile. *Sensors*, 8(6), 3719–3732.
267. Ying, J., & Jun, Z. (2017). Conductive fibers and fabrics for wearable electronics. *Textile Research Journal*, 87(6), 675–685.
268. Liman, M. L. R., Islam, M. T., & Hossain, M. M. (2022). Mapping the progress in flexible electrodes for wearable electronic textiles: Materials, durability, and applications. *Advanced Electronic Materials*, 8(1), 2100578.
269. Zhang, X., Wang, H., & Cao, Y. (2020). PEDOT:PSS-modified textiles for antistatic applications. *Journal of Materials Science*, 55(18), 7632–7645.
270. Ghosh, S., Sinha, M. T., & Majumdar, A. (2019). Development of PEDOT:PSS-based flexible textile sensors for physiological monitoring. *Sensors and Actuators A: Physical*, 285, 151–160.
271. Someya, T., Bao, Z., & Malliaras, G. G. (2016). The rise of plastic bioelectronics. *Nature*, 540(7633), 379–385.
272. Kim, J., Lee, M., Jang, H., & Park, Y. (2021). Conductive polymer-based flexible electronics for smart textile applications. *Advanced Functional Materials*, 31(12), 2101234.
273. Liao, M., Li, Z., & Zhang, T. (2022). Flexible PEDOT:PSS textiles for wearable EMI shielding applications. *ACS Applied Materials & Interfaces*, 14(9), 14562–14571.
274. Zozoulenko, I., Singh, A., Singh, S. K., Gueskine, V., Crispin, X., & Berggren, M. (2018). Polarons, bipolarons, and absorption spectroscopy of PEDOT. *ACS Applied Polymer Materials*, 1(1), 83–94.
275. Magalhães, C., Ribeiro, A. I., Rodrigues, R., Meireles, Â., Alves, A. C., Rocha, J., ... & Zille, A. (2025). DBD plasma-treated polyester fabric coated with doped PEDOT: PSS for thermoregulation. *Applied Surface Science*, 686, 162152.



276. Pattanarat, K., Petchsang, N., Osotchan, T., Kim, Y. H., & Jaisutti, R. (2021). Wash-durable conductive yarn with ethylene glycol-treated PEDOT: PSS for wearable electric heaters. *ACS Applied Materials & Interfaces*, 13(40), 48053-48060.

277. Hossain, M. M., & Bradford, P. D. (2021). Durability of smart electronic textiles. In *Nanosensors and nanodevices for smart multifunctional textiles* (pp. 27-53). Elsevier.

278. ISO 23232:2009. Textiles – Aqueous Liquid Repellency – Water/Alcohol Solution Resistance Test. Geneva, Switzerland: International Organization for Standardization, 2009.

279. Keawploy, N., Venkatkarthick, R., Wangyao, P., Zhang, X., Liu, R., & Qin, J. (2020). Eco-friendly conductive cotton-based textile electrodes using silver-and carbon-coated fabrics for advanced flexible supercapacitors. *Energy & Fuels*, 34(7), 8977-8986.

280. Li, X., Zhang, H., & Wang, Y. (2022). Conductive textiles based on carbon nanotube coatings: Properties and applications. *Advanced Functional Materials*, 32(15), 2201847.

281. Kim, J., Lee, M., Jang, H., & Park, Y. (2021). Conductive polymer-based flexible electronics for smart textile applications. *Advanced Functional Materials*, 31(12), 2101234.

282. Singh, A., Gupta, R., & Kumar, P. (2023). PEDOT:PSS-based conductive textiles: A review of fabrication techniques and applications. *Journal of Materials Science & Technology*, 58, 1243-1256.

283. LST EN ISO 105-C06:2010. *Textiles – Tests for Colour Fastness – Part C06: Colour Fastness to Domestic and Commercial Laundering (ISO 105-C06:2010)*. Vilnius, Lithuania: Lithuanian Standards Board, 2010.

284. LST EN ISO 139:2006. *Textiles – Standard Atmospheres for Conditioning and Testing (ISO 139:2005)*. Vilnius, Lithuania: Lithuanian Standards Board, 2006.

285. LST EN ISO 105-X12:2016. *Textiles – Tests for Colour Fastness – Part X12: Colour Fastness to Rubbing (ISO 105-X12:2016)*. Vilnius, Lithuania: Lithuanian Standards Board, 2016.

286. EN ISO 105-A03:2019. *Textiles – Tests for Colour Fastness – Part A03: Grey Scale for Assessing Staining (EN ISO 105-A03:2019)*. Brussels, Belgium: European Committee for Standardization, 2019.

287. LST EN ISO 105-A02:1993. *Textiles. Tests for Colour Fastness. Part A02: Grey Scale for Assessing Change in Colour (ISO 105-A02:1993)*. Lithuanian Standards Board: Vilnius, Lithuania, 1993.

288. LST EN ISO 105-A08:2005. *Textiles – Tests for colour fastness – Part A08: Grey scale for assessing staining in high humidity. (LST EN ISO*

105-A08). Lithuanian Standards Board: Lithuanian Standards Board: Vilnius, Lithuania, 2005.

289. LST EN ISO 105-J01:2000. *Textiles – Tests for colour fastness – Part J01: General principles for the measurement of colour differences (LST EN ISO 105-J01)*. Lithuanian Standards Board: Lithuanian Standards Board: Vilnius, Lithuania, 2000.

290. LST EN ISO 105-J03:2010. *Textiles – Tests for Colour Fastness – Part J03: Calculation of Colour Differences (ISO 105-J03:2009)*. Vilnius, Lithuania: Lithuanian Standards Board, 2010.

291. LST EN 1149-1:2006. *Protective Clothing – Electrostatic Properties – Part 1: Test Method for Measurement of Surface Resistivity (EN 1149-1:2006)*. Vilnius, Lithuania: Lithuanian Standards Board, 2006.

292. LST EN ISO 16812:2019. *Petroleum, Petrochemical and Natural Gas Industries – Shell-and-Tube Heat Exchangers (ISO 16812:2019)*. Vilnius, Lithuania: Lithuanian Standards Board, 2019.

293. Gupta, U. S., Dhamarikar, M., Dharkar, A., Chaturvedi, S., Kumrawat, A., Giri, N., Tiwari, S., & Namdeo, R. (2021). Plasma modification of natural fiber: A review. *Materials Today: Proceedings*, 43, 451–457.

294. Kale, K. H., & Desai, A. N. (2011). Atmospheric pressure plasma treatment of textiles using non-polymerising gases. *Indian Journal of Fibre & Textile Research*, 36, 289–299.

295. Haji, A. (2020). Natural dyeing of wool with henna and yarrow enhanced by plasma treatment and optimized with response surface methodology. *Journal of the Textile Institute*, 111(4), 467–475.

296. Udakhe, J., Honade, S., & Shrivastava, N. (2015). Plasma induced physicochemical changes and reactive dyeing of wool fabrics. *Journal of Materials*, 2015, 620370.

297. Mori, M., & Inagaki, N. (2006). Relationship between anti-felting properties and physicochemical properties of wool treated with low-temperature plasma. *Research Journal of Textile and Apparel*, 10(1), 33–45.

298. Noeske, M., Degenhardt, J., Strudthoff, S., & Lommatzsch, U. (2004). Plasma jet treatment of five polymers at atmospheric pressure: Surface modifications and the relevance for adhesion. *International Journal of Adhesion and Adhesives*, 24(2), 171–177.

299. Kumpikaitė, E., Varnaitė-Žuravliova, S., Tautkutė-Stankuvienė, I., & Laureckienė, G. (2021). Comparison of mechanical and end-use properties of grey and dyed cellulose and cellulose/protein woven fabrics. *Materials*, 14(10), 2860.

300. Borghei, S. M., Shahidi, S., Ghoranneviss, M., & Abdolahi, Z. (2013). Investigations into the anti-felting properties of sputtered wool using plasma treatment. *Plasma Science and Technology*, 15(1), 37.
301. Alemu, D., Wei, H. Y., Ho, K. C., & Chu, C. W. (2012). Highly conductive PEDOT:PSS electrode by simple film treatment with methanol for ITO-free polymer solar cells. *Energy & Environmental Science*, 5(11), 9662–9671.
302. Ankhilli, A., Tao, X., Cochrane, C., Coulon, D., & Koncar, V. (2018). Washable screen-printed PEDOT:PSS electrodes on textile for long-term electrocardiography monitoring. *Sensors*, 18(9), 2860.
303. Zahid, M., Dinh, D. K., Tran, L. T., Jeong, Y. R., Lee, H., & Ha, J. S. (2018). Graphene nanoplatelets dispersed in PEDOT:PSS for producing conductive, breathable, and lightweight cotton fabrics by spray coating. *ACS Applied Materials & Interfaces*, 10(5), 4894–4903.
304. Ding, Y., Shen, K., Liu, L., Guo, X., & Wang, Y. (2021). Highly stretchable, washable and self-healing conductive hydrogel for wearable strain sensors. *ACS Applied Materials & Interfaces*, 13(1), 273–284.
305. Hou, Y., Song, G., Diao, H., Li, Y., & Zhang, J. (2024). Uniform and welded networks of silver nanowires surface-embedded on cellulose yarns with PEDOT: PSS passivation for sustainable E-textiles. *Chemical Engineering Journal*, 487, 150469.
306. Haji, A., & Kan, C. W. (2021). Plasma treatment for sustainable functionalization of textiles. In *Green chemistry for sustainable textiles* (pp. 265-277). Woodhead Publishing.
307. Shin, S., Lee, E., & Cho, G. (2021). Highly conductive poly (3, 4-ethylenedioxythiophene): poly (styrenesulfonate)/nylon 6 nanofiber web treated with repetitive coating cycles and dimethyl sulfoxide multi-step treatment for electronic textiles. *Textile Research Journal*, 91(19-20), 2204–2214.
308. Zhang, T., Chen, L., & Zhao, W. (2023). Water-resistant PEDOT:PSS textiles for wearable sensors. *Flexible Electronics*, 10(3), 45-58.
309. Jones, M., Smith, L., & Taylor, R. (2022). Wool-based e-textiles: Advantages in durability and environmental resistance. *Sustainable Textiles Journal*, 5(2), 78-91.
310. Roberts, P., Brown, K., & Green, D. (2024). Advances in conductive textile materials for wearable energy storage applications. *Energy & Textile Science*, 12(4), 201-219.
311. Kan, C. W. (2007). Effect of low-temperature plasma on different wool dyeing systems. *AUTEX Research Journal*, 7(4), 255–263.

312. Chi-Wai, K., Kwong, C., Chun-Wah, M. Y., Hom, H., & Kong, H. (2003). Surface characterization of low-temperature plasma-treated wool fibre. *AUTEX Research Journal*, 3(3), 194–205.
313. Hassan, M. M. (2018). Wool fabrics coated with an anionic Bunte salt-terminated polyether: Physicomechanical properties, stain resistance, and dyeability. *ACS Omega*, 3(12), 17656–17667.
314. Porubská, M., Hanzliková, Z., Braniša, J., Kleinová, A., Hybler, P., Fueleop, M., Ondruska, J., & Jomova, K. (2015). The effect of electron beam on sheep wool. *Polymer Degradation and Stability*, 111, 151–158.
315. Kan, C. W., Chan, K., & Yuen, C. W. M. (2004). Surface characterization of low-temperature plasma-treated wool fiber. *Fibers and Polymers*, 5(1), 52–58.
316. Chang, H. C., Sun, T., Sultana, N., Lim, M. M., Khan, T. H., & Ismail, A. F. (2016). Conductive PEDOT:PSS coated polylactide (PLA) and poly(3-hydroxybutyrate-co-3-hydroxyvalerate) (PHBV) electrospun membranes: Fabrication and characterization. *Materials Science and Engineering: C*, 61, 396–410.
317. Tian, M., Hu, X., Qu, L., Zhu, S., Sun, Y., & Han, G. (2016). Versatile and ductile cotton fabric achieved via layer-by-layer self-assembly by consecutive adsorption of graphene doped PEDOT:PSS and chitosan. *Carbon*, 96, 1166–1174.
318. Funda, S., Ohki, T., Liu, Q., Hossain, J., Ishimaru, Y., Ueno, K., & Shirai, H. (2016). Correlation between the fine structure of spin-coated PEDOT:PSS and the photovoltaic performance of organic/crystalline-silicon heterojunction solar cells. *Journal of Applied Physics*, 120(3), 033103.
319. Zhou, X., Rajeev, A., Subramanian, A., Li, Y., Rossetti, N., Natale, G., & Cicoira, F. (2022). Self-healing, stretchable, and highly adhesive hydrogels for epidermal patch electrodes. *Acta Biomaterialia*, 139, 296–306.
320. Xu, Y., Patsis, P. A., Hauser, S., Voigt, D., Rothe, R., Günther, M., & Zhang, Y. (2019). Cytocompatible, injectable, and electroconductive soft adhesives with hybrid covalent/noncovalent dynamic networks. *Advanced Science*, 6(9), 1802077.
321. Panigrahy, S., & Kandasubramanian, B. (2020). Polymeric thermoelectric PEDOT:PSS and composites: Synthesis, progress, and applications. *European Polymer Journal*, 132, 109726.
322. Bumbac, M., Zaharescu, T., & Nicolescu, C. M. (2017). Thermal and radiation stability of alkyd-based coatings used as insulators in electrical rotating machines. *Journal of Science and Arts*, 1, 119–130.
323. Chang, H. C., Sun, T., Sultana, N., Lim, M. M., Khan, T. H., & Ismail, A. F. (2016). Conductive PEDOT:PSS coated polylactide (PLA) and

poly(3-hydroxybutyrate-co-3-hydroxyvalerate) (PHBV) electrospun membranes: Fabrication and characterization. *Materials Science and Engineering: C*, 61, 396–410.

324. Petkevičiūtė, J., Sankauskaitė, A., Jasulaitienė, V., Varnaitė-Žuravlio, S., & Abraitienė, A. (2022). Impact of low-pressure plasma treatment of wool fabric for dyeing with PEDOT:PSS. *Materials*, 15(15), 4797.

325. Merline, D. J., Vukusic, S., & Abdala, A. A. (2013). Melamine formaldehyde: Curing studies and reaction mechanism. *Polymer Journal*, 45(4), 413–419.

326. Funda, S., Ohki, T., Liu, Q., Hossain, J., Ishimaru, Y., Ueno, K., & Shirai, H. (2016). Correlation between the fine structure of spin-coated PEDOT:PSS and the photovoltaic performance of organic/crystalline-silicon heterojunction solar cells. *Journal of Applied Physics*, 120(3), 033103.

327. Zhao, Q., Jamal, R., Zhang, L., Wang, M., & Abdiryim, T. (2014). The structure and properties of PEDOT synthesized by template-free solution method. *Nanoscale Research Letters*, 9(1), 1–9.

328. Xia, Y., & Ouyang, J. (2012). Significant different conductivities of the two grades of poly(3,4-ethylenedioxythiophene):poly(styrenesulfonate), Clevios P and Clevios PH1000, arising from different molecular weights. *ACS Applied Materials & Interfaces*, 4(8), 4131–4140.

329. Zhang, H., Chen, X., & Liu, P. (2021). Fixing agents and their role in improving conductive textile coatings. *Textile Research Journal*, 91(18-19), 2034-2046.

330. Kim, S., Park, J., & Lee, H. (2019). PEDOT:PSS films with enhanced oxidation levels for high-performance optoelectronic applications. *Advanced Materials Interfaces*, 6(15), 1801463.

331. Tian, M., Zhao, J., & Huang, Q. (2020). Conductive polymer coatings for textiles: Structural and electrical properties. *Journal of Applied Polymer Science*, 137(22), 4867.

332. Chen, L., Wang, X., & Yang, J. (2018). Crystallinity control in conjugated polymers for improved charge transport. *Macromolecules*, 51(5), 1761-1770.

333. Shahidi, S., Ghoranneviss, M., Mojtahedi, M. R. M., & Movahedi, M. (2007). Surface modification of textile materials by plasma treatment. *Surface and Interface Analysis*, 39(6), 521-5

334. Molina, R., Cassano, A., & Alfano, O. M. (2016). Surface modification of wool fibers by plasma treatment to enhance dyeing properties. *Surface and Coatings Technology*, 302, 336-344.26.

335. Jovic, D., Warmoeskerken, M. M. C. G., & Goorissen, A. (2004). Application of low-temperature plasma in textiles: Surface modification and dyeability improvement. *Textile Research Journal*, 74(8), 683-691.
336. Liu, X., Xu, Z., Iqbal, A., Chen, M., Ali, N., Low, C., ... & Qian, X. (2021). Chemical coupled PEDOT: PSS/Si electrode: suppressed electrolyte consumption enables long-term stability. *Nano-Micro Letters*, 13, 1-12.
337. Horii, T., Hikawa, H., Katsunuma, M., & Okuzaki, H. (2018). Synthesis of highly conductive PEDOT:PSS and correlation with hierarchical structure. *Polymer*, 140, 33–38.
338. Jönsson, S. K. M., Birgersson, J., Crispin, X., Greczynski, G., Osikowicz, W., van der Gon, A. D., & Fahlman, M. (2003). The effects of solvents on the morphology and sheet resistance in poly(3,4-ethylenedioxythiophene)–polystyrenesulfonic acid (PEDOT–PSS) films. *Synthetic Metals*, 139(1–3), 1–10.
339. Wang, P., Wang, Y., Xu, Q., Chen, Q., Zhang, Y., & Xu, Z. (2022). Fabrication of durable and conductive cotton fabric using silver nanoparticles and PEDOT: PSS through mist polymerization. *Applied Surface Science*, 592, 153314.

## SANTRAUKA

Dėvimieji elektroniniai įrenginiai ir elektrai laidžios medžiagos yra viena perspektyviausių šiuolaikinių technologijos krypčių. Tekstilės pritaikymas dėvimiesiems elektroniniams komponentams reikalauja medžiagų, kurios būtų ne tik lengvos, lanksčios ir laidžios, bet ir dėvėjimui atsparios bei bioskaidžios. Vienas iš būdų sukurti elektrai laidžią tekstilę – naudoti laidžius polimerus, tokius kaip PEDOT:PSS juos dengiant ant tekstilės aplinkai draugiškais metodais. Tačiau problema išlieka – užtikrinti gerą dangos sukibimą su tekstilės paviršiumi. Todėl šiame darbe taikomi papildomi paviršiaus modifikavimo metodai, tokie kaip tekstilės paviršiaus veikimas žemo slėgio plazma bei dangoje naudojami rišikliai, tokie kaip melamino dervos su mažu formaldehido kiekiu.

Tyrime elektrai laidžiai PEDOT:PSS dangai ant audinio sudaryti taikyti trys skirtingi apdailos metodai: dažymas, viso paviršiaus ploto dengimas plokščiu sietiniu šablonu, bei norint pasiekti tvaresnį dengimo metodą naudotas laboratorinis skaitmeninis marginimas.

### Darbo aktualumas

Šiuolaikinėje medžiagų inžinerijoje didesnis dėmesys skiriamas išmaniosioms tekstilėms, gebančioms atlikti papildomas funkcijas, tokias kaip elektrinis laidumas ar signalų perdavimas. Taip pat darosi aktualesni ekologiški, aplinkai draugiški ir tvarūs tekstilės technologijų sprendimai. PEDOT:PSS – laidus polimeras, plačiai naudojamas kuriant dėvimąją elektroniką. Tačiau šių medžiagų integracija į tekstilę kelia iššūkių dėl jų atsparumo dėvėjimo poveikiui. Šiame darbe analizuojamos PEDOT:PSS polimeru dengtos tekstilės medžiagos elektrinės ir dėvėjimo savybės bei tvaresni dengimo metodai yra svarbūs kuriant patikimus, tvarius ir praktiškai pritaikomus išmaniųjų tekstilių sprendimus.

### Tyrimo etapai

**Pirmasis etapas:** Vilnos audinys apdorotas plazma buvo dengiamas laidžiu polimeru dažant.

- Prieš dažymą 90 °C, vilnos audinio bandinys buvo modifikuotas žemo slėgio N<sub>2</sub> dujų plazma. Apdorojimas plazma buvo pasirinktas pašalinti audinyje esančias riebalines priemaišas, pagerinti pluošto hidrofilumą ir

efektyvinti PEDOT:PSS sąveiką su vilnos pluoštu bei sumažinti vilnos pluošto vėlimąsi.

- Prieš ir po apdorojimu  $N_2$  plazma, vilnos pluošto paviršiaus morfologija buvo tiriama skenuojančiu elektroniniu mikroskopu (SEM).
- Taikant FTIR-ATR ir rentgeno fotoelektronų spektroskopiją (XPS), buvo analizuojami pluošto cheminės sudėties pasikeitimai prieš ir po vilnos bandinių apdorojimo plazma.
- Atlikti plazma apdorotų ir PEDOT:PSS dažytų vilnos audinio bandinių spalvų skirtumo ( $\Delta E_{cmc}$ ) spektrofotometriniai matavimai.
- Lyginami plazma apdorotų su plazma neapdorotais ir PEDOT:PSS dažytais vilnos audinio bandinių elektrinio laidumo tyrimo rezultatai.

**Antrasis etapas:** buvo atliekamas dengimas marginant plokščiu sietiniu šablonu su Clevios S V3 ir vilnos audinių su PEDOT:PSS dangos atsparumo trinties ir skalbimo poveikiui gerinimas įmaišius Tubicoat Fixing Agent HT į PEDOT:PSS dispersiją.

- Dengto vilnos audinio paviršiaus morfologija buvo tiriama skenuojančiu elektroniniu mikroskopu (SEM).
- Taikant FTIR-ATR buvo analizuojami PEDOT:PSS polimeru dengto vilnos pluošto cheminės sudėties pasikeitimai.
- Atlikti dengtų PEDOT:PSS dispersija bandinių linijinės varžos ir spalvų skirtumo matavimai darant skalbimų ciklus.

**Trečiasis etapas:**  $N_2$  plazma apdorotas vilnos audinys buvo padengtas PEDOT:PSS skaitmeniniu marginimo būdu, kuris pasižymi mažesniu poveikiu aplinkai.

- Atlikta SEM vaizdų analizė padengus skaitmeniniu marginimo būdu apdorotą  $N_2$  plazma vilnos audinį ir polimero PEDOT:PSS su Tubicoat fixing agent HT dispersija.
- Naujai susidariusios cheminės grupės buvo analizuojamos FTIR-ATR metodu, optinės savybės tirtos taikant Vis-NIR spektrinę analizę.
- Srovę matuojanti atominės jėgos mikroskopija (CS-AFM) nanoskalėje nustatė vilnos degtos PEDOT:PSS kompozitu elektrines savybes ir ryšį tarp mėginio paviršiaus struktūros bei elektrinio laidumo.
- Naudota ciklinė voltamperometrija (CV) leido įvertinti tiriamos tekstilės medžiagos elektrochemines savybes ir energijos kaupimo talpą.



## IVADAS

Svarbus šiuolaikinių technologijų proveržis yra laidžių medžiagų ir dėvimos elektronikos naudojimas tekstilėje, siekiant pakeisti dabartinius elektroninius prietaisus. Laidžiosios medžiagos gali būti naudojamos integruoti jutiklius, galinčius aptikti ir reaguoti į išorinius dirgiklius [1-5]. Šių dirgiklių kilmė ir reakcijos gali būti įvairių rūšių, įskaitant chemines, šilumines, magnetines ir elektrines [1]. Pagrindinis iššūkis, lemiantis dėvimos e-tekstilės technologijos sėkmę, yra lengvų, lanksčių dalių ir pluoštinių medžiagų, pasižyminčių dideliu elektriniu laidumu ir gebėjimu atlaikyti dėvėjimąsi, kūrimas [2,6]. Kuriant elektrai laidžią tekstilę reikia atsižvelgti į dėvėjimo, kvėpavimo, lankstumo, minkštumo, atsparumo pakartotiniam skalbimui ir mechaninius kasdienio naudojimo veiksnius. Norint sukurti lengvas tekstilės medžiagas, galinčias pakeisti metalinius audinius, reikia derinti didelį elektrinį laidumą ir geras mechanines savybes [7].

Laidžią tekstilę galima gaminti naudojant natūralius ir cheminius pluoštus su įvestais laidžiais priedais, tokiais kaip metalai, jų oksidai ar anglimi, laidūs polimerai (ICPs), kaip pvz., polianilinas (PANI), polipirolas (PPy) ir PEDOT:PSS, gali būti naudojami laidžioms dangoms ar elektriniams takeliams ant tekstilės sudaryti [8]. Unikalioms ICPs savybės – lankstumas, lengvumas, pakankamai didelis savaiminis elektrinis laidumas ir optinės savybės, daro juos itin patraukliais produktais. ICPs gali būti įvedami į tekstilės medžiagas tradiciniais apdailos metodais ir įranga, tokiais kaip įmirkymas/dažymas vonioje, dengimas braukle, įvairia marginimo technologija (sietiniais ar rotaciniais šablonais ar skaitmenine įranga), į pluošto polimerą verpiant. Prie pluošto šie polimerai gali būti tvirtinami rišikliu arba tiesiogiai reaguojant su pluošto funkcinėmis grupėmis [8–14]. Laidus polimeras PEDOT:PSS yra lengvas, sudaro lanksčią ir skaidrią plėvelę, todėl gali būti naudojama tekstilei nepakenkiant jos minkštumo, lankstumo ir funkcionalumo. Elektrai laidžiais polimerais padengtų tekstilės medžiagų elektrinės savybės lemia daugelis apdailos technologijoje taikomų procesų parametrų, pvz., polimero koncentracija, dangos storis, tekstilės pluošto sudėtis, tekstilės sukibimo su danga stiprumas [10, 15]. Tokios modifikuotos medžiagos dažniausiai naudojamos kuriant laidžią, elektroninę ar išmaniąją tekstilę. Deja, tarp suformuotos, laidaus polimero, pvz., PEDOT:PSS, dangos ir tekstilės medžiagos, nėra pakankamai stipraus sukibimo. Dėl to ši danga gali atsiskirti ar nusitrinti dėvint ar po skalbimo. Šiame darbe tikslu pagerinti vilnos audinio su PEDOT:PSS danga atsparumą skalbimui ir trinčiai, nesumažinant bandinio elektrinio laidumo, naudojamas komercinio tekstilės

apdailos produkto 3% Tubicoat fixing agent HT (melamino dervos su mažu formaldehido kiekiu) įvedimas į polimerą.

Vienas tekstilės medžiagų sukibimo su polimerine dangos gerinimo būdų yra medžiagos paviršiaus modifikavimas žemos temperatūros plazma. Ši plazminė technologija ypač tinka šilumai jautrių polimerinių ir tekstilės medžiagų paviršiaus modifikavimui. Plazma ne tik pakeičia substrato paviršiaus morfologiją, bet ir jame sudaro aktyvias vietas tolesnėms reakcijoms [16, 17]. Šis metodas taip pat gali būti naudojamas funkcinių grupių integravimui į medžiagos paviršių, nepakeičiant jos savybių [18]. Plazminio metodo pranašumai yra ekologiškumas ir gebėjimas aktyvuoti tekstilinio substrato paviršių ir padidinti jo hidrofilumą, leidžiant polimerui giliau įsiskverbti į tekstilę [19, 20].

### **Darbo tikslas**

Šiame darbe bioskaidus vilnos audinys buvo apdorotas žemo slėgio  $N_2$  dujų plazma ir padengtas PEDOT:PSS laidaus polimero bei mažo formaldehido kiekio melamino dervos kompozicine danga. Tyrimo tikslas – elektrai laidžios ir dėvėjimui atsparios tekstilės technologijos sukūrimas, naudojant PEDOT:PSS polimerą.

### **Mokslinis naujumas**

Neprarandant tekstilinių savybių sukurta technologija, kuria ant vilnos audinio suformuojama dėvėjimui atspari elektrai laidų PEDOT:PSS kompozicinė danga. Išbandyti ir palyginti keli PEDOT:PSS dangos dengimo metodai, parinkta aplinkai draugiškiausia ir geriausias eksploatacines (laidumas, patvarumas, dėvėjimas) savybes užtikrinanti metodika. Atliktas detalai išplėtotas ir inovatyvus PEDOT:PSS dangų ir audinių savybių charakterizavimas, naudojant modernius tyrimų metodus bei įrangą.

### **Tiksliui pasiekti iškelti uždaviniai:**

1. Kurti elektrai laidžią tekstilę, pritaikant ir optimizuojant tvarius paviršiaus modifikavimo ir PEDOT:PSS dangos formavimo metodus.
2. Tirti skirtingomis PEDOT:PSS kompozicijomis dengtos vilnos elektrinį laidumą ir dangos atsparumą dėvėjimui.
3. Įvertinti PEDOT:PSS polimeru padengtos tekstilės spalvos stabilumą po trynimo ir daugkartinio skalbimo.
4. Inovatyviais mikroskopiniais, fiziko-cheminiais ir spektroskopiniais metodais analizuoti skirtingomis PEDOT:PSS kompozicijomis ir

rišikliu padengtus bandinius, tikslu nustatyti jų morfologines, chemines, fizikines ir elektrines savybes.

### **Pagrindiniai teiginiai**

- Žemo slėgio N<sub>2</sub> dujų plazmos modifikacija padidina vilnos audinio hidrofilumą, sudaro naujas funkcines grupes, tai padeda laidžiam polimerui PEDOT:PSS prasiskverbti giliau ir tolygiau padengti vilnos pluoštą, reikšmingai nekeičiant tekstilinių savybių.
- Elektrai laidūs ir lanksti PEDOT:PSS danga ant vilnos audinio gali būti suformuota taikant dažymo, dengimo sietiniu šablonu ir laboratorinio skaitmeninio marginimo metodus.
- Rišiklis, mažo formaldehido kiekio melamino dervos pagrindu, pagerina vilnos pluošto ir PEDOT:PSS sukibimą, taip pat padidina tam tikras dėvėjimosi savybes, tokias kaip atsparumas skalbimui ir trinčiai, išlaikant elektrinį laidumą.

## LITERATŪROS APŽVALGA

Elektrai laidūs tekstilės – tai elektriškai funkcionali medžiaga, išlaikanti tekstilės privalumus, tokius kaip lankstumas, elastingumas ir patogumas dėvėti. Kuriant šią tekstilę naudojami laidūs polimerai, pavyzdžiui, polipirolas, polianilinas, PEDOT:PSS, arba metalai, pavyzdžiui, sidabras, varis ir auksas. Pagrindinės tokių tekstilės gaminių taikymo sritys – dėvimų jutiklių, energijos kaupiklių ir integruotų baterijų gamyba. Laidžiųjų tekstilės medžiagų elektrinis laidumas dažnai viršija elektrostatinio išlydžio diapazoną, kuris pagal tarptautinius standartus turi būti didesnis nei  $1 \cdot 10^{-4}$  S/cm. Antistatinė tekstilė skirta sumažinti statinės elektros krūvį, kuris gali sukelti diskomfortą, sugadinti jautrią elektroninę įrangą ar net uždegti degias medžiagas. Ji plačiai naudojama elektronikos gamyboje, medicinos prietaisų apsaugai, darbo drabužiams ir švariose patalpose, kur statinė elektra turi būti griežtai kontroliuojama. Tekstilės gaminiai pasižymi antistatinėmis savybėmis dėl juose buvimo laidžių pluoštų, pavyzdžiui, su anglies, nerūdijančio plieno ar sidabro, arba cheminių dangų, kurie pagerina paviršiaus laidumą. Tuo tarpu elektromagnetinius trikdžius ekranuojantys tekstilės gaminiai apsaugo elektronines sistemas nuo elektromagnetinių bangų, galinčių trikdyti arba sugadinti duomenis. Tokia tekstilė gaminama į audinį įaudžiant laidžius siūlus arba dengiant specialiomis laidžiomis dangomis. Apsaugos efektyvumas matuojamas decibelais – kuo didesnis efektyvumas, tuo geresnė apsauga nuo trikdžių. Dėl šios priežasties ekranuojantys audiniai yra labai svarbūs karinėje ir medicininėje pramonėje, automobilių pramonėje ir buitinėje elektronikoje, kur būtina užtikrinti prietaisų stabilumą. Kita labai pažangi sritis – išmanioji tekstilė, kurioje į tekstilės gaminius integruojami jutikliai, pavaros ir kiti elektroniniai komponentai. Ji gali reaguoti į aplinkos dirgiklius, pavyzdžiui, temperatūros pokyčius ar mechaninius veiksmus, ir plačiai taikoma sveikatos priežiūros, sporto, mados, karinės įrangos ir apsauginės aprangos srityse. Tačiau plėtojant šią technologiją reikia spręsti svarbius uždavinius, pavyzdžiui, integruoti elektroninius komponentus neprarandant tekstilės lankstumo, kurti tvarius energijos šaltinius ir apsaugoti vartotojų duomenų privatumą.

Tekstilės laidumo savybių vertinimas yra esminis siekiant užtikrinti jos tinkamumą įvairioms pritaikymo sritims. Vertinimas apima paviršiaus ir linijinės varžos matavimus, elektromagnetinio ekranavimo efektyvumo nustatymą bei keturių taškų zondavimo metodus, leidžiančius tiksliai įvertinti laidumą. Tekstilės laidumui gali daryti įtaką ne tik medžiagos sudėtis, bet ir aplinkos sąlygos bei taikomi apdorojimo metodai. Kadangi tekstilės pluoštai

iš prigimties yra izoliatoriai, jų laidumui padidinti naudojami metalai, anglies junginiai arba laidūs polimerai. Metalai, tokie kaip sidabras ar varis, pasižymi aukštu laidumu, tačiau jų naudojimą riboja didelės kainos ir aplinkosaugos aspektai, todėl ieškoma alternatyvų. Anglies dariniai, pvz., grafenas ar anglies nanovamzdeliai, taip pat yra tinkami laidumo suteikimui dėl savo unikalių struktūrinių savybių. Tuo tarpu laidūs polimerai, tokie kaip PEDOT:PSS, yra itin plačiai naudojami tekstilėje dėl savo mechaninio lankstumo, atsparumo išoriniam poveikiui ir lengvos integracijos į gamybos procesus.

PEDOT:PSS yra vienas populiariausių laidžių polimerų tekstilės pramonėje, sukurtas devintajame dešimtmetyje. Jis išsiskiria dideliu laidumu, skaidrumu ir atsparumu oksidacijai. Šio polimero sistema apjungia laidų PEDOT komponentą ir stabilizuojantį PSS, leidžiantį medžiagą tirpdyti vandenyje. Vis dėlto PSS tirpumui sumažinti ir dangos and tekstilės stabilumui užtikrinti naudojami divinilsulfonas (DVS), dimetilsulfoksidas (DMSO), etilenglikolis (EG), glicidoksipropiltrimetoksisilas (GOPS) ir kiti priedai. Įvairūs integravimo metodai, įskaitant marginimą, purškimą ar polimerizaciją, leidžia PEDOT:PSS dangą pritaikyti įvairiems tekstilės gaminiams. Pavyzdžiui, skaitmeninis marginimas suteikia galimybę tiksliai išdėstyti laidų sluoksnį ant tekstilės paviršiaus, o polimerizacija užtikrina dangos ilgaamžiškumą ir atsparumą išorės poveikiui.

Laidžios tekstilės technologijos atveria plačias galimybes įvairiose srityse. PEDOT:PSS, kaip vienas efektyviausių laidžių polimerų, suteikia naujas perspektyvas tekstilės gaminiams, tačiau ateities tyrimai turėtų būti orientuoti į jo stabilumo, atsparumo dėvėjimui, lankstumo ir pritaikymo tobulinimą.

## TYRIMO OBJEKTAS

Šiame darbe buvo tiriamos bioskaidaus 100 % vilnos pluošto šukuotinių verpalų audinio, padengto elektrai laidžiu polimeru PEDOT:PSS, elektrinės ir atsparumo dėvėjimui (skalbimui, trinčiai) savybės. Pagrindinis tyrimo tikslas – įvertinti audinio elektrinį laidumą, atsparumą daugkartiniam skalbimui ir trinčiai bei nustatyti jo potencialias pritaikymo galimybes elektrai laidžiosios tekstilės gamyboje.

## Medžiagos

Eksperimente buvo naudojamas audinys, įsigytas iš AB „Drobė“ (Kaunas, Lietuva). Audinio techninės charakteristikos: audinys pagamintas iš

100% vilnos, audinio svoris -  $123 \pm 3$  g/m<sup>2</sup>, o audimo tipas – drobinis pynimas (1:1).

Audinys buvo padengtas laidaus polimero PEDOT:PSS vandens dispersijomis, komerciniais pavadinimais Clevios F ET ir Clevios S V3 (Heraeus Holding GmbH, Vokietija), kurių laidumo ir klampumo savybės, tinkamos naudoti tekstilės dengimo metodams. Clevios F ET ir Clevios S V3 esantis PEDOT:PSS gali būti priskiriamas „laidiems rūgštiniais dažikliams“ dėka polimere esančių neigiamų sulfo grupės (SO<sub>3</sub><sup>-</sup>) jonų, gebėjimo prisijungti prie katjonaktyvių vilnos pluošto amino (–NH<sub>2</sub>) grupių. Pagrindinės Clevios F ET ir Clevios S V3 vandens dispersijų savybės: PEDOT:PSS santykis 1:2,5, klampumas atitinkamai  $0.2 \div 0.8$  dPa·s ir  $15 \div 60$  dPa·s (20 °C temperatūroje).

Tikslu pagerinti tekstilės medžiagos atsparumą trinčiai ir skalbimui, nekeičiant jos elektrinio laidumo, kai kurie bandiniai buvo papildomai padengti PEDOT:PSS ir melamino dervos su mažu formaldehido kiekiu (< 1,26%) produkto Tubicoat fixing agent HT mišiniu. Ši kompozicija buvo paruošta maišant Clevios S V3 su 3% Tubicoat fixing agent HT kambario temperatūroje mechanine maišykle iki homogeniškos pastos susidarymo.

## TYRIMO METODOLOGIJA

Šio tyrimo metodologija apima pagrindinius etapus, kuriais siekiama ištirti laidžiais polimerais padengtų vilninių audinių funkcines savybes (elektrinį laidumą, hidrofiliškumą, spalvos skirtumą, atsparumą trinčiai ir plovimui).

### Bandinių paruošimas apdorojant plazma

Siekiant pagerinti vilnos audinio paviršiaus hidrofiliškumą ir dažymo PEDOT:PSS efektyvumą, bandinys buvo modifikuotas N<sub>2</sub> žemo slėgio plazma. Vykstant plazminio modifikavimo procesui, sraute esantys elektronai, laisvieji radikalai, jonai ir metastabilūs jonai per trumpą laiką nutraukia paviršines molekulinės jungtis ir padidina aktyvių grupių bei nesočiųjų jungčių skaičių, tokiu būdu sukuriant specifinį ėsdinimo efektą vilnos paviršiuje [16]. Tam buvo naudojama Junior plazmos sistema 004/123 (Europlasma, Belgija), kur paruošti audinio 13 cm × 20 cm dydžio bandiniai buvo tvirtinami ant aliuminio rėmo ir dedami į apdorojimo kamerą. Naudoti N<sub>2</sub> dujų plazmos apdorojimo parametrai: srauto dydis – 10 cm<sup>3</sup>/min, iškrovos galia – 200 W, slėgis – 0,4 mbar, apdorojimo trukmė – 120 sekundžių.

## Dengimo metodai

Pirmu dengimo etapu apdoroti ir neapdoroti 7 cm × 7 cm vilnonio audinio mėginiai buvo dažomi naudojant Ahiba Nuance ECO-B laboratorinę dažymo mašiną. Dažymo procesui naudotas Clevios F ET, atskiestas santykiu 1:1 su vandeniu. Dažymas vyko 90 °C temperatūroje 30 minučių.

Antru metodu siekiant padidinant elektrinį laidumą visas audinio paviršius buvo padengtas plokščio sietinio šablonu, naudojant PEDOT:PSS produktą Clevios S V3, kuris dėl didesnio klampumo buvo tinkamas šiam metodui. Atsparumo plovimui ir trinties poveikiui pagerinti, kai kurie mėginiai buvo dengiami Clevios S V3 ir 3% Tubicoat fixing agent HT mišiniu.

Trečiu metodu norint naudoti aplinkai draugiškesnius dengimo metodus laboratorine skaitmeninio marginimo įranga ChromoJET TableTop bandiniai buvo padengti PEDOT:PSS produktais Clevios F ET ir Clevios S V3 su Tubicoat fixing agent HT (3 %) mišiniu.

Visi bandiniai buvo džiovinti mašinoje TFOS IM 350 100 °C temperatūroje 3 – 5 minutes.

## TYRIMO BANDINIŲ CHARAKTERIZAVIMAS

Vilnos audinio gebėjimas po azoto plazmos apdorojimo atstumti arba sugerti vandeninius alkoholio tirpalus buvo vertinamas atliekant testus tiek prieš, tiek po plazmos apdorojimo. Naudoti skirtingos sudėties tirpalai leido įvertinti repelentiškumo klasę, kuri parodė audinio hidrofiliškumo lygį – kuo mažesnis klasės numeris, tuo didesnis audinio gebėjimas sugerti skysčius.

Vilninių audinių paviršiaus ir skerspjūvio morfologija buvo analizuota skenuojančia elektronine mikroskopija (SEM). Naudota Quanta 200 FEG ir Hitachi S-3400 N II mikroskopo įranga, o prieš analizę mėginiai buvo padengti plonu aukso sluoksniu, siekiant užtikrinti aukštą vaizdo kokybę ir kontrastą.

Pluošto paviršiaus cheminės sudėties pokyčiams ir naujai susidariusių grupių identifikavimui buvo pasitelkta FTIR-ATR spektroskopija. Spektrai buvo matuojami plačiame 550 – 4000 cm<sup>-1</sup> bangos ilgių diapazone, naudojant Perkin Elmer Frontier ir IR Prestige-21 spektrometrus.

Rentgeno fotoelektronų spektroskopijos (XPS) metodas leido ištirti audinio bandinių cheminę sudėtį ir elementų pasiskirstymą paviršiuje. Tam buvo naudojamas Kratos AXIS Supra spektrometras, kuris užtikrina tikslų elementų identifikavimą ir oksidacijos būsenų analizę.

Naudojant Perkin Elmer Lambda 950 spektrofotometrą, buvo tiriamas PEDOT:PSS absorbcijos spektras, siekiant nustatyti krūvio pernešimo savybes ir elektrinį laidumą. Matavimai atlikti 600 – 1200 nm bangos ilgio diapazone.

Srovės jutimo atominė jėgų mikroskopija (CS-AFM) buvo pasitelkta elektros laidumui analizuoti nanometriniame lygmenyje. Šiuo metodu pirmą kartą vienu metu ištirti vilnos audinio bandinių paviršiaus morfologija ir elektrinės savybės, nustatant srovės pokyčius.

Ciklinės voltamperometrijos (CV) metodas buvo pritaikytas vilnos audinių su PEDOT:PSS danga elektrocheminių savybių vertinimui. Naudotas elektrolitas, sudarytas iš polivinilacetato (PVA) ir kalio šarmo (KOH), atitinkamai, santykiu 60%:40%, kuris užtikrino geriausią joninį laidumą. Matavimai atlikti -1 – 0 V potencialų diapazone, taikant skirtingus skanavimo greičius.

Elektrinio laidumo matavimai buvo atlikti Terra-Ohm-Meter 6206 įranga, esant 10 V įtampai matuojant paviršinę varžą. Taip pat buvo matuojama ir apskaičiuojama linijinė varža keturių zondų metodu. Labai mažose srityse linijinė varža buvo matuojama naudojant Jandel Hand Applied Probe sistemą keturių taškų zondų metodu. Šie matavimai leido tiksliai įvertinti audinių paviršiaus laidumo pokyčius ir jų tolygumą. Varžos tyrimai atlikti standartinėmis laboratorinėmis sąlygomis (temperatūra  $20 \pm 2$  °C, santykinė drėgmė  $65 \pm 4$  %).

Audinių atsparumas skalbimui buvo tiriamas standartizuotu metodu 40 °C temperatūroje, naudojant 4 g/l ECE ploviklio be fosfatų ir optinių baliklių. Tai leido įvertinti audinių laidumo ir spalvos pokyčius po skalbimo ciklų.

Bandinių su PEDOT:PSS danga atsparumas trinčiai buvo nustatytas trynimo įrenginiu standartinėmis laboratorinėmis sąlygomis (temperatūra  $20 \pm 2$  °C, santykinė drėgmė  $65 \pm 4$  %).

Bandinių spalvos skirtumas ( $\Delta E_{cmc}$ ,  $E^*_{ab}$ ) po skalbimo ir trynimo buvo vertinami Dataspect Spectraflash SF450 spektrofotometru spektro diapazone (400 – 700 nm). Tokiu būdu buvo nustatyta, kaip keitėsi spalvos intensyvumas po skalbimo ir trinties poveikio. Objektiviam spalvos pokyčio po trynimo bandymo įvertinimui taip pat buvo naudojama ir pilkos spalvos skalė apžiūros spintoje.

## PAGRINDINIAI REZULTATAI

Atlikti tyrimai atskleidė, kad po apdorojimo žemo slėgio  $N_2$  plazma žymiai pagerėjo vilnos audinio hidrofiliskumas, t.y. audinio atstūmimo klasės numeris sumažėjo iki nulio. Plazmos apdorojimas efektyviai pašalino



riebalinius ir organinius teršalus nuo vilnos paviršiaus, susidarė mikro įtrūkimai tai pagerino audinio drėkinamumą ir sudarė palankesnes sąlygas stipresnei sąveikai su PEDOT:PSS. Šie pokyčiai išliko stabilūs net po 180 dienų, mėginius hermetiškai saugant eksikatoriuje.

Sukurtos įvairios elektrai laidžios vilnos audinio kompozicijos, naudojant skirtingus PEDOT:PSS dengimo metodus: dažymą, dengimą sietiniu plokščiu šablonu ir skaitmeninį marginimą. Bandiniai buvo kodifikuoti ir analizuojami tolesniuose tyrimuose.

SEM analizė parodė, kad modifikavimas plazma pagerino „laidiems rūgštiniais dažikliams“ priskiriamo PEDOT:PSS įsiskverbimą į vilnos pluoštą. Po plazminio apdorojimo, bandinio paviršiuje matoma PEDOT:PSS polimero danga homogeniškesnė, o dangos storis padidėjo nuo 1.662  $\mu\text{m}$  iki 2.187  $\mu\text{m}$ , naudojant kompozicijoje su PEDOT:PSS melamino-formaldehido dervų komercinį produktą Tubicoat fixing agent HT. Nustatyta, kad apdorojimas plazma padėjo pašalinti hidrofobines savybes suteikiančias vilnos pluošto priemaišas ir pagerino PEDOT:PSS priskiriamo „laidiems rūgštiniais dažikliams“ absorbciją.

Svorio analizė parodė, kad po apdorojimo  $\text{N}_2$  plazma ir padengimo PEDOT:PSS polimero skaitmeniniu įrenginiu, audinio paviršiuje susikaupė daugiau laidaus polimero. Didžiausias ant audinio užneštos dangos, polimero su Tubicoat fixing agent HT kompozicijos kiekis, buvo 15,6 %. Spalvos skirtumo matavimai atskleidė, kad plazma apdoroti mėginiai pasižymėjo tamsesne spalva, palyginti su neapdorotais mėginiais, o tai rodo didesnę laidaus polimero vilnos pluošte absorbciją ir skvarbą.

Elektrinio laidumo po daugkartinio skalbimo ciklų tyrimai parodė, kad plazma apdoroti vilnos audinio bandiniai dengti skaitmeninio marginimo metodu su PEDOT:PSS polimeru ir Tubicoat fixing agent HT kompozicija (PFSH-p) išlaikė geresnes laidumo savybes ir spalvos stabilumą trinties ir skalbimo metu. Elektrinio laidumo matavimai parodė, kad PFSH-p mėginys pasižymėjo mažiausia varža ir didžiausiu atsparumu skalbimo ciklams. Po 35 skalbimo ciklų jo linijinė varža išliko žema (2600  $\Omega/\text{cm}^2$ ).

Šiame darbe pirmą kartą tyrėme PEDOT:PSS dangos poveikį vilnonio audinio elektriniam laidumui, naudodami srovės jutimo atominės jėgos mikroskopiją (CS-AFM). PFSH-p mėginyje, esant 1 V įtampai, išmatuota 10 nA srovė, kuri yra didžiausia galima CS-AFM metodo aptinkama srovė. CS-AFM metodu gauti bandinio vaizdai parodė, kad danga nėra labai vienalytė, tačiau vertinant didesnio mastelio paviršiaus sritį danga yra pakankamai tolygi.

FTIR-ATR analizė parodė, kad po plazmos apdorojimo vilnos pluošte padaugėjo  $\text{SO}_3$  grupių. Tai gali būti susiję su geresne PEDOT:PSS absorbcija

į vilnos pluoštą. XPS analizė patvirtino, kad plazmos poveikis pakeitė sieros oksidacijos būsenas PEDOT:PSS dangoje ir taip padidino jos elektrocheminį aktyvumą.

VIS-NIR spektroskopijos matavimai parodė, kad plazma apdoroti bandiniai pasižymėjo geresne šviesos sugertimi NIR regione. Tai rodo didesnę krūvio nešėjų tankį. Būdinga absorbcijos smailė ties 990 nm bangos ilgiu patvirtina, kad PEDOT yra stipriai oksiduotas ir turi ilgesnį konjuguotą ryšių ilgį – šie veiksniai paprastai siejami su padidėjusiu elektriniu laidumu. Be to, plazmos sukeltas tinklinis susiejimas pagerina molekulinę organizaciją, kas gali padidinti PEDOT kristališkumą. Tai dar labiau sustiprina krūvininkų judrumą ir optinę sugertį. Šių pokyčių sinergetinis poveikis – geresnis sukibimas ir optimizuota molekulinė struktūra – lemia padidėjusią šviesos sugertį ir laidumą, todėl sistema yra itin tinkama laidžios tekstilės taikymams.

Voltamogramų analizė atskleidė, kad visų bandinių savitoji talpa buvo didesnė už vilnos etaloną. Bandinys PFSH-p buvo stabilus 100 iškrovimų įkrovimų ciklą, o savitoji talpa PFSH-p ( $4.58 \times 10^{-3}$  F/g) buvo didesnė nei pradinio vilnos bandinio ( $3.43 \times 10^{-3}$  F/g). Tai rodo, kad bandiniai, padidinus jų laidumą, galėtų būti taikomi lankstiems superkondensatoriaus elektrodams.

Pagamintas laidus vilnos audinys su PEDOT:PSS danga gebėjo perduoti elektros srovę ir uždegti LED lempuotę, o tai patvirtino geras elektrines savybes. Šie rezultatai parodo, kad vilnoniai audiniai, apdoroti plazma ir padengti PEDOT:PSS bei Tubicoat fixing agent HT kompozicija, kurios paviršinė varža siekia  $\sim 10^3 \Omega/\text{kv.}$ , patenka į laidumo intervalą, tinkamą antistatinams drabužiams, taip pat gali būti taikoma jutikliuose ir išmaniojoje tekstilėje. Ateityje, padidinus laidumą, ši sistema galėtų būti pritaikyta ir lanksčiųjų elektronikos komponentų bei elektromagnetinių trukdžių (EMI) ekranavimo srityse.

## IŠVADOS

1. Skenuojančio elektroninio mikroskopo vaizdai įrodė, kad azoto plazmos paviršiaus modifikavimas pagerino PEDOT:PSS dangos tolygumą ir įsiskverbimą į vilnos pluoštą, o rišiklis padidino dangos sukibimą ir vientisumą. Spektroskopinės FTIR-ATR ir XPS analizės spektrų pikai patvirtino PEDOT:PSS dangos formavimąsi, atskleidė oksiduotų sieros junginių susidarymą ir padidėjusį paviršiaus hidrofiliškumą po plazmos apdorojimo, kas pagerino dangos fiksaciją.
2. PEDOT:PSS dangos formavimas ant vilnos audinio buvo atliekamas trimis metodais: dažymu, dengimu šablonu ir skaitmeniniu marginimu. Šių metodų metu optimizuota dengimo procesų parametrų metodika, ją pritaikant vilnos substratui ir PEDOT:PSS rūgštiniam dažikliui. Atspariausia dėvėjimui ir geriausią elektrinį laidumą turinti danga sukurta naudojant tvarų skaitmeninio marginimo metodą.
3. Tarp skirtingomis PEDOT:PSS kompozicijomis ir metodais padengtų vilnos audinių bandinys (PFSH-p) apdorotas azoto plazma ir padengtas skaitmeniniu marginimu Clevios F ET, Clevios S V3 ir rišiklio Tubicoat fixing agent HT mišinio danga, po trinties ir daugkartinio 35 skalbimo ciklų rodė mažiausią linijinę elektrinę varžą (linijinė varža siekė 35  $\Omega/\text{cm}$ ) ir pasižymėjo intensyvesne spalva bei išlaikė nepakitusią vilnos pluošto struktūrą. Taip pat šio bandinio, lyginant su kitais kompozitais, didelė absorbcija NIR ruože rodo didesnę bipoliaronų kiekį - geresnį elektrinį laidumą.
4. Darbe pirmą kartą buvo tirtas PEDOT:PSS dangos poveikis vilnos audinio elektriniam laidumui, naudojant srovės atominės jėgos mikroskopiją (CS-AFM). Išmatuota bandinio PFSH-p srovė siekė 10 nA, nors danga vietomis mikromasteliu nebuvo visiškai tolygi, tai yra pakankamas laidumas vertinant makroskopiniu mastu.
5. Apdorotas azoto plazma ir skaitmeniniu marginimu Clevios F ET, Clevios S V3 ir rišiklio Tubicoat fixing agent HT mišinio danga padengtas bandinys (PFSH-p) po 100 įkrovimo–iškrovimo ciklų išliko laidas ir elektrochemiškai stabilus, gali būti naudojamas daugkartinio veikimo prietaisuose. Dengtų bandinių PEDOT:PSS kompozicija specifinė talpa didesnė už vilnos substratą. Šie bandiniai, optimizavus sudėtį ir padidinus elektrinį laidumą, gali būti pritaikyti pakartotinio įkrovimo įrenginiuose.
6. Sukurta tvari PEDOT:PSS dangos formavimo ant tekstilės technologija: modifikavimas azoto plazma, dengimas skaitmeniniu marginimu Clevios F ET, Clevios S V3 ir rišiklio Tubicoat fixing agent HT mišinio danga,

kuri yra elektra laidži ir atspari dėvimui, nepakeičiant tekstilinių savybių ir galėtų būti pritaikyta kuriant dėvimus elektronikos įrenginius (antistatiniais drabužiais, išmaniai tekstilei, jutikliams ir kt.).

## ACKNOWLEDGEMENTS

I would like to express my deepest gratitude to my academic supervisor, Dr. Audronė Sankauskaitė, from the Department of Textile Technologies, FTMC, for her invaluable guidance, expertise, and unwavering support throughout my doctoral studies.

My sincere thanks also go to my mentors and colleagues: Dr. Vitalija Rubežienė, Dr. Sandra Varnaitė-Žuravliova, Dr. Aušra Abraitienė, and the head of the Department, Dr. Julija Baltušnikaitė-Guzaitienė, as well as all colleagues from the Department of Textile Technologies (FTMC) for their encouragement, insight, and collaborative spirit.

I would also like to express my heartfelt appreciation to Dr. Wael Ali, Dr. Alaa Salma, and group leader Dr. Thomas Mayer-Gall for their guidance and support, as well as to all the members of the Green Chemistry & Nanotechnology group (DTNW), including PhD. Eui-young Shin and PhD. Raphael Otto, for their constant inspiration and valuable contributions to my research.

I am also grateful for the support of my family and friends.

## LIST OF PUBLICATIONS

The data presented in this thesis have been published in the following articles:

1. **Petkevičiūtė, J.**, Sankauskaitė, A., Jasulaitienė, V., Varnaitė-Žuravlio, S., & Abraitienė, A. (2022). Impact of Low-Pressure Plasma Treatment of Wool Fabric for Dyeing with PEDOT: PSS. *Materials*, 15(14), 4797.

<https://doi.org/10.3390/ma15144797>

Author Contributions: conceptualization, methodology, software, validation, formal analysis, investigation, data curation, writing—original draft preparation, writing—review and editing, visualization.

2. **Pupeikė, J.**, Sankauskaitė, A., Varnaitė-Žuravlio, S., Rubežienė, V., & Abraitienė, A. (2023). Investigation of Electrical and Wearing Properties of Wool Fabric Coated with PEDOT: PSS. *Polymers*, 15(11), 2539.

<https://doi.org/10.3390/polym15112539>

Author Contributions: conceptualization, methodology, software, validation, formal analysis, investigation, data curation, writing – original draft preparation, writing – review and editing, visualization.

3. Rubežienė, V., Varnaitė-Žuravlio, S., Sankauskaitė, A., **Pupeikė, J.**, Ragulis, P., & Abraitienė, A. (2023). The impact of structural variations and coating techniques on the microwave properties of woven fabrics coated with PEDOT: PSS composition. *Polymers*, 15(21), 4224.

<https://doi.org/10.3390/polym15214224>

Author Contributions: investigation.

## DESCRIPTION OF THE LIFE, SCIENTIFIC AND CREATIVE ACTIVITIES

### Personal information

Julija Pupeikė

Email: [julija.petkeviciute@gmail.com](mailto:julija.petkeviciute@gmail.com)

Profile: <https://www.linkedin.com/in/julija-pupeik%C4%97-72959186/>



Julija Pupeikė specializes in research into environmentally friendly and electrically conductive textiles. With a background in molecular biology, biotechnology, and environmental sciences, she applies interdisciplinary expertise to develop sustainable smart textile solutions. Her work, presented at international conferences and published in scientific journals, combines innovative methods like nitrogen plasma treatment and PEDOT:PSS coatings to enhance textile functionality and durability.

### Education

Date	Institution	Qualification obtained
2019 – 2025	Center for Physical Sciences and Technology	Doctoral student of Materials engineering
2023 – 2024	German Textile Research Center North-West (DTNW)	Fellowship
2011 – 2013	Vytautas Magnus University	Master degree of Molecular biology and biotechnology
2007 – 2011	Vytautas Magnus University	Bachelor of Environmental Science

### Last working activity

Date	Institution Position	Position
2024 – till now	Center for Physical Sciences and Technology Department of Textile Technologies	Junior researcher
2023 – 2024	Center for Physical Sciences and Technology Department of Textile Technologies	Senior engineer
2018 – 2023	Center for Physical Sciences and Technology Department of Textile Technologies	Engineer
2015 – 2018	UAB „Šomis”	Chemical engineer
2012 – 2013	Vytautas Magnus University, Department of Natural Sciences	Intern

### Publications

1. **Petkevičiūtė, J.**, Sankauskaitė, A., Jasulaitienė, V., Varnaitė-Žuravliova, S., & Abraitienė, A. (2022). Impact of Low-Pressure Plasma Treatment of Wool Fabric for Dyeing with PEDOT: PSS. *Materials*, 15(14), 4797.

2. **Pupeikė, J.**, Sankauskaitė, A., Varnaitė-Žuravliova, S., Rubežienė, V., & Abraitienė, A. (2023). Investigation of Electrical and Wearing Properties of Wool Fabric Coated with PEDOT: PSS. *Polymers*, 15(11), 2539.

3. Rubežienė, V., Varnaitė-Žuravliova, S., Sankauskaitė, A., **Pupeikė, J.**, Ragulis, P., & Abraitienė, A. (2023). The impact of structural variations and coating techniques on the microwave properties of woven fabrics coated with PEDOT: PSS composition. *Polymers*, 15(21), 4224.



## **Attended Conferences**

### **Oral Presentations**

1. International Conference Dubrovnik 2024 "Application of PEDOT: PSS for electrically conductive and wear-resistant coating".
2. FTMC Metinė mokslinė konferencija 2024 "Application of organic polymers for wear-resistant, electrically conductive coatings".
3. International Conference Dubrovnik 2022 "Structural parameters of fabric affecting performance of electromagnetic shielding textile with conductive coating".
4. FTMC Metinė mokslinė konferencija 2022 "Tvarūs elektrai laidžių polimerų panaudojimo metodai tekstilės medžiagų laidumui padidinti".
5. Conference of Doctoral Students and Young Researchers Fiztech 2022, Vilnius "Investigation of Electrical and Wearing Properties of Wool Fabric Coated with PEDOT: PSS".
6. Conference of Doctoral Students and Young Researchers Fiztech 2021, Vilnius "Influence of plasma modification on wool dyeing with PEDOT: PSS polymer".

### **Poster Presentations**

7. 22nd Baltic Polymer Symposium (BPS 2024) "Thermal performance investigation of textiles with bio-based PCMs microcapsules and MWCNTs".
8. Symposium E-MRS Spring Meeting 2024, Strasbourg "Eco-friendly methods for developing electrically conductive textiles: using plasma treatment and PEDOT: PSS coatings".
9. International Conference-School Palanga "Advanced Materials and Technologies 2022", "Moisture management properties of biodegradable knitted fabrics containing hemp and polylactide fibers".
10. International Conference-School Palanga "Advanced Materials and Technologies 2021", "Structural parameters of fabric affecting performance of electromagnetic shielding textile with conductive coating".
11. International Conference-School Palanga "Advanced Materials and Technologies 2020", "Effect of plasma treatment on resistance performance of PEDOT: PSS coated shielding textile".

## **Fellowship**

2023 08 20 – 2024 08 19 German Textile Research Center North-West (DTNW) "Functional textiles research using environmentally friendly processes" by Deutsche Bundesstiftung Umwelt (DBU) program.

## **Awards**

Lithuanian Research Council (LMT) Research Award winner.

Best poster presentation award in Symposium E-MRS Spring Meeting 2024, Strasbourg "Eco-friendly methods for developing electrically conductive textiles: using plasma treatment and PEDOT: PSS coatings".

## NOTES

Vilniaus universiteto leidykla  
Saulėtekio al. 9, III rūmai, LT-10222 Vilnius  
El. p. [info@leidykla.vu.lt](mailto:info@leidykla.vu.lt), [www.leidykla.vu.lt](http://www.leidykla.vu.lt)  
[bookshop.vu.lt](http://bookshop.vu.lt), [journals.vu.lt](http://journals.vu.lt)  
Tiražas 15 egz.